



EDUARDO GUIMARÃES RATIER DE ARRUDA

**“2-(1H-IMIDAZOL-2-YL)HETEROARYL LIGANDS AND THEIR FE(II), RU(II)
AND CU(II) COMPLEXES”**

**“LIGANTES 2-(1H-IMIDAZOL-2-IL)HETEROARIL E SEUS COMPLEXOS DE
FE(II), RU(II) e CU(II)”**

**CAMPINAS
2015**



UNIVERSIDADE ESTADUAL DE CAMPINAS
INSTITUTO DE QUÍMICA

EDUARDO GUIMARÃES RATIER DE ARRUDA

**“2-(1H-IMIDAZOL-2-YL)HETEROARYL LIGANDS AND THEIR FE(II), RU(II)
AND CU(II) COMPLEXES”**

Orientador(a)/Supervisor: PROF. DR. ANDRÉ LUIZ BARBOZA FORMIGA

***“LIGANTES 2-(1H-IMIDAZOL-2-IL)HETEROARIL E SEUS COMPLEXOS DE
FE(II), RU(II) e CU(II)”***

Dissertação de Mestrado apresentada ao Instituto de Química da Universidade Estadual de Campinas para obtenção do título de Mestre em Química na área de Química Inorgânica.

Master's thesis presented to the Institute of Chemistry of Unicamp to obtain the title Master's in Chemistry in the area of Inorganic Chemistry.

ESTE EXEMPLAR CORRESPONDE À VERSÃO FINAL DA DISSERTAÇÃO DEFENDIDA POR EDUARDO GUIMARÃES RATIER DE ARRUDA E ORIENTADA PELO PROF. DR. ANDRÉ LUIZ BARBOZA FORMIGA.

Assinatura do Orientador

CAMPINAS
2015

Ficha catalográfica
Universidade Estadual de Campinas
Biblioteca do Instituto de Química
Simone Lucas Gonçalves de Oliveira - CRB 8/8144

Ar69L Arruda, Eduardo Guimarães Ratier de, 1990-
Ligantes 2-(1H-imidazol-2-il)heteroaril e seus complexos de Fe(II), Ru(II) e Cu(II) / Eduardo Guimarães Ratier de Arruda. – Campinas, SP : [s.n.], 2015.

Orientador: André Luiz Barboza Formiga.
Dissertação (mestrado) – Universidade Estadual de Campinas, Instituto de Química.

1. N-heterociclos. 2. Química de coordenação. 3. Imidazol. 4. Ferro. 5. Rutênio.
I. Formiga, André Luiz Barboza. II. Universidade Estadual de Campinas. Instituto de Química. III. Título.

Informações para Biblioteca Digital

Título em outro idioma: 2-(1H-imidazol-2-yl)heteroaryl ligands and their Fe(II), Ru(II) and Cu(II) complexes

Palavras-chave em inglês:

N-heterocycles

Coordination chemistry

Imidazole

Iron

Ruthenium

Área de concentração: Química Inorgânica

Titulação: Mestre em Química na área de Química Inorgânica

Banca examinadora:

André Luiz Barboza Formiga [Orientador]

Carlos Roque Duarte Correia

Marian Rosaly Davolos

Data de defesa: 19-02-2015

Programa de Pós-Graduação: Química

BANCA EXAMINADORA

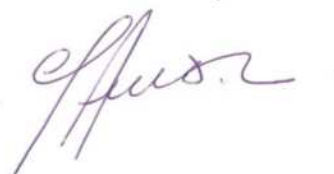
Prof. Dr. André Luiz Barboza Formiga (Orientador)



Profa. Dra. Marian Rosaly Davolos (IQ-UNESP - Araraquara)



Prof. Dr. Carlos Roque Duarte Correia (IQ-UNICAMP)



Este exemplar corresponde à redação final da
Dissertação de Mestrado defendida pelo aluno
EDUARDO GUIMARÃES RATIER DE ARRUDA,
aprovada pela Comissão Julgadora em 19 de fevereiro
de 2015.



Prof. Dr. André Luiz Barboza Formiga

(Presidente da Banca)

Quotes

Dias de sol

Abençoada seja a angústia, por que em igual proporção será o alívio.

Abençoada seja a despedida e a falta, porque novo gosto e belas cores terá a presença que se seguirá ao júbilo do encontro.

Abençoado seja o desejo que nos aperta o peito, porque faz nos agarrarmos à vida e aos sonhos e que apesar de tormento, nos leva à diante.

Abençoado portanto seja esse dia de sol, porque logo desponta trovosa tormenta a lavar os céus e a banhar meu ser cansado da refrega.

Sergio Augusto Venturinelli Jannuzzi

“In the beginning God created the heavens and the earth.”

Genesis 1.1

“All have their worth and each contributes to the worth of the others.”

J.R.R. Tolkien, The Silmarillion

“It’s a dangerous business, Frodo, going out your door. You step onto the road, and if you don’t keep your feet, there’s no knowing where you might be swept off to.”

J.R.R. Tolkien, The Lord of the Rings

“Never trust the storyteller. Only trust the story.”

Neil Gaiman, The Sandman, Vol. 6: Fables and Reflections

“Reality is frequently inaccurate.”

Douglas Adams, The Restaurant at the End of the Universe

“My goal is simple. It is a complete understanding of the universe, why it is as it is and why it exists at all.”

Stephen Hawking

“Don’t Panic.”

Douglas Adams, The Hitchhiker’s Guide to the Galaxy

Acknowledgements

Inicialmente, gostaria de agradecer ao Criador pela vida e criação da entidade responsável pela curiosidade que motiva a minha vida, a matéria. Obrigado pela oportunidade de aprender e trabalhar com a certeza que estou exercendo meu papel na construção da estrada da ciência.

Agradeço aos meus pais, Dr. Eduardo José de Arruda e Ive Guimarães Ratier de Arruda pelo amor, pelos ensinamentos, valores e exemplos. Obrigado pelo DNA e por serem a ilha segura no oceano da vida. Agradeço meu irmão Aly Guimarães Ratier de Arruda por ser o chato que eu mais amo, amigo, cabeça, exemplo e “engenheiro” da vida. À Melany Maria, minha *dachshund* valquíria, por me ajudar a desestressar e lembrar que humanidade passa por amar e proteger até a mais simples das criaturas. Agradeço a minha irmã Regiane, seu marido Fabiano e minhas sobrinhas Isabella e Amanda pelo apoio, carinho e suporte.

Agradeço ao minha avó-materna Zenir, por me ensinar que força vem de dentro. Aos meus tios Everton e Ester, pelos braços sempre abertos para me receber, pelo carinho, amizade e até o churrasco com aquela farofinha que só a tia faz. Agradeço ao meu primo Felipe pelas conversas e dicas de cinema, música e livros. À minha prima-irmã Marianna, por ser minha melhor amiga, aluna, professora, exemplo de superação e por ser sempre carinhosa com esse ser que vos escreve. A Bridinha e

Billy, vocês também fazem parte da vitória. Aos meus avós-paternos José e Dirce, pelo carinho e aquela comidinha que nunca provei melhor.

Agradeço a minha família de Campinas, Eliana Gama Lukas pelo amor de mãe, amizade, pelos almoços de domingo e pelo exemplo de batalhadora que não deixa as circunstâncias abalarem. Aos meu primos Kaleb, Raquel e Júlia, pela amizade, suporte e carinho. Nominalmente, Kaleb pelo exemplo de batalhador, Raquel pelas risadas e carinho (Caio, você também), Julika pela amizade e por ser a irmã caçula do grupo.

Agradeço ao carinho da família Lopes, obrigado Patrícia Maria Morato Lopes pela amizade, carinho de mãe e os maravilhosos finais de semana. À Gabriela pela amizade e companhia durante os bons momentos e a escrita da tese. E à Nininha, pelos lambeijos e carinho canino. Agradeço aos meus amigos Cleiton Zambiasi, Bruno Matos Paz, Helena Mannocho Russo, Cristiana Nilsson Buzolin, Cristina Adamo, Rafael Panzetti, Michele Moretti, Raquel Sisti e Anthony pela ajuda e apoio durante essa nova etapa.

Agradeço ao meu irmão e amigo Sergio Augusto Venturinelli Jannuzzi, pelo suporte na ciência e na vida, sua família, Neuza, Deo e Amanda, pelo apoio durante a caminhada. Agradeço a Sabrina Gracia Santos pelos momentos de alegria, choro e bobearas. À Helen Meneses pela amizade, ótimas conversas e ajuda durante o processo da ciência. À Irlene Maria Silva pelo suporte emocional, pelos abraços e melhores livros. Ao Douglas Hideki Nakahata pela amizade, apoio e suporte durante a escrita da dissertação. E à Stella de Almeida Gonsales pela ajuda no início da pesquisa e companherismo.

Agradeço as minhas queridas alunas de iniciação científica Carolina Gallupo e

Naíma Mohamed Orra pela oportunidade de ajudá-las e aprender com elas. Obrigada pela companhia e pelo ar “trevoso”. Também a Renata Sanches, Mariana Casado e Maiara Costa pela oportunidade de ajudá-las nos seus projetos de pesquisa. A Flávia Elisa Galdina e Bianca Cheregatti pela companhia durante o dia-a-dia do laboratório.

Agradeço a Vera Katic pela amizade e ajuda imprescindível com a correção da escrita. Ao Bruno Morandi Pires pelo apoio e longas discussões sobre voltametria cíclica. Ao Kalil Cristhian Figueiredo Toledo pela ajuda e pelo humor do dia-a-dia. À Pâmyla Layene dos Santos pela amizade e por dividir o fardo do período de defesas. Também a Mariana Carvalhaes Gallo pelas risadas e dicas tão preciosas.

Agradeço a Camilla Abbehausen pelas discussões e presença durante a evolução das idéias. Obrigado Marcos Alberto de Carvalho, Márcio Cristiano Monteiro, Luis Enrique Santa Cruz Huamaní, Raphael Enoque Ferraz de Paiva, Fernando Bergamini, Marjorie Mendonça, Júlia Helena Bormio Nunes, Rafael Michelin e Lily pela companhia e apoio. Agradeço a Nina Torres Zanvettor e Nicolas Chernavsky pela amizade e caronas. E a todos os colegas dos laboratórios do Instituto de Química.

Um agradecimento mais que especial para Cintia Massae Saito por ser a salvação do laboratório e uma aliada de peso no trabalho de bancada. Também a Bárbara Comunian, não só pelo apoio técnico, mas por uma amizade tão agradável e cheia de músicas.

Agradeço a meu orientador, Prof. Dr. André Luiz Barboza Formiga pela oportunidade, pela confiança depositada e pelas discussões tão enriquecedoras. Ao Prof. Dr. Pedro Paulo Corbi pela ajuda, apoio constante, ouvido para desabafo e exemplo de foco científico. À Profa. Dra. Regina Buffon pelas conversas e discussões. Agradeço também à Profa. Dra. Kristine Pierloot e seus alunos Simon Hallaert,

Quan Phung e Nick Van Steerteghem pela oportunidade e acolhimento durante a minha estada na KU Leuven/Bélgica,

Agradeço aos colaboradores deste trabalho: Ao Douglas Hideki Nakahata pela ajuda na discussão sobre os ligantes. Ao Sergio Augusto Venturinelli Jannuzzi nas medidas de solvatocromismo do 2-(1H-imidazol-2-il)pirazinapentacianidoferrato(II) e idéias sobre polimerização controlada. Ao Bruno Morandi Pires e ao Prof. Dr. Juliano Alves Bonacin pelas medidas de voltametria cíclica e discussão do comportamento eletroquímico do complexo de pentacianidoferrato(II). Ao Dr. Marcelo Alexandre de Farias e a Prof^a. Dr^a. Maria do Carmo Gonçalves pelos experimentos de Cu(I)-ATRP, todo o estudo da polimerização e caracterização do poliestireno. Ao Dr. Ronaldo Adriano Timm e ao Prof. Dr. Lauro T. Kubota pelas medidas de voltametria cíclica do complexo de Cu(II) e atribuições. Aos Dr. Surender K. Sharma, Dr. Giorgio Zoppellaro e Prof. Dr. Marcelo Knobel pelos estudos de magnetismo em estado sólido do complexo de Cu(II).

Agradeço a todos os professores e funcionários do Instituto de Química, ao CNPq pela bolsa de mestrado e a todos os colegas, técnicos e amigos que foram fundamentais nessa etapa.

Do fundo do meu coração obrigado!

EDUARDO GUIMARÃES RATIER DE ARRUDA

Academic formation

Nov-Dec/2014	Research internship at computational coordination chemistry group	KU Leuven, Belgium
	Master in Chemistry (Inorganic Chemistry) (ongoing)	University of Campinas, Brazil
2012	Bachelor in Chemistry (3 rd out of 70 students)	University of Campinas, Brazil

Additional formation

Mar/2013	Introduction to FORTRAN. CENAPAD/SP - University of Campinas, UNICAMP, Campinas, Brazil.
Jan/2012	Electronic Structure of Coordination Complexes - University of Campinas, UNICAMP, Campinas, Brazil.

Publications

M. C. Gallo, B. M. Pires, K. C. F. Toledo, S. A. V. Jannuzzi, **E. G. R. Arruda**, A. L. B. Formiga, J. A. Bonacin. *The use of modified electrodes by hybrid systems gold nanoparticles/Mn-porphyrin in electrochemical detection of cysteine. Synthetic Metals* (Just accepted - DOI:10.1016/j.synthmet.2014.10.024)

Scientific projects

Aug/2009-Dec/2012	<i>Synthesis, characterization and biological assays of the 2,6-Di(1H-imidazol-2-yl)pyridine and his transition metal complexes.</i> Institute of Chemistry, Unicamp. Department of Inorganic-Chemistry.
-------------------	--

Awards

2012	<i>Lavoisier Award of Best Student of Chemistry in the period of 2009-2012.</i> Regional Council of Chemistry, 4th Region.
------	--

Main congress contributions

- ³ **E. G. R. Arruda**, S. A. Gonsales, P. P. Corbi, M. Lancellotti A. L. B. Formiga. *Synthesis, structural characterization and biological assays of the 2,6-Di(imidazol-2-yl)pyridine copper(II) complex.* Poster. XVI Brazilian Meeting on Inorganic Chemistry, Florianopolis, Brazil, Aug/2012.
- ² **E. G. R. Arruda**, E. J. Arruda, G. A. Casagrande, T. A. D. Rodrigues, C. T. Carvalho, F. E. L. Correa, K. M. P. OLIVEIRA *Synthesis and characterization of complex L-aspartate-Cu(II) and L-aspartate-Fe(III) for control Aedes aegypti (Diptera: Culicidae).* Oral. XVI Brazilian Meeting on Inorganic Chemistry, Florianopolis, Brazil, Aug/2012.
- ¹ **E. G. R. Arruda**, S. A. Gonsales, A. L. B. Formiga. *Structural Characterization of the 2,6-Bis(imidazol-2-yl)pyridine copper(II) complex.* Poster. 35th Annual Meeting of the Brazilian Chemical Society,guas de Lindia, Brazil, May/2012.

Abstract

2-(1H-IMIDAZOL-2-YL)HETEROARYL LIGANDS AND THEIR FE(II), RU(II) AND CU(II) COMPLEXES.

Focusing on the development of new ligands for coordination and supramolecular chemistry, a class of the 1H-imidazol-2-yl N-heteroaryl derivatives were investigated. Complexes with transition metals were planned to verify the electronic properties and multidentate behaviour of the ligands. A fourth ligand with a tridentate binding site and its copper(II) complex were studied in order to evaluate an application in controlled polymerization catalysis.

In the first chapter, a series of 2-(1H-imidazol-2-yl)heteroaryl ligand were synthesized and characterized. Their ^1H and ^{13}C NMR were assigned and the pK_aH values were obtained in order to evaluate the σ -donor ability of the ligand. The effect of the six-membered N-heterocycle over the electronic structure of the 2-(1H-imidazol-2-yl) moiety was evaluated and showed that the electron-withdrawing effect of the azine/diazine that can be used to modulate the ligand-metal bond.

In the second chapter, a homoleptic ruthenium(II) complex with 2-(1H-imidazol-2-yl)pyridine (Himpy) was synthesized, purified and characterized. Due to the non-symmetry of the ligand, the synthesis of two isomers (*meridional* or *facial*) were

possible. The obtained product $[\text{Ru}(\text{Himpy})_3](\text{PF}_6)_2$ was the *meridional* isomer (*mer*) and it was fully characterized using ^1H NMR techniques. The UV-Vis absorption spectrum of the compound showed a complex metal-to-ligand charge-transfer (MLCT) transition and its solvatochromic behaviour.

In the third chapter, in order to evaluate the monodentate binding site of the 2-(1H-imidazol-2-yl)pyrazine ligand a pentacyanidoferrate(II) complex was synthesized. The characterization confirmed that the coordination occurs with the 2-pyrazine moiety via the N4 and free imidazol-2-yl moiety. The cyclic voltammetry showed the redox-active character of the ligand and the pH-dependency of the metal and ligand redox potential. The electronic spectrum was also found to be pH-dependent allowing the study of the correlation between the observed data, the electrochemical data and the electronic structure of the complex.

In the fourth chapter, the 2,6-di(1H-imidazol-2-yl)pyridine (H_2dimpy) was used as a catalyst for Cu(I)-mediated atom transfer radical polymerization (ATRP) for styrene polymerization in bulk and in DMF, as solvent. Due to the low solubility of the complex, only the system with solvent led to a controlled polymerization that resulted in a monomodal polystyrene with relative low polydispersity index (1.3). Similar results were obtained with terpyridine alkyl-derivatives. On the other hand, without the solvent, a green intermediate (Cu(II)) precipitated leading to a non-controlled polymerization. Therefore, confirming the importance of the solubilization of the Cu(II) intermediate in the system. Additionally, a Cu(II) complex was synthesized to investigate the catalyst intermediate. The complex 1:1:1 Cu(II): H_2dimpy :Cl was obtained and characterized by ESI-MS, FT-IR, UV-Vis, cyclic voltammetry and also the structure was obtained by single-crystal XRD.

The crystal showed the $[\text{Cu}_2(\text{H}_2\text{dimpy})_2(\mu\text{-Cl})_2](\text{PF}_6)_2 \cdot 2 \text{H}_2\text{O}$ dimeric complex, with the copper ion in a distorted square-based pyramid geometry ($\tau = 0.301$) with chloride bridge. The magnetic characterization of the crystal showed a ferromagnetic coupling that was also confirmed by U-DFT calculations.

Resumo

LIGANTES 2-(1H-IMIDAZOL-2-IL)HETEROARIL E SEUS COMPLEXOS DE FE(II), RU(II) E CU(II).

Tendo como foco o desenvolvimento de novos ligantes para química de coordenação e supramolecular, os compostos do tipo 1H-imidazol-2-il N-heteroaril foram estudados no que tange a modulação de suas propriedades pelo anel N-heterocíclico de seis membros. Os seus complexos com metais de transição foram planejados para verificar as propriedades eletrônicas e o caráter multidentado dessa classe de ligantes. Por fim, um quarto ligante com um sítio tridentado e seu complexo de cobre(II) foram estudados para avaliar a sua aplicação em uma catálise de polimerização controlada.

No primeiro capítulo, uma série de ligantes da classe dos 2-(1H-imidazol-2-il)heteroaril foram sintetizados e caracterizados. Os espectro de RMN de ^1H e ^{13}C foram atribuídos e os seus valores de pK_a foram obtidos para uma avaliação da capacidade σ -doadora dos ligantes. Um estudo comparativo foi realizado e a influência do anel N-heterocíclico de 6 membros sobre a estrutura eletrônicas do anel imidazólico foi avaliado. Foi observado que o caráter retirador da azina/diazina pode ser utilizado para modular a ligação metal-ligante.

No segundo capítulo, o complexo homoléptico de rutênio(II) com o ligante 2-(1H-

imidazol-2-il)piridina (Himpy) foi sintetizado, purificado e caracterizado. Devido a não-simetria do ligante, era esperado a presença de dois possíveis isômeros (*meridional* or *facial*). Porém, o produto obtido $[\text{Ru}(\text{Himpy})_3](\text{PF}_6)_2$ apresentou apenas o isômero *meridional* e este foi caracterizado através de várias técnicas de RMN de ^1H . O espectro de absorção no UV-Vis do composto apresentou uma transição de transferência de carga do tipo metal-ligante e seu comportamento solvatocrômico.

No terceiro capítulo, para avaliar o sítio de coordenação monodentado com ligante 2-(1H-imidazol-2-il)pirazina um complexo de pentacianoferrate(II) foi sintetizado. A caracterização confirmou a coordenação pelo N4 do grupo 2-pirazina e a presença do grupo imidazol-2-il descoordenado. A voltametria cíclica mostrou o caráter redox-ativo do ligante e a dependência com pH dos potenciais redox do metal e do ligante. O espectro de eletrônico também se mostrou uma dependência com o pH, possibilitando um estudo correlacionando os espectros obtidos, os dados eletroquímicos e a estrutura eletrônica do complexo.

Por fim, no quarto capítulo o ligante 2,6-di(1H-imidazol-2-il)piridina (H_2dimpy) foi utilizado como catalisador para uma polimerização radicalar controlada por transferência de átomo (ATRP) mediada por Cu(I) de poliestireno em “bulk” e em DMF, como solvente. Devido a baixa solubilidade do complexo, apenas o sistema com solvente levou a uma polimerização controlada gerando um produto monomodal e com um baixo índice de polidispersividade (1.3), similar aos resultados obtidos com derivados alquilados de terpiridina. Porém sem o solvente, um intermediário verde de Cu(II) precipitou durante a reação, levando a uma polimerização não-controlada. Uma vez confirmada a importância da solubilidade com intermediário de Cu(II) no meio reacional. Adicionalmente, um complexo de Cu(II) foi sintetizado como

modelo para investigar o intermediário catalítico. O complexo com proporção 1:1:1 Cu(II):H₂dimpy:Cl foi obtido e caracterizado por ESI-MS, FT-IR, UV-Vis, voltametria cíclica e sua estrutura foi resolvida por difração de raios X de monocristal. A cristal mostrou o complexo dimérico [Cu₂(H₂dimpy)₂(μ-Cl)₂](PF₆)₂ · 2 H₂O, onde o íon de cobre está em uma geometria de pirâmide de base quadrada distorcida ($\tau=0.301$) com pontes de cloreto. A caracterização magnética do cristal mostrou um acoplamento ferromagnético entre os íons de cobre em acordo com o resultado observado por cálculos de U-DFT.

Contents

Abbreviations, Acronyms and Symbols	xxvi
List of Tables	xxix
List of Figures	xxxi
1 2-(1H-imidazol-2-yl)heteroaryl ligands	1
1.1 Introduction	1
1.2 Results and discussion	2
1.2.1 NMR spectroscopy characterization	2
1.2.2 Comparative studies	10
1.3 Conclusion	12
1.4 Experimental	13
1.4.1 Materials and methods	13
1.4.2 Synthesis of 2-(1H-imidazol-2-yl)pyridine - Himpy	14
1.4.3 Synthesis of 2-(1H-imidazol-2-yl)pyrimidine - Himpmp	15
1.4.4 Synthesis of 2-(1H-imidazol-2-yl)pyrazine - Himpz	15
1.4.5 Determination of pK_{aH}	16

2	<i>mer</i>-[Ru(Himpy)₃](PF₆)₂	19
2.1	Introduction	19
2.2	Results and discussion	21
2.2.1	Structural characterization	21
2.3	Conclusion	30
2.4	Experimental	30
2.4.1	Materials and methods	30
2.4.2	Synthesis of 2-(1H-imidazol-2-yl)pyridine - Himpy	32
2.4.3	Synthesis of [Ru(Himpy) ₃](PF ₆) ₂	33
3	Na₃[Fe(CN)₅(Himpz)]	35
3.1	Introduction	35
3.2	Results and discussion	38
3.2.1	Synthesis and characterization	38
3.2.2	Electrochemical characterization	42
3.3	Conclusion	46
3.4	Experimental	48
3.4.1	Materials and methods	48
3.4.2	Synthesis of 2-(1H-imidazol-2-yl)pyrazine - Himpz	49
3.4.3	Synthesis of Na ₃ [Fe(CN) ₅ (Himpz)]	50
3.4.4	Determination of pK _{aH}	51
4	H₂dimpy as a ligand for Cu(I)-mediated ATRP	53
4.1	Introduction	53
4.2	Results and discussion	55

4.2.1	Syntheses	55
4.2.2	Ligand characterization	55
4.2.3	Cu(I)-ATRP assays	56
4.2.4	Copper(II) complex	60
4.3	Conclusion	70
4.4	Experimental	71
4.4.1	Materials and methods	71
4.4.2	Ligand Synthesis	73
4.4.3	Preparation of polystyrene via ATRP	74
4.4.4	Complex synthesis	75
4.4.5	DFT calculations	75
5	Conclusion and Perspectives	81
5.1	Conclusion	81
5.2	Perspectives	82
	Bibliography	84

Abbreviations, Acronyms and Symbols

ACN	Acetonitrile
AcOH	Acetic Acid
AN	Gutmann Acceptor Number
ATRP	Atom Transfer Radical Polymerization
bpy	2,2'-bipyridine
COSY	Correlation Spectroscopy
CRP	Controlled Radical Polymerization
CV	Cyclic Voltammetry
DMF	Dimethylformamide
DMSO	Dimethyl sulfoxide
ESI-MS	Electrospray Ionization Mass Spectrometry
ESI-QTOF	Electrospray Ionization Quadrupole Time-of-Flight
EtOAc	Ethyl Acetate
FT-IR	Fourier Transform Infrared Spectroscopy
GCE	Glassy Carbon Electrode
GPC	Gel Permeation Chromatography
Himp _m	2-(1H-imidazol-2-yl)pyrimidine
Himpy	2-(1H-imidazol-2-yl)pyridine

Himpz	2-(1H-imidazol-2-yl)pyrazine
H ₂ dimpy	2,6-Di(imidazol-2-yl)pyridine
HMBC	Heteronuclear Multiple-Bond Correlation
HSQC	Heteronuclear Single Quantum Coherence
HOMO	Highest Occupied Molecular Orbital
LUMO	Lowest Unoccupied Molecular Orbital
MeOH	Methanol
MLCT	Metal-to-Ligand Charge Transfer
MS	Mass Spectrometry
NaOMe	Sodium Methoxide
NMR	Nuclear Magnetic Resonance
phen	Phenanthroline
pK _a	Logarithmic Acidity Constant
PS	Polystyrene
py	Pyridine
pz	Pyrazine
SHE	Standard Hydrogen Electrode
SQUID	Superconducting Quantum Interference Device Magnetometer
terpy	2,2';6',2''-terpyridine
THF	Tetrahydrofuran
U-B3LYP	Unrestricted Becke three-parameter, Lee-Yang-Parr
U-DFT	Unrestricted Kohn-Sham approach to Density Functional Theory
UV-Vis	Ultraviolet-Visible Absorption Spectroscopy

XRD

X-Ray Diffraction

List of Tables

1.1	Assignment of the ^1H NMR spectrum of the Himpy in d^6 -DMSO.	3
1.2	Assignment of the ^{13}C NMR spectrum of the Himpy in d^6 -DMSO.	5
1.3	Assignment of the ^1H NMR spectrum of the Himp _m in d^6 -DMSO.	6
1.4	Assignment of the ^{13}C NMR spectrum of the Himp _m in d^6 -DMSO.	8
1.5	Assignment of the ^1H NMR spectrum of the Himp _z in d^6 -DMSO.	9
1.6	Assignment of the ^{13}C NMR spectrum of the Himp _z in d^6 -DMSO.	10
1.7	Chemical shift (δ) of the hydrogens in the 1H-imidazol-2-yl moiety for the ligands in d^6 -DMSO. For the imidazole, the literature data was obtained in D_2O ¹	10
1.8	Chemical shift (δ) of the C7 carbon in the 1H-imidazol-2-yl moiety for the ligands in d^6 -DMSO. ¹	11
1.9	Experimentally calculated $\text{pK}_{a\text{H}}$ of the ligands.	11
1.10	Experimental conditions for $\text{pK}_{a\text{H}}$ determination.	17
3.1	Assignment of the signals of ^1H NMR spectrum of the complex $\text{Na}_3[\text{Fe}(\text{CN})_5(\text{Himpz})]$ in D_2O	40
3.2	Assignment of the signals of ^{13}C NMR spectrum of the complex $\text{Na}_3[\text{Fe}(\text{CN})_5(\text{Himpz})]$ in D_2O	42

3.3	Half wave potentials obtained from cyclic voltammetry (V vs SHE)	
	in pH values of 4, 7 and 10 and the pK_a values of the N-heterocycle	
	protonation equilibria.	45
3.4	Experimental conditions for pK_{aH} determination.	51
4.1	Molecular parameters obtained for the PS homopolymers.	57
4.2	Data from the single-crystal XRD of the $[Cu_2(H_2dimpy)_2(\mu-Cl)_2](PF_6)_2 \cdot$	
	$2 H_2O$ complex	61
4.3	Selected bond distances and angles from the single-crystal XRD of	
	the complex	62
4.4	Data from the single-crystal XRD of the $[Cu_2(H_2dimpy)_2(\mu-Cl)_2](PF_6)_2 \cdot$	
	$2 H_2O$ complex sample at room temperature.	76
4.5	Magnetic coupling analysis obtained with broken-symmetry U-B3LYP/def2-	
	TZVP. The XRD experimental geometry was used neglecting water	
	and PF_6^-	76

List of Figures

1.1	Structure of the ligands with numbered hydrogens.	3
1.2	¹ H NMR spectrum of the Himpy obtained in the 600 MHz spectrometer.	4
1.3	Annular prototropic tautomeric equilibrium present on the ligand Himpy, favored by protic solvents.	4
1.4	¹³ C NMR spectrum of the Himpy obtained in the 500 MHz spectrometer.	5
1.5	¹ H NMR spectrum of Himpm obtained in the 600 MHz spectrometer	6
1.6	Structure of the ligands with numbered carbons and nitrogens.	7
1.7	¹³ C NMR spectrum of the Himpm obtained in the 500 MHz spectrometer.	7
1.8	¹ H NMR spectrum of the Himpz obtained in the 500 MHz spectrometer.	8
1.9	¹³ C NMR spectrum of the Himpz obtained in the 500 MHz spectrometer.	9
1.10	Intramolecular hydrogen bond upon protonation of the Himpm.	12

2.1	UV-Vis spectra of the $[\text{Ru}(\text{Himpy})_3](\text{PF}_6)_2$ and of the ligand Himpy in MeOH.	21
2.2	^1H NMR spectrum of the complex $[\text{Ru}(\text{Himpy})_3](\text{PF}_6)_2$ in $\text{DMSO}-d_6$ obtained in the 500 MHz spectrometer.	22
2.3	^1H - ^1H NMR COSY spectrum of the complex $[\text{Ru}(\text{Himpy})_3](\text{PF}_6)_2$ in $\text{CH}_3\text{CN}-d_3$ obtained in the 400 MHz spectrometer.	24
2.4	^1H NMR spectrum of the complex $[\text{Ru}(\text{Himpy})_3](\text{PF}_6)_2$ in $\text{CH}_3\text{CN}-d_3$ with double irradiation at 6.66 ppm obtained in the 400 MHz spectrometer.	25
2.5	Assigned ^1H NMR spectrum of the complex <i>mer</i> - $[\text{Ru}(\text{Himpy})_3](\text{PF}_6)_2$ in $\text{CH}_3\text{CN}-d_3$ obtained in the 400 MHz spectrometer.	26
2.6	ESI-QTOF-MS of the $[\text{Ru}(\text{Himpy})_3](\text{PF}_6)_2$ in a $\text{H}_2\text{O}/\text{MeOH}$ solution, the peak at 512.50 is an internal contamination of the equipment.	28
2.7	UV-Vis spectra of the <i>mer</i> - $[\text{Ru}(\text{Himpy})_3](\text{PF}_6)_2$ in different solvents.	29
2.8	Linear relation between the intraligand band energy and the Gutmann AN for MeOH, EtOH and H_2O .	29
3.1	UV-Vis absorption spectra of the complex $\text{Na}_3[\text{Fe}(\text{CN})_5(\text{Himpz})]$ in water and of the ligand Himpz in MeOH.	39
3.2	^1H NMR of the $\text{Na}_3[\text{Fe}(\text{CN})_5(\text{Himpz})]$ complex in D_2O .	40
3.3	^{13}C NMR of the $\text{Na}_3[\text{Fe}(\text{CN})_5(\text{Himpz})]$ complex in D_2O .	41

3.4	Cyclic voltammograms of 1.10^{-3} mol L $^{-1}$ aqueous solutions of pentacyanidoferrate(II) complexes containing the Himpz ligand in Britton-Robinson buffer solution in at a) pH 4.0, b) pH 7.0, c) pH 10.0 containing KCl 0.1 mol L $^{-1}$. Scan rate 100 mV s $^{-1}$	43
3.5	Cyclic voltammograms of 1.10^{-3} mol L $^{-1}$ aqueous solutions of himpz in Britton-Robinson buffer solutions containing KCl 0.1 mol L $^{-1}$. Scan rate 100 mV s $^{-1}$	44
3.6	Variation of the electronic absorption spectra of Na $_3$ [Fe(CN) $_5$ Himpz] by increasing stepwise the pH by titration with NaOH 0.05 mol L $^{-1}$. The arrows show the evolution of the spectra during the titration and each line represents a pH increase of 0.23 in average.	47
4.1	Chemical equation of the styrene Cu(I)-ATRP assays.	56
4.2	GPC curves of PS-s and PS-b homopolymers.	57
4.3	^1H NMR spectrum of the PS-s with inset showing the 4.60-4.35 ppm range magnification obtained in the 500 MHz spectrometer.	58
4.4	ORTEP image of the complex $[\text{Cu}_2(\text{H}_2\text{dimpy})_2(\mu-\text{Cl})_2](\text{PF}_6)_2 \cdot 2 \text{H}_2\text{O}$	61
4.5	FT-IR spectra of the copper(II) complex and the H $_2$ dimpy ligand.	64
4.6	A) Experimental magnetic susceptibility in the 2-300 K temperature range and theoretical fittings based on two different models (B and C) for exchange interaction in dimeric $[\text{Cu}_2(\text{H}_2\text{dimpy})_2(\mu-\text{Cl})_2](\text{PF}_6)_2 \cdot 2 \text{H}_2\text{O}$	66

4.7	Spin density obtained from U-B3LYP/def2-TZVP using the experimental geometry of the dimeric $[\text{Cu}_2(\text{H}_2\text{dimpy})_2(\mu\text{-Cl})_2]^{2+}$ unit in the triplet state ($S = 1$).	67
4.8	UV-Vis spectra of the H_2dimpy in MeOH and the copper(II) complex in H_2O .	68
4.9	Cyclic voltammetry of the complex in acetonitrile at 100 m V s^{-1} .	69
4.10	ESI-(+)-MS spectrum of the copper complex in MeOH/ H_2O .	77
4.11	ESI-(+)-MS-MS spectrum of the peak at $m/z = 309$ corresponding to the $[\text{Cu}(\text{H}_2\text{dimpy})\text{Cl}]^+$ fragment.	78
4.12	UV-Vis spectra of the copper(II) complex and CuCl_2 in H_2O .	79
4.13	UV-Vis spectra of the copper(II) complex in H_2O and in the solid state.	79

Chapter 1

2-(1H-imidazol-2-yl)heteroaryl ligands

1.1 Introduction

The planning and synthesis of coordination compounds has been attracting a lot of attention during the last years. Beside the variety of possible architectures, it is possible to modulate their properties such as magnetism, luminescence, molecular recognition and so forth. However, the preparation of these rational designed compounds still are a challenge for the synthetic inorganic chemistry.²⁻⁵

Aromatic N-heterocycles ligands have been studied for a long period in coordination chemistry due to their rigid structures and their conjugated electronic systems that favors the formation of coordination compounds with strong light absorption in the visible region.^{6,7} The complexes of imidazole ligands are prominent not only because of their optical properties, but also for the possibility of deprotonation or derivatization of the N-H group, thus altering the electronic structure and reactivity of the compound.^{8,9}

Henceforth, the planning of transition metal complexes with aromatic ligands and multiple coordination sites is a tendency in supramolecular chemistry. Compounds

with multiple metallic centers connected by conjugated systems are of great technological interest. They can be used in solar energy conversion, as pigments in photovoltaic cells, as catalysts and as electrochemical sensors.^{10,11}

The development of new ligands that lead to complexes with interesting properties for both academia and technological application, like photocatalysts and photovoltaic cells pigments, is a well-exploited field.^{12,13} However, combine the rational complexes synthesis with supramolecular strategies to optimize the interesting properties is relative new approach.^{14–16} Therefore by uniting both fields, supramolecular species generated by the new ligands could be built up.

In this work a series of 2-(1H-imidazol-2-yl)heteroaryl have been synthesized, using a simple one-pot reaction,¹⁷ and characterized. Their ¹H and ¹³C NMR spectra were assigned and a comparative study was made in order to evaluate the effect of the number and position of the nitrogens in the structure over their electronic properties.

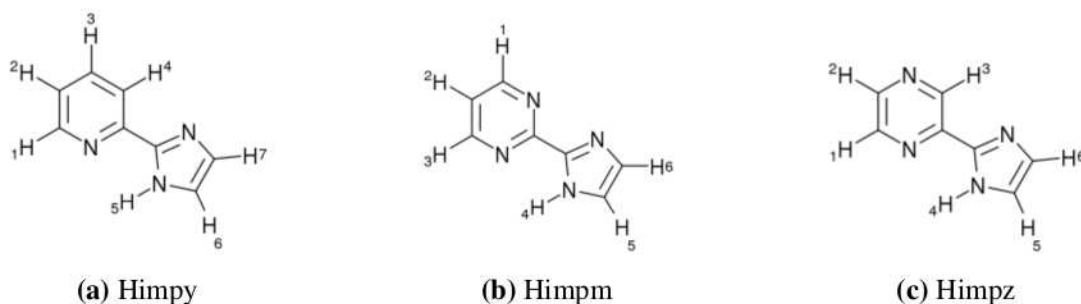
1.2 Results and discussion

1.2.1 NMR spectroscopy characterization

2-(1H-imidazole-2-yl)pyridine - Himpy

The product was mainly characterized using ¹H NMR and is shown in Figure 1.2. The signals assignments were done, presented in Table 1.1, and are in agreement with literature.¹⁷ The numbered structures used in the assignments are shown in Figure 1.1a.

For the imidazole moiety, only one signal for the H6/H7 was observed, this is due to the annular prototropic tautomerism, shown in Figure 1.3, which is common in

**Figure 1.1:** Structure of the ligands with numbered hydrogens.**Table 1.1:** Assignment of the ^1H NMR spectrum of the Himpy in d_6 -DMSO.

δ (ppm)	Signal type	J (Hz)	Integration	Hydrogen
7.16	s	-	2	H6/H7
7.35	ddd	7.5, 4.8, 1.2	1	H2
7.88	td	7.5, 1.8	1	H4
8.04	dt	7.5, 1.2	1	H3
8.59	ddd	4.8, 1.8, 1.2	1	H1
12.68	s (br)	-	-	H5

polyazins like pyrimidines, triazoles and tetrazoles.^{1,18,19} Consequently, the hydrogens H6 and H7 from the imidazole ring are equivalent and a single broad signal at 7.16 ppm could be observed, which integrates for two hydrogens. This tautomeric equilibrium is facilitated by protic solvents and the water content in d_6 -DMSO favors the tautomerism.

Broadening of signals was also favored by the quadrupolar effect caused by ^{14}N , mainly the hydrogen atoms bonded to nitrogen.²⁰ Therefore it is a main effect that causes broadening of H5 signal.

On the ^{13}C NMR, shown in Figure 1.4, it was possible to observe six well-defined signals and one broad low-intense signal. Consequently, this result corroborates the annular prototropic tautomerism, illustrated in Figure 1.3b for the carbons.

Due to the fast interconversion between the tautomers, the signals from carbons

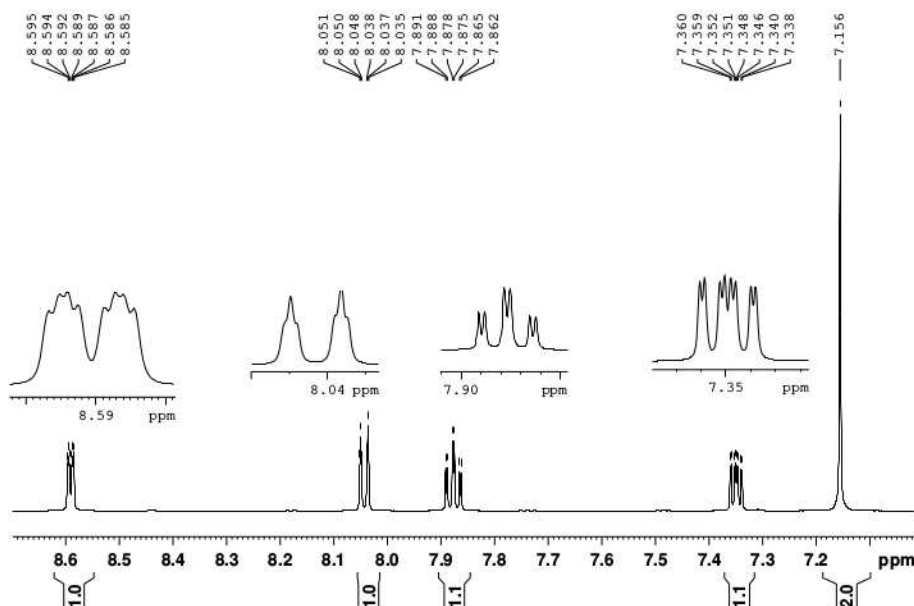


Figure 1.2: ^1H NMR spectrum of the Himpy obtained in the 600 MHz spectrometer.

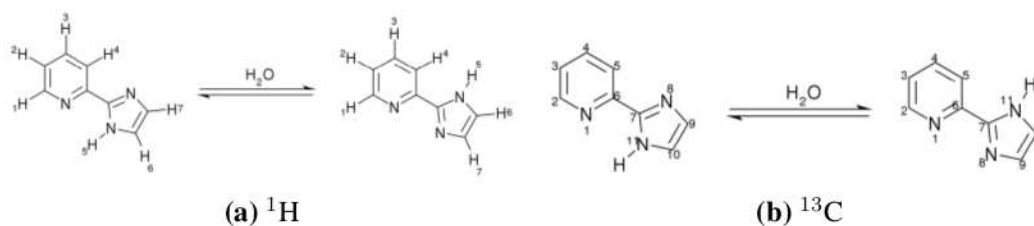


Figure 1.3: Annular prototropic tautomeric equilibrium present on the ligand Himpy, favored by protic solvents.

C9 and C10 coalesce, generating a broad signal. The signal attribution from ^{13}C NMR was made, shown in Table 1.2 and is in agreement with it.¹⁷

2-(1H-imidazole-2-yl)pyrimidine - Himpm

The ^1H NMR spectrum, shown in Figure 1.5, demonstrates three signals, two being from the pyrimidine ring and one for the imidazole ring. Once again, the prototropic annular tautomerism is present, which turns the hydrogen pairs (H1, H3) and

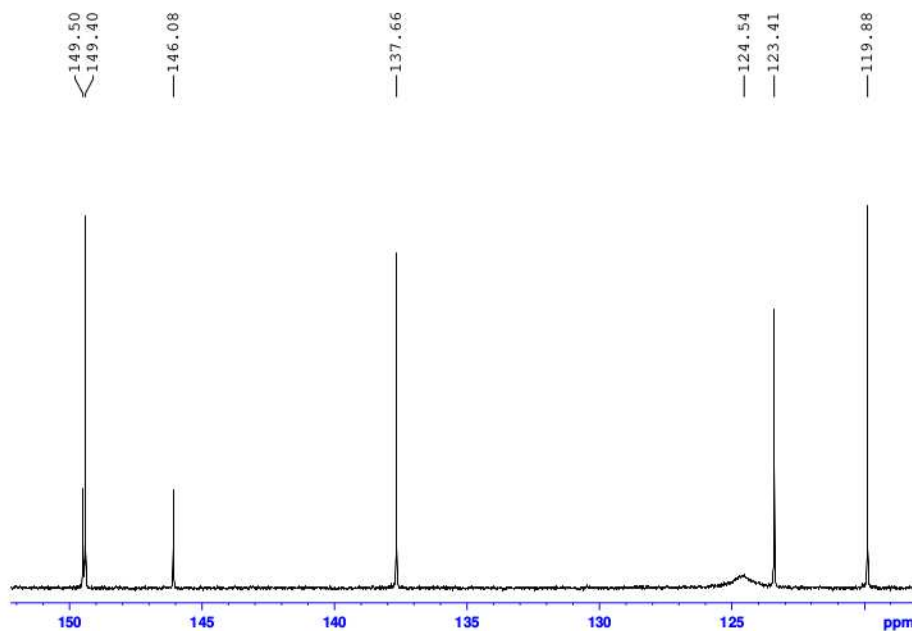


Figure 1.4: ^{13}C NMR spectrum of the Himpy obtained in the 500 MHz spectrometer.

Table 1.2: Assignment of the ^{13}C NMR spectrum of the Himpy in $\text{d}^6\text{-DMSO}$.

	C3	C5	C9/C10	C4	C7	C2	C6
δ (ppm)	119.97	123.52	124.56	137.72	146.23	149.40	149.49

(H5, H6) equivalent, increasing the symmetry (C_s to C_2) and reducing the number of signals from five to three signals. This is corroborated by the signal observed for the pair (H1, H3), a duplet, and for H2, a triplet, indicating the chemical equivalence between the meta hydrogens for the 2-substituted pyrimidine.

The structure of Himpm with numbered hydrogen and the signal attribution is shown in Figure 1.1b and in Table 1.3, respectively.

Figure 1.7 and 1.6a show the ^{13}C NMR spectrum of the Himpm and the structure with numbered carbon and nitrogen used for assignments, respectively.

It was possible to observe four signals instead of six, due to the prototropic annu-

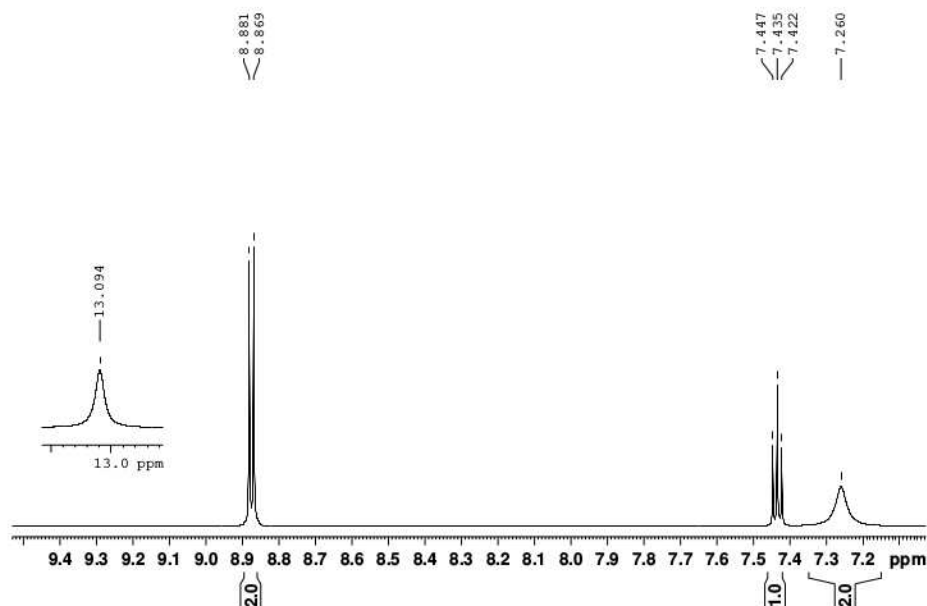


Figure 1.5: ^1H NMR spectrum of Himpm obtained in the 600 MHz spectrometer

Table 1.3: Assignment of the ^1H NMR spectrum of the Himpm in $\text{d}^6\text{-DMSO}$.

δ (ppm)	Signal type	3J (Hz)	Integration	Hydrogen
7.26	s	-	2	H4/H5
7.44	t	4.8	1	H2
8.88	d	4.8	2	H1/H3
13.09	s (br)	-	1	H5

lar tautomerism, that makes the carbon pairs (C4, C6) and (C9 and C10) equivalent.

The assignments were made using two-dimensional ^1H - ^{13}C NMR techniques, heteronuclear single quantum coherence (HSQC) and heteronuclear multiple-bond correlation (HMBC) spectroscopies. The assignments are shown on Table [1.4](#).

The results obtained were consistent with literature.¹⁷



Figure 1.6: Structure of the ligands with numbered carbons and nitrogens.

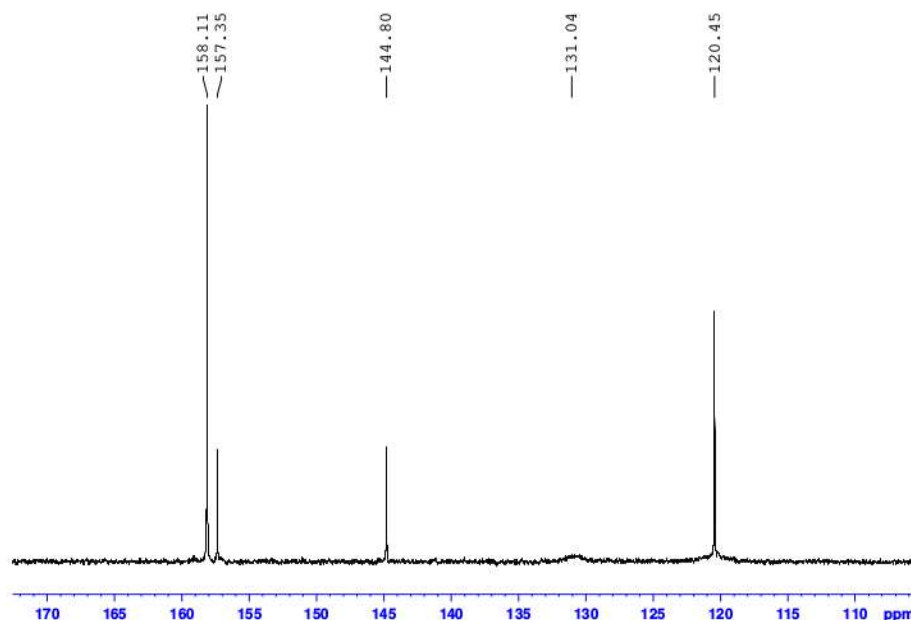


Figure 1.7: ^{13}C NMR spectrum of the Himpm obtained in the 500 MHz spectrometer.

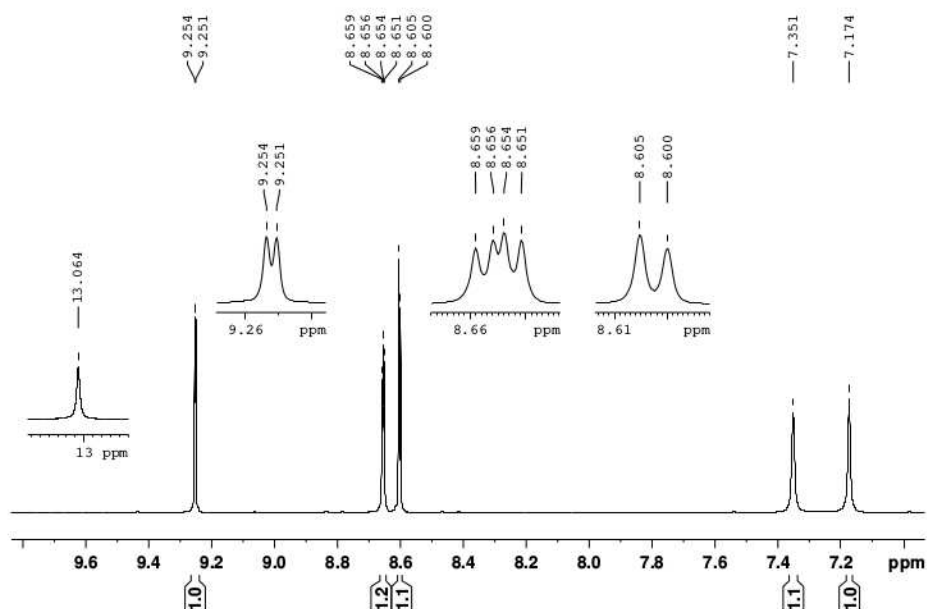
2-(1H-imidazole-2-yl)pyrazine - Himpz

The obtained ^1H NMR spectrum was in agreement with the expected for a mono-substituted pyrazine, where the three signals from pyrazine are in the 8.6-9.3 ppm region. In the case of imidazole, the spectrum is highly sensible to the prototropic annular tautomerism. When a protic solvent is present (wet sample) the H5 and H6 became chemically equivalent and a single signal is observed in 7.26 ppm. The Himpz shown a minor hydrophilic character when compared with the Himpy and

Table 1.4: Assignment of the ^{13}C NMR spectrum of the Himp in d^6 -DMSO.

	C5	C9/C10	C7	C2	C4/C6
δ (ppm)	120.45	130.68	144.80	157.35	158.12

Himp. Therefore it has allowed the acquisition of a spectrum where the signals of the H5 and H6 of imidazole were chemically non-equivalent, as it could be seen in Figure 1.8. The structure and numbering used for attribution and the experimental data are given in Figure 1.1c and Table 1.5

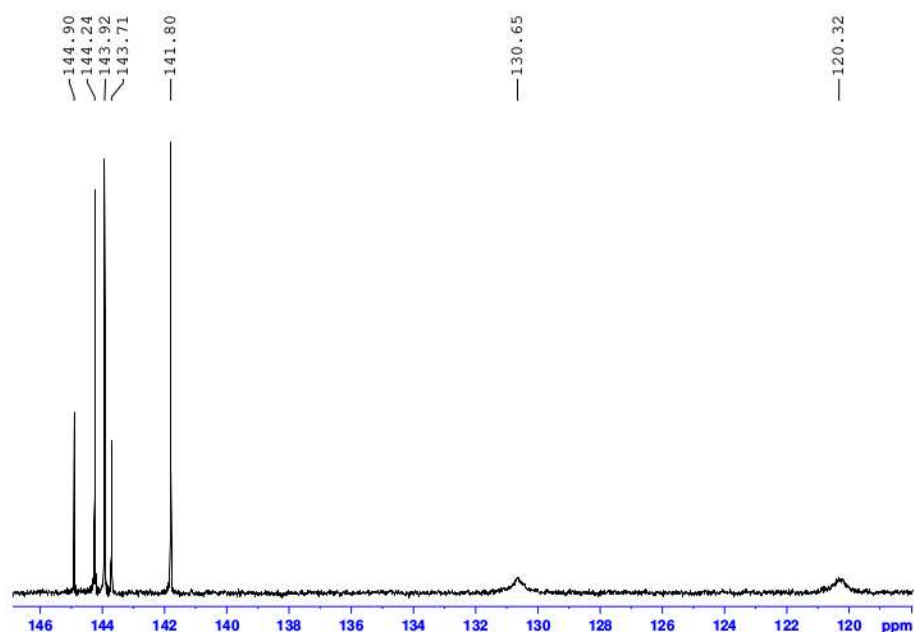
**Figure 1.8:** ^1H NMR spectrum of the Himpz obtained in the 500 MHz spectrometer.

Due to the slow rate of interconversion between the tautomers, all seven signals expected for the ^{13}C NMR were observed, as it could be seen in the Figure 1.9. It was possible to differentiate the carbons from imidazole, with a shift of 10 ppm. However, the signals obtained were broad due to the influence of the prototropic annular tautomerism even in a unfavorable medium. The complete attribution was possi-

Table 1.5: Assignment of the ^1H NMR spectrum of the Himpz in $\text{d}^6\text{-DMSO}$.

δ (ppm)	Signal type	J (Hz)	Integration	Hydrogen
7.17	s	-	1	H5
7.35	s	-	1	H6
8.60	d	2.5	1	H2
8.66	dd	2.5, 1.5	1	H1
9.25	d	1.5	1	H3
13.06	s	-	1	H4

ble by two-dimensional ^1H - ^{13}C HSQC and HMBC NMR. The results and structure with carbon numbering used for attribution are given in Table 1.6 and Figure 1.6b, respectively.

**Figure 1.9:** ^{13}C NMR spectrum of the Himpz obtained in the 500 MHz spectrometer.

The results obtained were consistent with the literature.¹⁷

Table 1.6: Assignment of the ^{13}C NMR spectrum of the Himpz in $\text{d}^6\text{-DMSO}$.

	C9	C10	C3	C7	C5	C6	C2
δ (ppm)	120.32	130.72	141.80	143.71	143.92	144.24	144.90

1.2.2 Comparative studies

A comparative study has been performed in order to evaluate the effect of the number of nitrogens and their position into the electronic structure of the ligands using the 1H-imidazol-2-yl moiety, that is common to all ligand as a probe. The ^1H NMR chemical shift for the imidazole hydrogens are shown in Table 1.7 and it could be seen that amine hydrogen is the H5 in Himpy and H4 in Himpz/Himpm, and the aryl hydrogens the H6/H7 in Himpy and H5/H6 in Himpz/Himpm. (See Figure 1.1)

Table 1.7: Chemical shift (δ) of the hydrogens in the 1H-imidazol-2-yl moiety for the ligands in $\text{d}^6\text{-DMSO}$. For the imidazole, the literature data was obtained in D_2O ¹

	Himpy	Himpm	Himpz	Imidazole
Amine hydrogen	12.68	13.09	13.06	-
Average of aryl hydrogens	7.16	7.26	7.26	7.14

Comparing the chemical shift for both hydrogens of the imidazol-2-yl moiety, the more relevant change occurs from the azine (pyridine) to a diazine (pyrimidine and pyrazine), however almost no difference was observed between the diazines. Therefore, the number of nitrogens is more important for the acidity of those hydrogens than their relative position.

The same was made using the C7 carbon (See Figure 1.3b and 1.6) as probe to evaluate the six-membered N-heterocycle over the electronic density of the imidazole. The results are shown in Table 1.8.

It was possible to observe that for the Himpy ligand the C7 is more deshielded

Table 1.8: Chemical shift (δ) of the C7 carbon in the 1H-imidazol-2-yl moiety for the ligands in d^6 -DMSO.¹

	Himpy	Himpm	Himpz	Imidazole
C7	146.23	144.80	143.71	135.46

when compared with the diazines. One might be surprised, however when it comes to the electronic communication between the rings, it is expected that the 2-pyrazyl moiety, the most acidic one (pK_{aH} 0.65),²¹ would delocalize the π -electronic density of the imidazol ring towards the diazine. Consequently, the density over the C7 increases towards the azine or diazine then decreasing the chemical shift. The observed series are consistent with the pK_{aH} of free six-membered N-heterocycles.^{21,22}

Due to the importance of the pK_{aH} over the properties of the N-heterocycles, they were experimentally calculated in H_2O for the three ligands and are shown in Table

1.9

Table 1.9: Experimentally calculated pK_{aH} of the ligands.

	Himpy	Himpm	Himpz	Pyridine ²³	Pyrimidine ²⁴	Pyrazine ²¹	Imidazole ²⁵
pK_{aH}	5.10	5.21	4.51	5.25	1.23	0.65	6.99

The Himpz was the ligand with the lowest pK_{aH} value, it is in agreement with the expected for a 1H-imidazol-2-yl moiety bonded to a electron-deficient group. The same is observed for the Himpy, however the 2-pyrimidine derivative have the highest pK_{aH} in series, even if the free pyrimidine pK_{aH} is lower than for the pyridine. This can be explained by the possibility of second intramolecular hydrogen bond (See Figure **1.10**) between the protonated imidazole moiety and the pyrimidine nitrogen. Leading to a more stable system when compared to the other ligands.

The pK_{aH} measurement can be related to the σ -donor ability of the ligand toward a coordination with a Lewis acid. Consequently, it is expected that in the Himpm

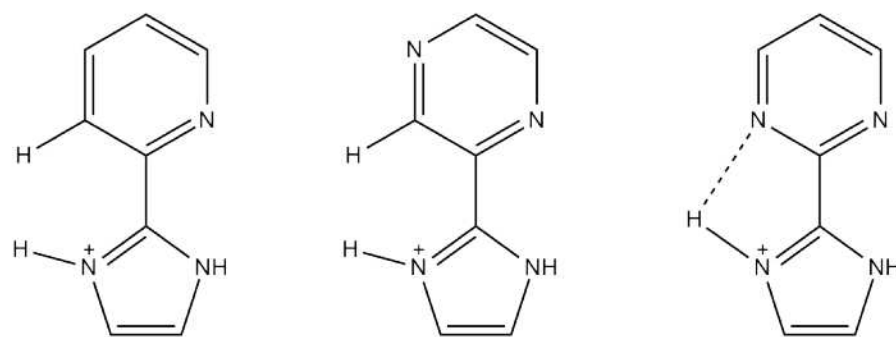


Figure 1.10: Intramolecular hydrogen bond upon protonation of the Himpz.

ligand complexes, σ -effect will be stronger when compared with the Himpz. Leading to a possible tuning of the transition metal complexes with a simple change in the position of the nitrogens in the diazine.

1.3 Conclusion

The 2-(1H-imidazol-2-yl)heteroaryl, with heteroaryl = pyridine, pyrimidine and pyrazine, were synthesized and characterized. The ^1H and ^{13}C spectra were assigned with aid of two-dimensional experiments. The comparative properties of those ligands were made using the 1H-imidazol-2-yl moiety as a probe and demonstrating the effect of the azine/diazine upon the electronic structures. The comparative results suggest that these ligands could be used to prepare transition metal complexes allowing the tuning of their properties in respect with slightly changes in the nitrogens number and position.

1.4 Experimental

1.4.1 Materials and methods

Materials

2-Pyridinecarbonitrile (99%), 2-pyrazinecarbonitrile (99%), 2-pyrimidinecarbonitrile (97%) 2,2-diethoxyethylamine (98%) and 2,2-dimethoxyethylamine (99%) were purchased from Sigma Aldrich. Methanol, acetic acid, hydrochloric acid, diethyl ether (Et₂O), ethyl acetate, dichloromethane, chloroform, acetonitrile, sodium hydroxide and sodium carbonate (99.5%) were purchased from Vetec-Sigma (Brazil). Sodium lumps were purchased from Riedel-de Haën. All reagents were used as received from commercial source, with no further purification, except when noted.

Physical Measurements

Electronic spectra in the 190-1100 nm range were acquired by using a 1.00 cm quartz cuvette in a diode array HP8453 UV/Visible absorption spectrophotometer equipped with a HP89090A Peltier.

Electrospray ionization mass spectrometry (ESI-MS) measurements were carried out using a Waters Quattro Micro API. Samples were evaluated in the positive mode in an 1:1 methanol:water solution with addition of 0.10% (v/v) formic acid.

The values of pH were measured using a Metrohm 827 pH Lab pHmeter.

Elemental analyses for carbon, hydrogen and nitrogen were performed using a Perkin Elmer 2400 CHN analyzer.

¹H and ¹³C NMR spectra were acquired in deuterated dimethylsulfoxide (DMSO) solutions using a Bruker Avance III - 500MHz (11.7T) and a 600MHz (14.09T)

spectrometers.

1.4.2 Synthesis of 2-(1H-imidazol-2-yl)pyridine - Himpy

The ligand was synthesized using the procedure described by Voss *et al.*¹⁷

A 100 mL round-bottom flask was filled with 2.60 g (25 mmol) of 2-pyridine-carbonitrile, 10 mL MeOH and 0.47 mL (2.5 mmol) of a 30% solution of NaOMe in MeOH. The mixture was stirred for 1 hour at 40 °C. 2.72 mL (25 mmol) of 2,2-dimethoxyethanamine followed by 2.75 mL of AcOH were added dropwise to the mixture and heated to reflux for 30 min. After the mixture was left to cool at rt, 30 mL of MeOH and 25 mL of HCl 6 mol L⁻¹ were added and the reaction was heated to reflux for 4.5 hours.

After, the solution was evaporated to dryness and a freshly prepared warm solution of a 1 g mL⁻¹ of K₂CO₃ was added dropwise, bringing the pH to 10. This resulted in a reddish suspension that, after cooled at rt, was filtered and the filtrate was extracted with 50 mL of CH₂Cl₂. The resulting red solution was evaporated to dryness and recrystallized in boiling EtOAc. The product was obtained as a reddish powder with a 52% yield. Anal. calc. for [(C₈H₇N₃)₄ · (H₂O)]: C 64.20; H 5.05; N 28.08; found: C 64.69; H 4.70 e N 28.16. ESI-MS (MeOH) m/z: 145.9 [H₂impy]⁺, 118.8 [(H₂impy)–(CN)]⁺ and 91.6 [(H₂impy)–2(CN)]⁺. ¹H NMR (600 MHz, DMSO-d₆) δ 8.58 (ddd, 1H, J= 4.8, 1.8, 1.2 Hz), 8.03 (dt, 1H, J= 7.5, 1.2), 7.87 (td, 1H, J= 7.5, 1.8), 7.34 (ddd, 1H, J= 7.5, 4.8, 1.2) and 7.15 (s, 1H). ¹³C NMR (125.7 MHz, DMSO-d₆) δ (ppm) 149.49, 149.40, 146.23, 137.72, 124.56, 123.52 and 119.97.

1.4.3 Synthesis of 2-(1H-imidazol-2-yl)pyrimidine - Himpm

The ligand was synthesized using the procedure described by Voss *et al.*¹⁷

To a 100 mL flask were added 2.62 g (25 mmol) of 2-pyrimidinecarbonitrile, 10 mL of MeOH and 0.47 mL of a 30% solution of NaOMe in MeOH. The mixture was kept under vigorous stirring at room temperature for 1.5 hour. Then, 1.63 mL (15 mmol) of aminoacetaldehyde dimethyl acetal were added, followed by dropwise addition of 2.75 mL of AcOH. The system was heated to reflux for 30 minutes. After cooling, 15 mL of MeOH and 12.5 mL of HCl 6 mol L⁻¹ were added and the system was again heated to reflux for 5 hours.

After the reaction time, the solvent was rotary evaporated and 27.5 mL of a warm K₂CO₃ 1 g mL⁻¹ solution were carefully added, forming a yellowish suspension which after cooling, was filtrated in a Buchner funnel. The precipitate was extracted with 3 × 50 mL of MeOH, forming a yellowish solution, which was rotary evaporated, and the precipitate was filtrated, washed with Et₂O and dried under vacuum. The product showed a pale yellow color, with yield of 68%. Elemental analysis calculated for (C₇H₆N₄): C 57.33; H 4.14; N 38.34; found: C 57.17, H 4.14 and N 38.86. ESI-MS (MeOH): 147.0 [H₂impm]⁺, 120.0 [(H₂impz)–(CN)]⁺ and 92.9 [(H₂impz)–2(CN)]⁺. ¹H NMR (600 MHz, DMSO-d₆) δ (ppm) 13.09 (s, 1H), 8.88 (d, 2H, *J* = 4.8), 7.44 (t, 1H, *J* = 4.8) and 7.26 (s, 2H). ¹³C NMR (125.7 MHz, DMSO-d₆) δ (ppm) 158.12, 157.35, 144.80, 130.68 and 120.45.

1.4.4 Synthesis of 2-(1H-imidazol-2-yl)pyrazine - Himpz

The ligand was synthesized using the procedure described by Voss *et al.*¹⁷

A 50 mL round-bottom flask was filled with 0.471 mL (5 mmol) of 2-pyrazine-carbonitrile, 5 mL MeOH and 0.47 mL (1 mmol) of a 30% solution of NaOMe in MeOH. The mixture was stirred for 20 minutes at rt.

0.727 mL (5 mmol) of 2,2-diethoxyethanamine followed by 0.6 mL of AcOH were added dropwise to the mixture and stirred for 1 hour at 50°C. After the mixture was left to cool at rt, 10 mL of MeOH and 2.5 mL of HCl 6 mol L⁻¹ were added and the resulting mixture was heated to reflux for 5 hours.

The solution was evaporated to dryness, resolubilised in 15 mL of water and extracted with 3 × 5 mL of Et₂O, resulting in a deep brown solution. The pH was adjusted to 8-9 with a NaOH 2 mol L⁻¹ solution then the volume was reduced to favor the product precipitation. The brown product was filtered and washed with Et₂O. The product was obtained as a brown powder with a 38% yield. Anal. calc. for (C₇H₆N₄)₃ · (NaCl): C 50.76; H 3.65; N 33.83; found: C 51.92; H 3.86 and N 33.95. ESI-MS (MeOH): 146.9 [H₂impz]⁺ and 119.8 [(H₂impz)–(CN)]⁺. ¹H NMR (500 MHz, DMSO-d₆) δ (ppm) 13.06 (s, 1H), 9.25 (d, 1H, *J* = 1.5), 8.66 (dd, 1H, *J* = 2.5, 1.5), 8.60 (d, 1H, *J* = 2.5), 7.35 (s, 1H) and 7.17 (s, 1H). ¹³C NMR (125.7 MHz, DMSO-d₆) δ (ppm) 144.90, 144.24, 143.92, 143.71, 141.80, 130.72 and 120.32.

1.4.5 Determination of pK_{aH}

The pK_{aH} values of ligands were measured spectrophotometrically according to Toma and Malin²⁶ using the expression

$$pH = pK_{aH} + \log \frac{[A]}{[HA]} \quad (1.1)$$

where $[A]$ and $[HA]$ are the molar concentration of base and protonated species respectively calculated using Beer's Law at the wavelengths indicated in Table 1.10. The initial acidic solution was titrated with NaOH 2 or 0.05 mol L⁻¹ depending on the proximity of the equivalence point. The pH value was determined using a calibrated pHmeter.

Table 1.10: Experimental conditions for pK_{aH} determination.

A	initial conc. ($\mu\text{mol L}^{-1}$)	initial pH	λ HA (nm)	λ A (nm)
Himpm	47	1.01	269	284
Himpy	50	0.99	283	293
Himpz	58	2.80	292	318

Chapter 2

mer-[Ru(Himpy)₃](PF₆)₂

2.1 Introduction

Chelating N-heterocycles ligands play an important role in coordination chemistry due to the diversity of properties that arise from the interaction between them and the metal center.^{2,27–30} Symmetric N-heterocycles chelating ligand, as bipyridines (bpy),³¹ phenanthroline (phen),^{32,33} and terpyridines (terpy),^{34,35} are well described in literature due their well-know and facile synthesis. Their metal complexes are also well-explored^{36,37} and applied in a broad range of areas, such as photocatalysis,^{38–40} supramolecular chemistry,^{35,41,42} bioinorganic^{43–45} and sensing.^{46–48}

The ruthenium complexes with bipyridines and terpyridines derivatives have an important role in coordination chemistry, mainly because of their well known electrochemical, spectroscopic and photoreactivity properties.^{35,49–51} The studies of Meyer et al regarding water oxidation and photochemistry with these complexes were important for a better understanding of the phenomena behind the observed properties.^{52–56} Nowadays, ruthenium compounds with other N-heterocyclic ligands are in full development, attempting to improve previously observed properties or un-

ravel new properties.^{57–61} However, complexes with those classical ligands still provide new questions and new answers despite their simplicity and well-studied behaviour.^{45,62–65}

The spectroscopic properties of ruthenium(II) complexes with N-heterocyclic ligands, mainly those associated to the metal-to-ligand charge transfer transition (MLCT), are deeply related to the chemical reactivity.^{54,66–69} Typically, N-heterocycles with low-lying π^* -orbitals can receive electron density from ruthenium, via photoexcitation (¹MLCT), leading to a transient charge-separation with the reduced-radical ligand and the oxidized metal ion. This excited state can relax via internal conversion and decay through an intersystem crossing, resulting in highly reactive long-lived triplet and responsible for the photoreactivity of those complexes.^{50,70–72}

Knowing the importance of the MLCT transition to the reactivity of the ruthenium complexes, we have decided to synthesize²⁸ the ruthenium(II) complex with 2-(1H-imidazol-2-yl)pyridine due to the non-symmetric donor-character. In the pyridyl moiety we expected a electron-deficient behaviour that favors the MLCT transition, whereas the imidazole moiety it is expected a high basicity that increases the electron density in the metal.^{73–76} Additionally, we expected to study the MLCT transition in this complex using experimental and theoretical methods to better understand the influence of the donation character of the ligand in the electronic structure.

2.2 Results and discussion

2.2.1 Structural characterization

The ligand Himpy was synthesized using the one-pot method described by Voss *et al* and the 1H and ^{13}C NMR spectra were consistent with the literature data.¹⁷ The Ru(II) complex was synthesized as described by Stupka *et al.*²⁸ The 1H NMR, in DMSO- d_6 , showed the presence of the free ligand, further confirmed by elemental analysis, suggesting that the purification proposed in the literature was not enough to purify the complex from the ligand excess used in the reaction. Consequently, a additional purification of the complex was carried out by washing the sample with $CHCl_3$, in order to dissolve ligand impurity. The residual powder was dissolved in CH_3CN , to remove any inorganic impurity (NH_4Cl mainly), filtered and evaporated to dryness.

After the purification, the UV-Vis spectra of complex and the ligand in MeOH were obtained as shown in Figure 2.1. The blue shift of the $\pi \rightarrow \pi^*$ bands of the ligand has been observed and a broad band in 440 nm, that is typically assigned to a MLCT transition. Both were in agreement with Stupka *et al.*²⁸

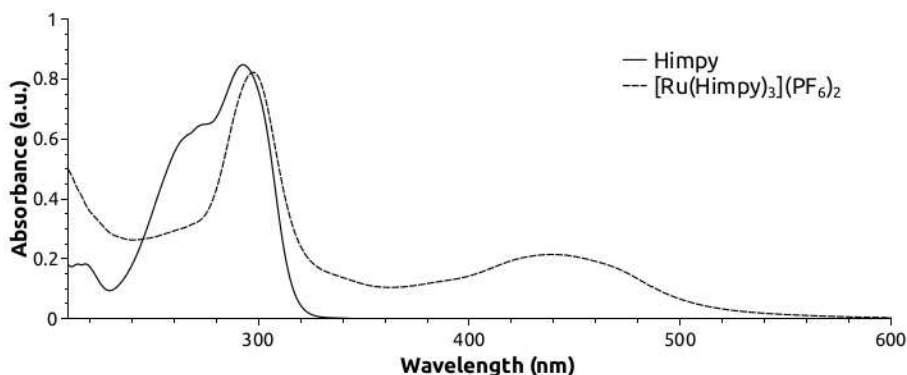


Figure 2.1: UV-Vis spectra of the $[Ru(Himpy)_3](PF_6)_2$ and of the ligand Himpy in MeOH.

Another ¹H NMR spectrum in DMSO-*d*₆ of the purified sample was taken and proved its purity, however after one day the spectrum was acquired again (Figure 2.2) and showed the signals of the free ligand in 8.60 and 7.37 ppm. Leading to the hypothesis of the ligand displacement by DMSO given that it is a coordinating solvent. In order to avoid the ligand exchange by the solvent, the ¹H NMR was reacquired in CH₃CN-*d*₃. Acetonitrile was chosen due the solubility of the complex and the low basicity solvent.

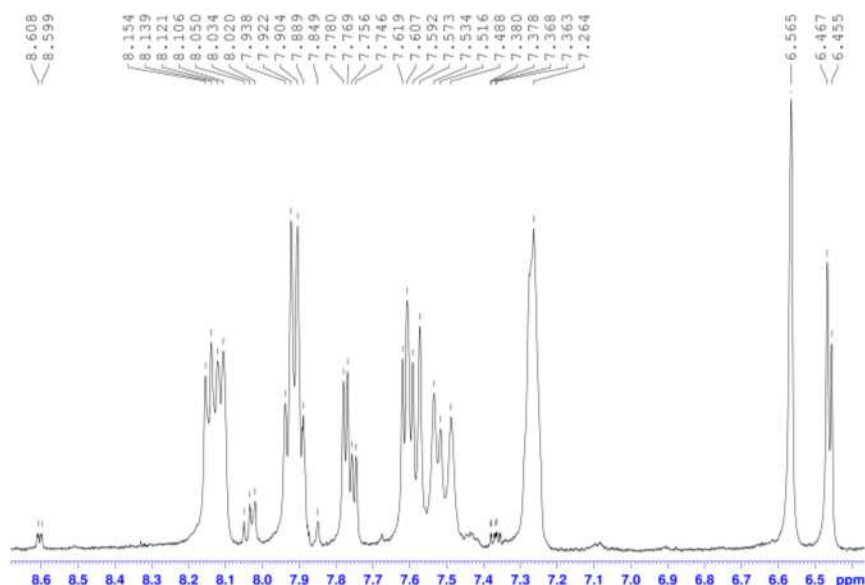


Figure 2.2: ¹H NMR spectrum of the complex [Ru(Himpy)₃](PF₆)₂ in DMSO-*d*₆ obtained in the 500 MHz spectrometer.

The ¹H NMR spectrum of the complex in CH₃CN-*d*₃ showed different signals pattern from the one described in literature.²⁸ This change in the pattern was associated to the proportion between the *meridional* (C₁ symmetry) and the *facial* (C₃) isomers, and in our spectrum it was only possible to see the signals associated only with the *mer* isomer. Suggesting that the discussion of isomers proportion made by

Stupka *et al* was misconceived due to the ligand equilibrium in dimethylsulfoxide, that is prevented in acetonitrile.

The imidazole signals were the probe that enabled the differentiation between the isomers. This is due to the symmetry of the complex that causes the emergence of only one signal, for the two hydrogens bonded to the carbons in the imidazol-2-yl moiety, in the *fac* isomer and three signals in the *mer* isomer. The signals coming from the 2-pyridyl moiety does not showed much sensibility to the symmetry of the complex, leading to a very complex signal that does not allow the isomer differentiation.

A ¹H-¹H NMR Correlation Spectroscopy (COSY) experiment have presented the correlation between the signals of the hydrogens in the 2-pyridyl moiety and between the hydrogens in the imidazol-2-yl moiety. This enabled the separation of the signals in two groups, one for each moiety. For the 2-pyridyl we find the signals in 7.24 (H2, see structure in Figure 2.5), 7.77 (H4), 7.93 (H1) and 8.02 (H3) ppm and for the imidazol-2-yl the signals in 6.60 (H7) and 7.40 (H6) ppm. The spectrum is shown in Figure 2.3.

For the imidazol-2-yl group it was expected a doublet signal for each hydrogen (H6 and H7) in the complex. That in the *mer* isomer, due the C₁ symmetry, leads to three doublet signals, one for each imidazole hydrogen bonded to carbon. This is observed in the signals centered in 6.60 ppm but for the signals centered in 7.40 ppm we have only observed one doublet signal (7.38 ppm) and one triplet-like signal (7.41 ppm).

In the *mer* isomer there is one imidazole *trans* to a pyridine and two imidazole *trans* to an imidazole. We have expected that two of the imidazole signals were

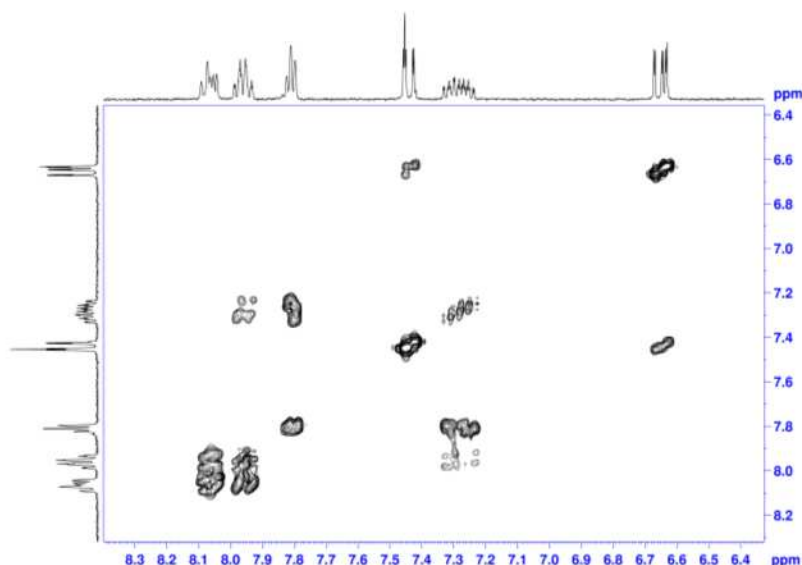


Figure 2.3: ^1H - ^1H NMR COSY spectrum of the complex $[\text{Ru}(\text{Himpy})_3](\text{PF}_6)_2$ in $\text{CH}_3\text{CN}-d_3$ obtained in the 400 MHz spectrometer.

closely related, indicating that the triplet-like signal could actually be two coalesced doublet signals coming from the imidazoles trans located to another imidazole.

In order to prove the aforementioned hypothesis the double irradiation ^1H NMR experiment was made and is shown in the Figure [2.4](#). When the signals centered in 6.60 ppm were saturated it was possible to observe the simplification of the signals in 7.40 ppm to three singlets, therefore, validating the hypothesis and enabling the assignment of the signals. The double irradiation also confirmed the assignment of 2-pyridyl signals and showed that the electronic communication between the hydrogens in the ligand remain strong as have been seen for the free ligand.

As a further evidence of the real nature of the triplet-like signal, centered in 7.41 ppm, a simple ^3J constant calculation was performed. Knowing that the value of the ^3J must be equal between the signals of the imidazol-2-yl hydrogens (H6 and H7)

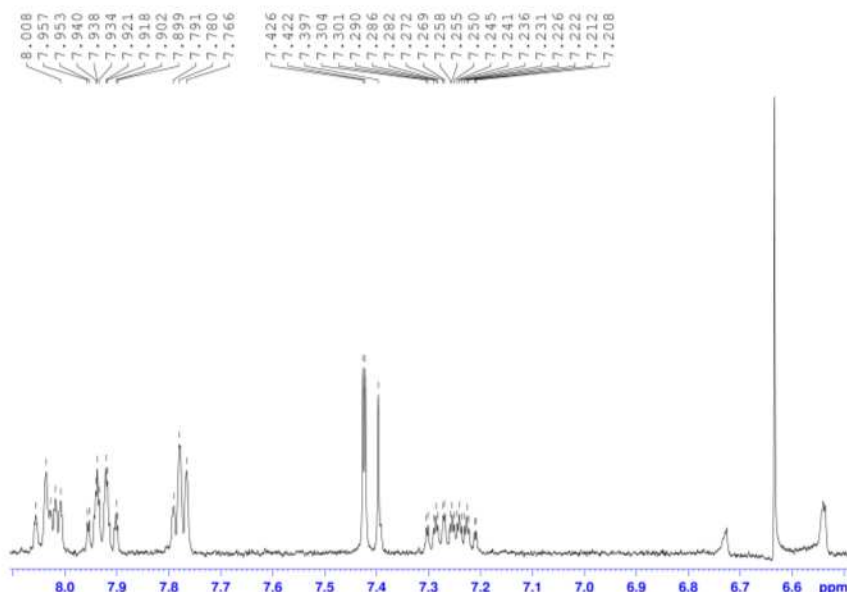


Figure 2.4: ^1H NMR spectrum of the complex $[\text{Ru}(\text{Himpy})_3](\text{PF}_6)_2$ in $\text{CH}_3\text{CN}-d_3$ with double irradiation at 6.66 ppm obtained in the 400 MHz spectrometer.

($^3J = 1.48$ Hz) and considering an impossible accuracy, we have calculated that if the peak in 7.4190 ppm were a doublet than the correlated peak should be in 7.4153 ppm and if the peak was at 7.4146 than the correlated peak should be at 7.4109 ppm. According to this the difference between the internal signals should be 0.0007 ppm. Considering the technique accuracy, this separation is not observable and leading to the coalescence of the internal peaks, resulting in a triplet-like signal.

Consequently by proving that the *mer* isomer in $\text{CH}_3\text{CN}-d_3$, more refined assignment was made using the fact that in this isomer we have two imidazol-2-yl groups chemically closely related (A and A'), due the trans position, and another more distinct (B). Then in the signals of the hydrogens H6 and H7, we have observed that there are two doublet with similar chemical shift (in this case so close that leads to a triplet-like signal) which we assigned as the A and A' imidazoles and the more

isolated doublet we assigned as the B imidazole.

Using all these information the ¹H NMR spectrum of the *mer*-[Ru(Himpy)₃](PF₆)₂ complex in CH₃CN-d₃ was assigned as shown in the Figure 2.5.

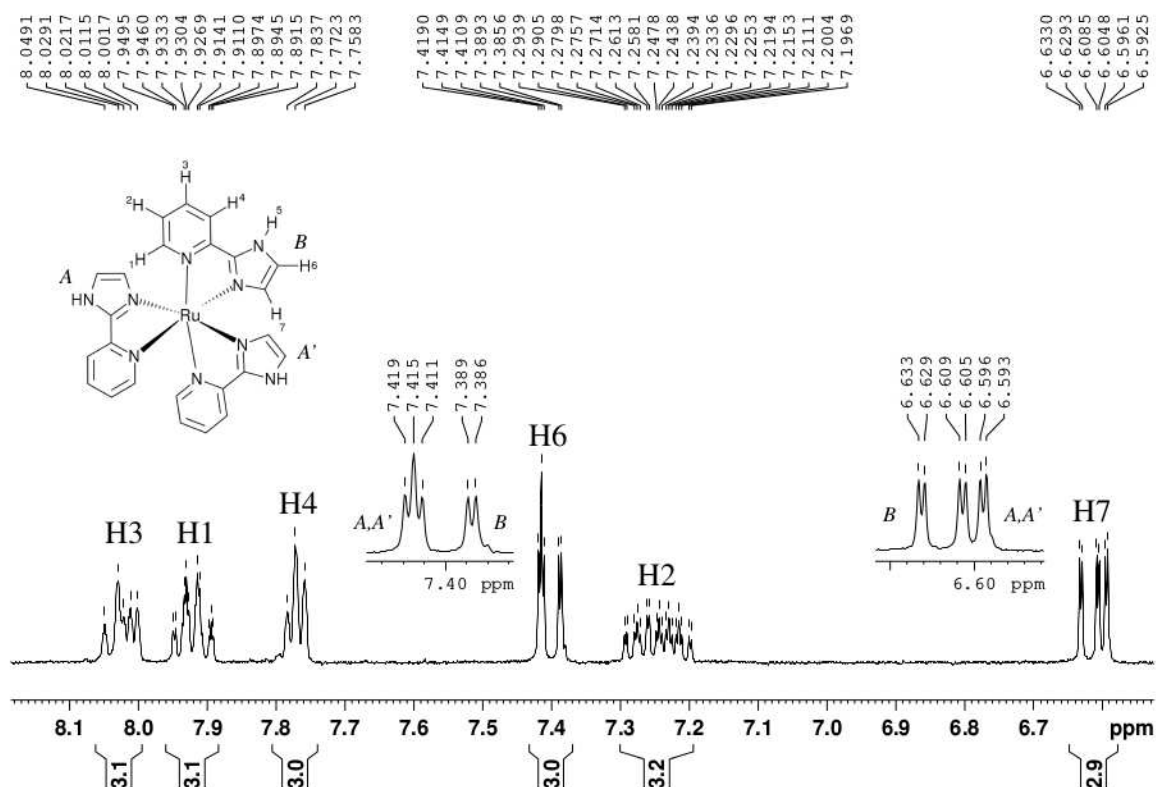


Figure 2.5: Assigned ¹H NMR spectrum of the complex *mer*-[Ru(Himpy)₃](PF₆)₂ in CH₃CN-d₃ obtained in the 400 MHz spectrometer.

Due to the low solubility of the complex in acetonitrile and other non-coordinating solvents, the ¹³C NMR spectrum was not possible to obtain in the saturated solution used in the experiment. The high resolution ESI-MS was performed and showed that the double charged molecular ion in *m/z* = 268.5, with the correct isotopic pattern and also showed fragments derived from the deprotonation of the ligand in the complex in *m/z* = 536.1, that has been extensively studied by Stupka *et al.*,²⁸ and from the exit

of one ligand in $m/z = 391.0$, as has been observed in the presence of a coordinating solvent. The spectrum is shown in Figure 2.6.

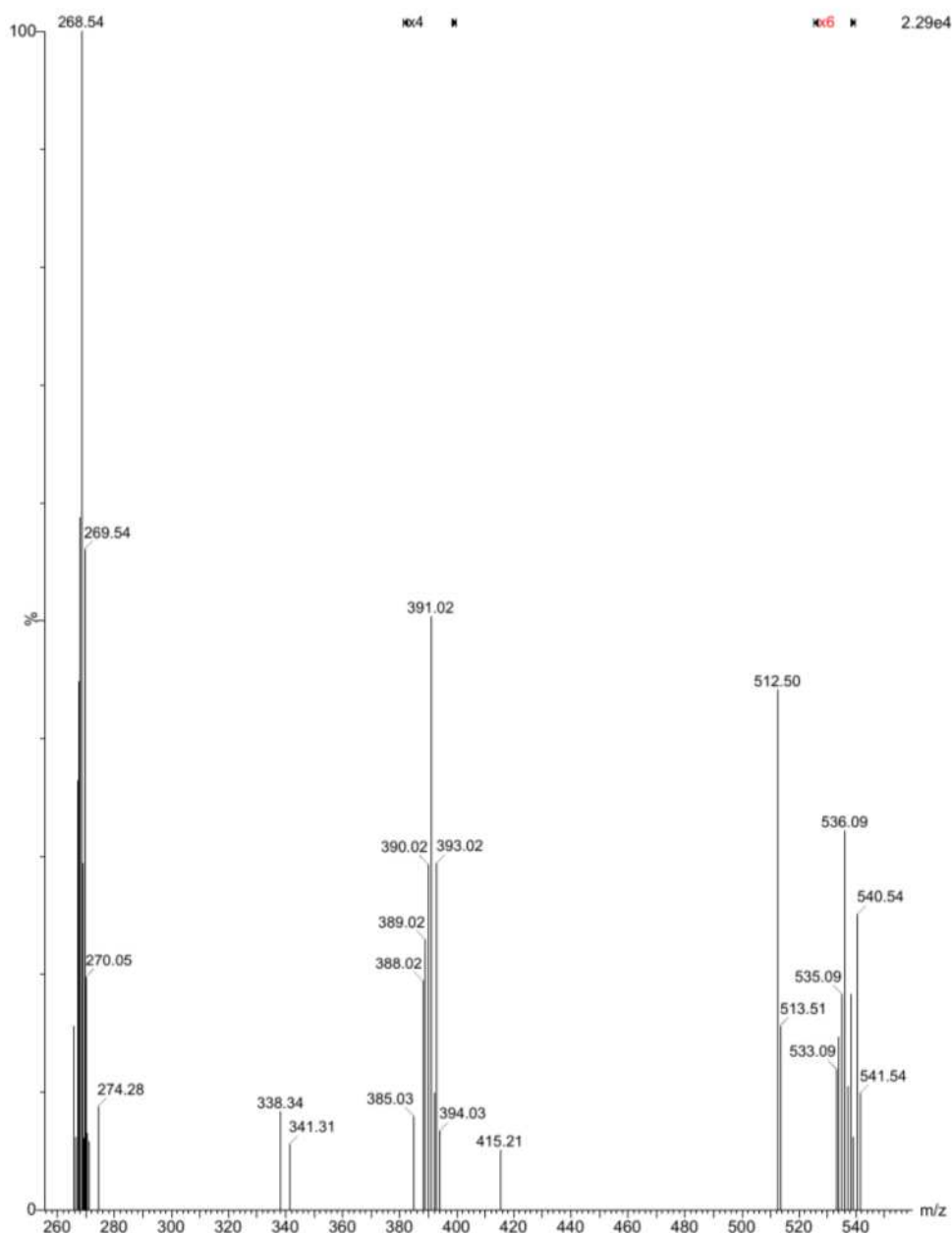


Figure 2.6: ESI-QTOF-MS of the $[Ru(HimpY)_3](PF_6)_2$ in a $H_2O/MeOH$ solution, the peak at 512.50 is an internal contamination of the equipment.

Knowing that we have the *mer*-isomer as major product, a spectroscopic study of the complex was proposed in order to better understand the nature of the bands observed in the UV-Vis absorption spectrum. The spectra of the complex were acquired in different solvents and as shown in Figure [2.7](#), it is possible to see the shift

of both bands with the solvent. For the intraligand band, the shift is more explicit due the maintenance of the band shape, this data was consistent with that observed for the [Ru(bpy)₃]²⁺.⁷⁷

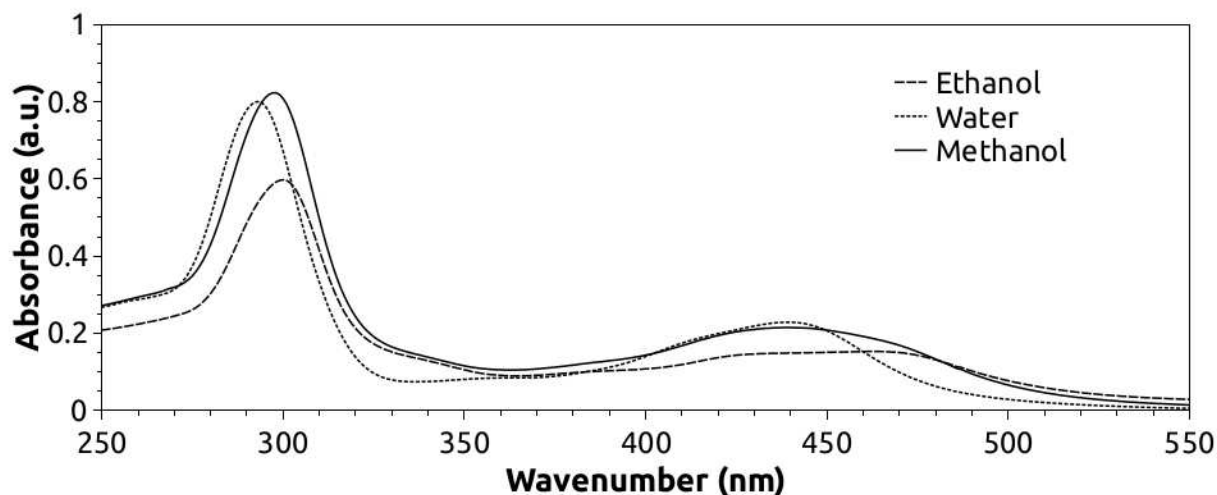


Figure 2.7: UV-Vis spectra of the *mer*-[Ru(Himpy)₃](PF₆)₂ in different solvents.

The observed shift for the intraligand band have a linear relation with the Gutmann acceptor number (AN),^{78–80} showing a negative solvatochromism, that is attributed to the different solvation interaction with the solute, mainly due to hydrogen-bond between the amine moiety of the imidazole and the protic solvents.^{81–83}

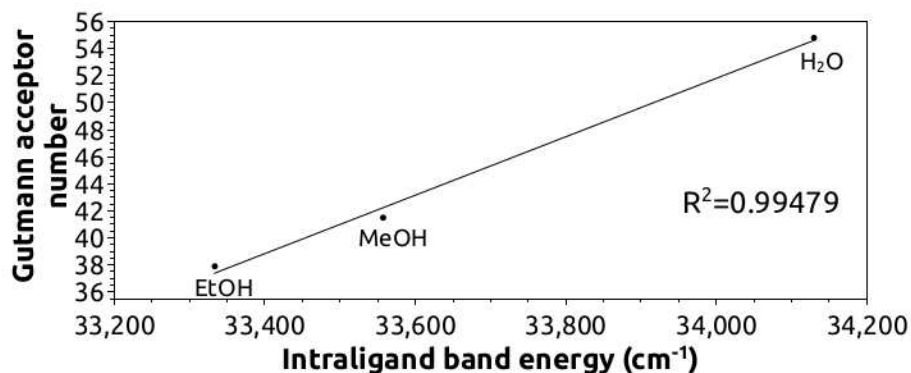


Figure 2.8: Linear relation between the intraligand band energy and the Gutmann AN for MeOH, EtOH and H₂O.

For the MLCT band, the result is similar as observed for the [Ru(bpy)₃]²⁺,⁸⁴ but

due to the lower symmetry the MLCT band is more complex and a carefully theoretical analysis of the absorption spectrum using multiconfigurational *ab initio* calculation will be performed.

2.3 Conclusion

The synthesis of the ligand Himpy and its ruthenium(II) complex were accomplished, according to the literature.^{17,28} However, for the complex further purification was needed to remove the ligand excess, observed via ¹H NMR and elemental analysis. The nuclear magnetic resonance showed that the complex decomposes in dimethyl sulfoxide and there was a need to change the solvent. Using acetonitrile as the ¹H NMR solvent, a complete assignment of the spectrum was made and showing that, in solution, the *mer*- isomer is the major product. Knowing this, a experimental spectroscopic study were made showing the solvatochromic behaviour of the complex.

2.4 Experimental

2.4.1 Materials and methods

Materials

2-Pyridinecarbonitrile (99%), 2,2-dimethoxyethylamine (99%), ammonium hexafluorophosphate ($\geq 95\%$) and ruthenium(III) chloride hydrate *ReagentPlus* were purchased from Sigma Aldrich. Methanol, acetic acid, hydrochloric acid, diethyl ether (Et₂O), ethyl acetate, dichloromethane, chloroform, acetonitrile and sodium

carbonate (99.5%) were purchased from Vetec-Sigma (Brazil). Sodium lumps were purchased from Riedel-de Haën. All reagents were used as received from commercial source, with no further purification, except when noted.

Physical Measurements

Electronic spectra in the 190-1100 nm range were acquired by using a 1.00 cm quartz cuvette in a diode array HP8453 UV/Visible absorption spectrophotometer equipped with a HP89090A Peltier.

Electrospray ionization mass spectrometry (ESI-MS) measurements were carried out using a Waters Quattro Micro API. Samples were evaluated in the positive mode in an 1:1 methanol:water solution with addition of 0.10% (v/v) formic acid.

Electrospray ionization quadrupole time-of-flight mass spectrometry (ESI-QTOF-MS) measurements were carried out in a Waters Synapt HDMS instrument (Manchester, UK). A sample of [Ru(Himpy)₃](PF₆)₂ was solubilized in 50 : 50 H₂O/MeCN (0.1% formic acid v/v) at a concentration of ca. 4 mg mL⁻¹, then further diluted 100-fold in the same solvent mixture and immediately analyzed. Resulting solutions were directly infused into the instruments ESI source at a flow rate of 15 mL min⁻¹. Typical acquisition conditions were capillary voltage: 3 kV, sampling cone voltage: 20 V, source temperature: 100 °C, desolvation temperature: 200 °C, cone gas flow: 30 L h⁻¹, desolvation gas flow: 900 L h⁻¹, trap and transfer collision energies: 6 and 4 eV, respectively. ESI mass spectra (full scans) and fragment ion spectra for quadrupole-isolated ions (QTOF-MS/MS) were acquired in reflectron V-mode at a scan rate of 1 Hz. For fragment ion spectrum experiments by collision-induced dissociation (argon as collision gas), the desired ion was isolated in the mass-resolving

quadrupole, and the collision energy of the trap cell was increased until sufficient fragmentation was observed. Prior to all analyses, the instrument was externally calibrated with phosphoric acid oligomers (H₃PO₄ 0.05% v/v in 50:50 H₂O/MeCN) ranging from *m/z* 99 to 980.

Elemental analyses for carbon, hydrogen and nitrogen were performed using a Perkin Elmer 2400 CHN analyzer.

¹H and ¹³C NMR spectra were acquired in deuterated acetonitrile (CD₃CN) and dimethyl sulfoxide (DMSO) solutions and using a Bruker Avance III - 400MHz (9.39T) and 500MHz (11.7T) spectrometers.

2.4.2 Synthesis of 2-(1H-imidazol-2-yl)pyridine - Himpy

The ligand was synthesized using the procedure described by Voss *et al.*¹⁷

A 100 mL round-bottom flask was filled with 2.60 g (25 mmol) of 2-pyridine-carbonitrile, 10 mL MeOH and 0.47 mL (2.5 mmol) of a 30% solution of NaOMe in MeOH. The mixture was stirred for 1 hour at 40 °C.

2.72 mL (25 mmol) of 2,2-dimethoxyethanamine followed by 2.75 mL of AcOH were added dropwise to the mixture and the reaction mixture was heated to reflux for 30 min. After the mixture cooled at the rt, 30 mL of MeOH and 25 mL of HCl 6 mol L⁻¹ were added and the reaction was heated to reflux for 4.5 hours.

After, the solution was evaporated to dryness and a freshly prepared warm solution of a 1 g.mL⁻¹ of K₂CO₃ was added dropwise, increasing pH to 10. This results in a reddish suspension that, after cooled at the rt, was filtered and the filtrate was extracted with 50 mL of CH₂Cl₂. The resulting red solution was evaporated to dryness and recrystallized in boiling EtOAc. The product was obtained as a reddish powder

with a 52% yield. Anal. calc. for [(C₈H₇N₃)₄ · (H₂O)]: C 64.20; H 5.05; N 28.08; found: C 64.69; H 4.70 e N 28.16. ESI-MS (MeOH) *m/z*: 145.9 [H₂impy]⁺, 118.8 [(H₂impy)–(CN)]⁺ and 91.6 [(H₂impy)–2(CN)]⁺. ¹H NMR (600 MHz, DMSO-*d*₆) δ 8.58 (ddd, 1H, *J*= 4.8, 1.8, 1.2 Hz), 8.03 (dt, 1H, *J*= 7.5, 1.2), 7.87 (td, 1H, *J*= 7.5, 1.8), 7.34 (ddd, 1H, *J*= 7.5, 4.8, 1.2) and 7.15 (s, 1H). ¹³C NMR (125.7 MHz, DMSO-*d*₆) δ (ppm) 149.49, 149.40, 146.23, 137.72, 124.56, 123.52 and 119.97.

2.4.3 Synthesis of [Ru(Himpy)₃](PF₆)₂

The complex was synthesized using the procedure described by Stupka *et al.*²⁸

0.3531 g (2.42 mmol) of Himpy and 0.1443 g (0.69 mmol) of RuCl₃ · (H₂O)_x were added to a round-bottom flask containing 30 mL of ethylene glycol and the mixture was heated to reflux for 1 hour.

After the solution was cooled to rt, 30 mL of a saturated solution of NH₄PF₆ was added dropwise, under stirring, resulting in an orange suspension, which was left overnight in the refrigerator. It was filtered, washed with 4 × 10 mL of H₂O and 4 × 10 mL Et₂O and dried under reduced pressure.

Further purification was performed by washing the powder with 8 × 10mL of CHCl₃. Additionally, the powder was dissolved in CH₃CN and the solution was filtered and evaporated to dryness. The purified powder was dried under reduced pressure until constant mass.

The product was obtained as an orange powder with a 35% yield. ESI-MS (ACN) *m/z*: 268.5 [Ru(Himpy)₃]²⁺, 536.1 [Ru(Himpy)₂(impy)]⁺ and 391.0 [Ru(Himpy)-(impy)]⁺ λ_{max} nm (L mol⁻¹ cm⁻¹) in MeOH: 296 (36929), 446 (15524), Anal. calc. for [Ru(C₈H₇N₃)₃](PF₆)₂ · 2 (CH₃CN): C 37.01; H 3.00; N 16.96; found: C 37.83; H

2.97 e N 16.27 ¹H NMR (600 MHz, DMSO-d₆) δ 8.02 (m, 3H), 7.93 (m, 3H), 7.77 (m, 3H), 7.40 (3 d, 3H, J = 1.6 Hz), 7.24 (m, 3H) and 6.60 (3 d, 3H, J = 1.6 Hz).

Chapter 3

$\text{Na}_3[\text{Fe}(\text{CN})_5(\text{Himpz})]$

3.1 Introduction

Coordination chemistry is an important tool in synthetic supramolecular chemistry due to the high yields and controlled geometries of the products and the possibility to include interesting properties associated to the metal centers.^{85–87} The development of ligands, especially with simple synthetic procedures, is of fundamental importance in the planning of new functional supramolecular systems.^{86,88} Click chemistry or one-pot synthesis of N-heterocycles are feasible and available strategies for high-yield synthesis of supramolecular ligands such as imidazoles, triazoles and tetrazoles whose interest stem from polydentacity, (de)protonation ability and easy derivatization after synthesis.^{17,89–91}

Pentacyanidoferrate complexes were extensively studied due to their electrochemical and spectroscopic properties.^{26,92–95} This class of compounds has the ability to coordinate to only a monodentate site of a ligand, making it an attractive complex to take place as an electrochemical or spectroscopic active center in a the supramolecular system.^{30,96–98} Moreover, its high affinity to N-heterocycles makes it an useful

probe to evaluate the properties of this kind of ligand, such as donor and acceptor abilities.^{26,92,99,100}

Redox potential and the energy of the metal-to-ligand charge transfer (MLCT) band in the visible region were shown to be a function of the pK_a and back-bonding ability of such ligands, thus evidencing the effects of electron donation or withdrawing of substituents of pyridine and pyrazine derivatives.^{26,101}

The reversible Fe(II)/Fe(III) redox process of cyanidoferrates allowed the development of many electrochemical sensors for biologically-relevant molecules such as cysteine.¹⁰² The N-heterocycle in this case was specifically planned to integrate a supramolecular assembly with carbon nanotubes. Upon dissociation of the N-heterocycle, pentacyanidoferrate can also be used as a precursor in the formation of Prussian blue-like structures that acts as active layer in electrocatalytical oxidation of ascorbic acid.¹⁰⁰ The current rationalization of the role of the N-heterocycle in the redox process consists in its ability to stabilize Fe(II) via back-donation. Ligand such as N-methylpyrazinium leads to lower oxidation potential than pyrazine owing the strong π back-bonding of the former.²⁶ A diazine used as bridging ligand in a ruthenium mixed-valence compound was shown to be a cation radical when oxidized.¹⁰³ The non-innocent character of diazines and derivatives in redox process of transition metals compounds is a field worth an investigation and which can take advantage of the well-known electrochemical properties of pentacyanidoferrate.

The energy of the MLCT band depends on the surrounding chemical environment, giving rise to solvatochromic behaviour characterized by preferential solvation by lower alcohols rather than water.^{104,105} We have showed that the preferential solvation can be shifted using a polymeric ligand such as poly(4-vinylpyridine), owing

intermolecular interactions of the solvated coil embedding pendant pentacyanido-ferrate moieties.³⁰ Recently, highly solvatochromic viologen-like ligands showed interesting behaviour as dyes responsive to solvent polarity.¹⁰⁶ The importance of intermolecular interaction between $[\text{Fe}(\text{CN})_5]^{3-}$ group and solvent molecules was demonstrated by multiconfigurational quantum mechanical calculations. Five explicit hydrogen-bonded water molecules resulted in MLCT energy closer to experimental value in comparison to the model of continuum polarizable medium. The agreement is even higher when fourteen molecules are explicitly placed solvating the $[\text{Fe}(\text{CN})_5]^{3-}$ group.⁹⁹ The idea that followed was to investigate experimentally whether modifications on the structure of the N-heterocycle could result in changes of the solvation sphere of $[\text{Fe}(\text{CN})_5]^{3-}$ group thus changing solvatochromic properties.

In the present work we explore the ligand 2-(1-H-imidazol-2-yl)pyrazine (Himpz), which is particularly interesting to bridge transition metals and form supramolecular structures. In order to pave the ground for doing so, we first aimed at the evaluation one of the two binding sites, that are the monodentate site in the pyrazine ring and a bidentate site gathering the imine nitrogen of imidazole and the other nitrogen of the pyrazine ring. We used pentacyanidoferrate to favor the coordination of the monodentate site whereas H^+ was used in the second site as a model Lewis acid instead of a transition metal. The effect of pH on the redox potential and on the MLCT energy were investigated and compared to pyrazinepentacyanidoferrate(II). The redox-active character of the N-heterocycle as well as the spectroscopic response to pH are key features to design molecular devices and responsive materials.

3.2 Results and discussion

3.2.1 Synthesis and characterization

The ligand 2-(1-H-imidazol-2-yl)pyrazine (Himpz) was synthesized using the one-pot method described by Voss *et al* and the ^1H and ^{13}C NMR spectra were consistent with the literature data.¹⁷

The pentacyanidoferrate(II) complex was synthesized, in high yield, using a well-known methodology for N-heterocyclepentacyanidoferrate(II) reported in the literature.^{26,92,93} The product showed a high water affinity that results in a deliquescent character. This affinity is confirmed by the elemental analysis that showed a 6.5 water molecules per complex.

The UV-Vis absorption spectrum of complex in H_2O is shown in the Figure 3.1. The bands in 224, 270 and 316 were assigned to $\pi \rightarrow \pi^*$ intraligand transitions and the band in 481 nm assigned as a MLCT transition. This MLCT band is responsible for the intense reddish-orange color of the solution. The λ_{MLCT} and the molar absorptivity observed for the $\text{Na}_3[\text{Fe}(\text{CN})_5(\text{Himpz})]$ complex were coherent with the literature for the pyrazinepentacyanidoferrate(II) complex $\text{Na}_3[\text{Fe}(\text{CN})_5(\text{pz})]$.¹⁰⁷

The FT-IR showed strong signals assigned to the asymmetric stretch of the cyanides in 2055 cm^{-1} and in 2095 cm^{-1} , that are consistent with low-spin $\text{Fe}(\text{II})\text{-d}^6$ N-heterocyclepentacyanidoferrates.¹⁰⁸

Due to his diamagnetic behaviour, the ^1H NMR in D_2O was acquired and is shown in the Figure 3.2. The signals of the 2-pyrazine moiety hydrogens shifted while the signals of the imidazol-2-yl moiety did not change upon coordination. It suggests the coordination via the 2-pyrazine moiety while the imidazol-2-yl remains uncoor-

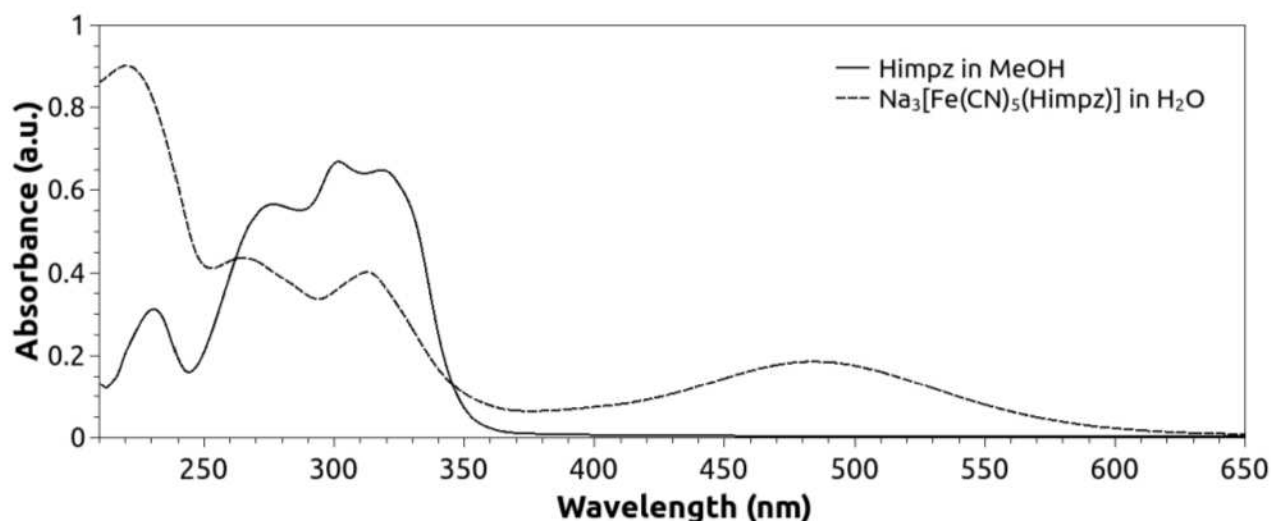


Figure 3.1: UV-Vis absorption spectra of the complex $\text{Na}_3[\text{Fe}(\text{CN})_5(\text{Himpz})]$ in water and of the ligand Himpz in MeOH.

dinated.

In the literature,¹⁷ it was observed that the imidazol-2-yl moiety is involved in a prototropic annular tautomerism, common to azolic systems,^{1,18,19} that leads to a chemical equivalence of the hydrogens H5 and H6. Due the protic solvent used (D_2O), the tautomeric equilibrium was observed in the ^1H NMR spectrum of the $\text{Na}_3[\text{Fe}(\text{CN})_5(\text{Himpz})]$ complex. It results in only one signal for both hydrogens (H5/H6), in 7.26 ppm, and also the disappearance of amine hydrogen due the deuterium exchange. This is coherent with the free imidazol-2-yl moiety in the complex, remaining available to participate in the prototropic annular tautomerism. Leading to the conclusion that the ligand coordinates by the 2-pyrazine ring. Nevertheless, this diazine have two coordination sites (N1 and N4) that can interact with the $[\text{Fe}(\text{CN})_5]^{3-}$ moiety. The ^1H NMR spectrum of the complex showed that the hydrogens H2 and H3 were deshielded while the hydrogen H1 was shielded that is consistent with the coordination by the nitrogen N4. The deshielding of the hydro-

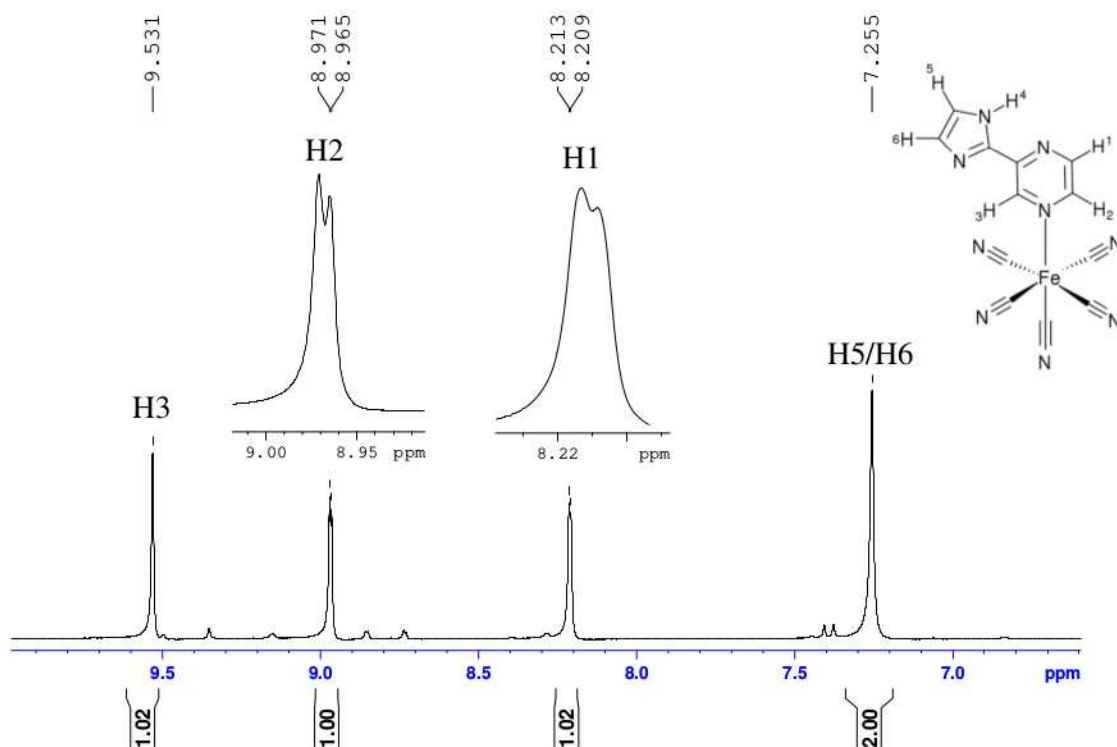


Figure 3.2: ^1H NMR of the $\text{Na}_3[\text{Fe}(\text{CN})_5(\text{Himpz})]$ complex in D_2O .

gens H2 and H3 is consequence of the acid character of the coordinated $\text{Fe}(\text{II})$ and the shielding of the H1 is due the π -acceptor character of the pyrazine ring.^{29,107}

The coupling pattern of the 2-pyrazine moiety also changes with the coordination. Once coordinated by the N4, the communication between the hydrogen H1 and H3 decreases, due to the decrease of the electronic density in the ring, leading to the decoupling of the signals. The assignment of signals obtained in the ^1H NMR spectrum of the complex is shown in the Table [3.1](#).

Table 3.1: Assignment of the signals of ^1H NMR spectrum of the complex $\text{Na}_3[\text{Fe}(\text{CN})_5(\text{Himpz})]$ in D_2O .

δ (ppm)	Signal type	J (Hz)	Integration	Hydrogen
7.26	s	-	2	H5/H6
8.21	d	3.0	1	H1
8.97	d	3.0	1	H2
9.53	s	-	1	H3

The ^{13}C NMR spectrum in D_2O was acquired and showed seven signals that were assigned using two-dimensional ^1H - ^{13}C experiments. Five signals were attributed to the Himpz and the other two to the axial and equatorial cyanides.

There were expected seven peaks for the ligand, but due the intense prototropic tautomerism these two signals assigned to C9 and C10 carbons are too broad and low intense. This is favored in a protic solvent like D_2O where the imidazol-2-yl moiety is involved in the hydrogen-deuterium exchange, leading to the disappearance of the those signals.

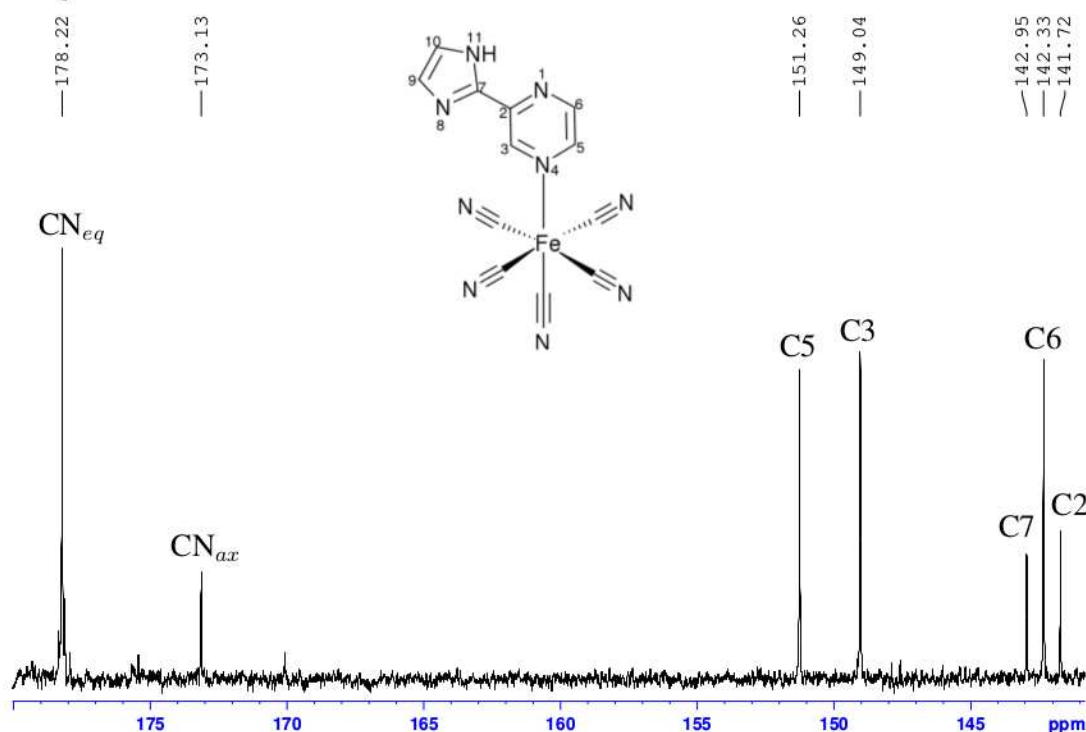


Figure 3.3: ^{13}C NMR of the $\text{Na}_3[\text{Fe}(\text{CN})_5(\text{Himpz})]$ complex in D_2O .

This results are in agreement that the coordination is via the 2-pyrazine moiety, did not prevent the imidazol-2-yl moiety of taking the part in the annular prototropic tautomerism equilibrium. The assigned ^{13}C NMR spectrum is shown in the Figure [3.3](#) and the assignment in the Table [3.2](#).

Table 3.2: Assignment of the signals of ^{13}C NMR spectrum of the complex $\text{Na}_3[\text{Fe}(\text{CN})_5(\text{Himpz})]$ in D_2O .

	C2	C6	C7	C3	C5	CN-axial	CN-equatorial
δ (ppm)	141.72	142.33	142.95	149.04	151.26	173.13	178.22

It was possible to see that in the complex the signals related to the carbons C3 and C5, neighbors of the coordinated nitrogen N4, were deshielded by the coordination with the Fe(II) and shifted in approximate +7 ppm. This is consistent with the coordination via the N4 of the 2-pyrazine moiety. On the other hand, the signal of the carbons C2 and C6 were shielded with the coordination and shifted between -2 to -3 ppm, in agreement with the hypothesis of π -acceptor character of the pyrazine ring.

The signal of the imidazol-2-yl carbon C7 do not change much with the coordination, only a slightly shielding (1.38 ppm) that is coherent with π -acceptance of the 2-pyrazine bonded to the imidazol-2-yl moiety. The cyanides signals were consistent with the literature data for N-heterocyclepentacyanidoferrate(II).^{109,110} Thus, the ^1H and ^{13}C NMR experiments confirmed the coordination of the ligand Himpz with the $[\text{Fe}(\text{CN})_5]^{3-}$ moiety via the nitrogen N4 and that the imidazol-2-yl is uncoordinated.

3.2.2 Electrochemical characterization

Cyclic voltammetry provides information about the character of the different ligands over the metal, which is reflected on the half wave potentials of the iron redox pair. Figure 3.4 shows the voltammogram of the pentacyanidoferrate (II) complexes containing the Himpz ligand.

The complex shows a quasi-reversible redox process at 0.64 V vs SHE ($\Delta E = 68$ mV) at 100 mV s^{-1} corresponding to the $[\text{Fe}(\text{CN})_5(\text{Himpz})]^{2-/3-}$ redox pair. This value is in agreement with other pentacyanidoferrate (II) complexes, where the redox

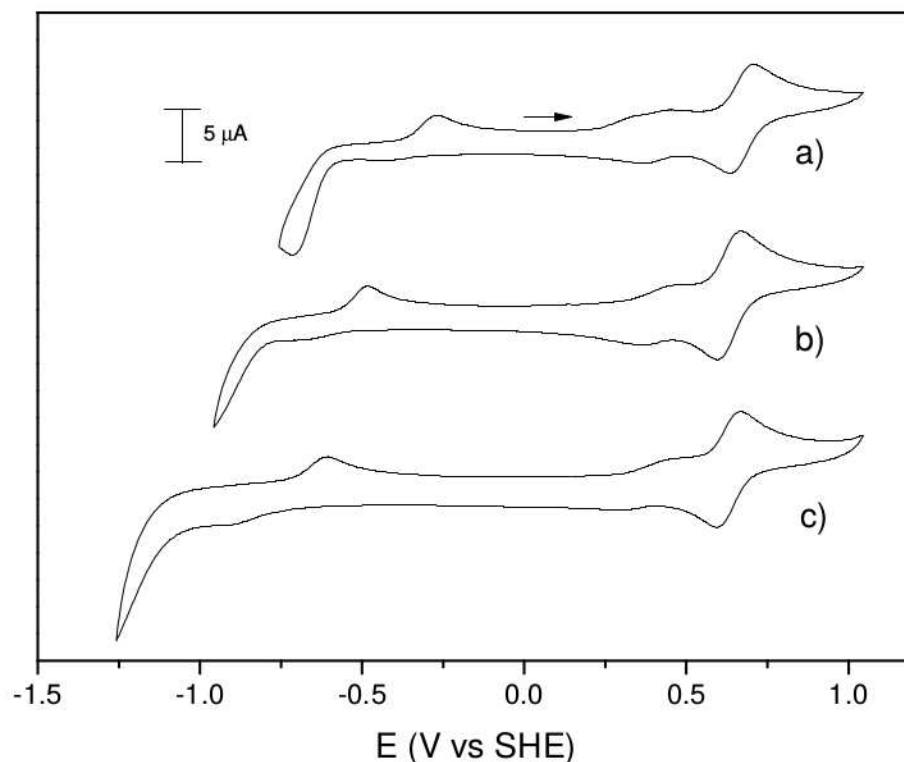


Figure 3.4: Cyclic voltammograms of $1.10^{-3} \text{ mol L}^{-1}$ aqueous solutions of pentacyanidoferrate(II) complexes containing the Himpz ligand in Britton-Robinson buffer solution in at a) pH 4.0, b) pH 7.0, c) pH 10.0 containing KCl 0.1 mol L^{-1} . Scan rate 100 mV s^{-1} .

potential is influenced by different ligands.

Higher values of half wave potentials are observed when the backbonding ability of the N-heterocycle increases. Thus, the results indicate that the Himpz ligand has a higher π -acceptor behavior than pyrazine over the pentacyanidoferrate(II) moiety.^{100, 111}

There is a shift of the half wave potentials from 0.67 V vs SHE at pH 4.0 to 0.63 V vs SHE at pH 7.0 and 10.0. From the cyclic voltammograms it is also possible to note a redox process with $E^{0'} = 0.424 \text{ V vs SHE}$, which we assigned to be ligand centered, even though further experiments need to be done in order to confirm these

hypothesis.

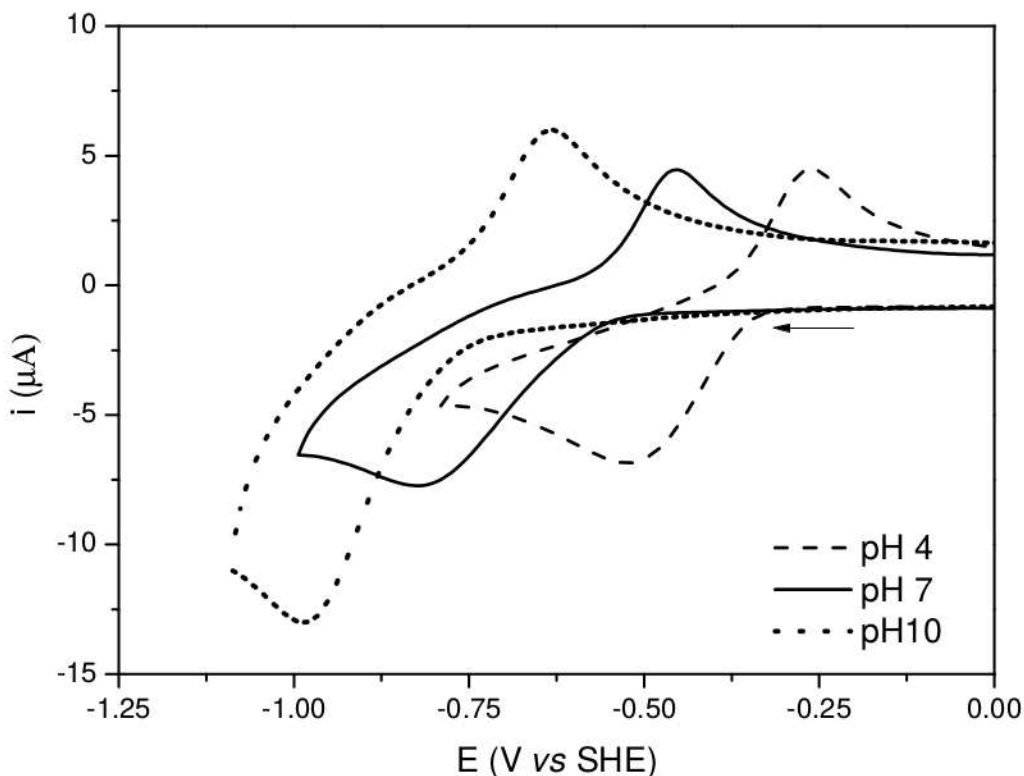


Figure 3.5: Cyclic voltammograms of $1.10^{-3} \text{ mol L}^{-1}$ aqueous solutions of himpz in Britton-Robinson buffer solutions containing $\text{KCl } 0.1 \text{ mol L}^{-1}$. Scan rate 100 mV s^{-1} .

The redox process in the cathodic region can be assigned to the redox process of pyrazine, which could be seen in the cyclic voltammograms of the free ligand (Figure 3.5). The half wave potentials decrease with pH increment, which is consistent with pyrazine electrochemical reduction that is highly dependent of the pH.¹¹² This process is observed in ligand and complex with similar redox potentials and the pH dependency. It suggests that the pyrazine electrochemical reduction is almost independent of the presence of the pentacyanidoferrate.

The values of the redox process for the Himpz, $\text{Na}_3[\text{Fe}(\text{CN})_5(\text{Himpz})]$, pyrazine

and its analogous pentacyanidoferrate(II) complex are shown in Table 3.3.

Table 3.3: Half wave potentials obtained from cyclic voltammetry (V vs SHE) in pH values of 4, 7 and 10 and the pK_a values of the N-heterocycle protonation equilibria.

	$\text{Fe}^{\text{II}}/\text{Fe}^{\text{III}}$			$\text{L}^{\bullet-}/\text{L}$			pK_a
	4	7	10	4	7	10	
pz					-0.66 ¹¹²		0.65 ²¹
Himpz				-0.39	-0.61	-0.81	4.51 ^a
$[\text{Fe}(\text{CN})_5\text{pz}]^{3-}$		0.55 ¹¹¹			^b		
$[\text{Fe}(\text{CN})_5\text{Himpz}]^{3-}$	0.67	0.63	0.63	-0.35	-0.60	-0.76	5.41

^a Value presented and discussed on Chapter 1 ^b This process was not observed by Toma *et al.*¹¹¹

The value of the pK_a of the ligand Himpz is in between the values of pyrazine (0.65)²¹ and imidazole (6.99).²⁵ This suggests that the protonation occurs in the imidazole moiety, whose electron density was diminished by the electron-withdrawing effect of the pyrazine moiety. Since the imidazole moiety in the $\text{Na}_3[\text{Fe}(\text{CN})_5(\text{Himpz})]$ is free to protonate, the pK_a was measured and is shown in Table 3.3. The value obtained is higher than for the free ligand, showing that the coordination via the pyrazine moiety increases the electron density over the ligand, possibly due to the π -acceptor character of the diazine.

Comparing the values of the redox potential for the $\text{Fe}(\text{II})/\text{Fe}(\text{III})$ process in function of the pH, it could be observed that the value increase 0.04 V only when pH is below the pK_a . This proves that the electroactive species is indeed the complex with protonated N-heterocycle $[\text{Fe}^{\text{II/III}}(\text{CN})_5\text{H}_2\text{impz}]^{2-/1-}$. Moreover, the shift in the redox process centered on the metal caused by the protonation also indicate the strong electron delocalization among the both diazine and imidazole rings.

The protonated species $[\text{Fe}(\text{CN})_5(\text{H}_2\text{impz})]^{2-}$ was observed in the UV-Vis spectrum of the complex in acidic solution and showed a shift in the MLCT to lower

energy when compared to the $[\text{Fe}(\text{CN})_5(\text{Himpz})]^{3-}$. We rationalize the effect of protonation in the redox potential as following: in low pH the protonation stabilize the LUMO containing the unpaired electron and the molecule is consequently more easily oxidized. In order to support the hypothesis that the reduction in the cathodic region is due to $\text{Himpz}^{\bullet-} \rightarrow \text{Himpz}$, we investigated the electronic absorption of its pentacyanidoferrate(II) complex in different pH values. The MLCT band is attributed to an electronic transfer from the HOMO, whose character is mainly Fe(3d), to LUMO $\pi_{b_1}^*$ of the N-heterocycle.⁹⁹ Owing the distinct character of the frontier orbitals the protonation of Himpz will stabilize mainly the LUMO. Therefore we expect that the energy of the MLCT in low pH would decrease. The opposite was already shown by Toma and Malin.²⁶ Lowering the pH from 5.0 to 0.3, they noticed an increase of the MLCT transition energy, that was attributed to the protonation of the cyanides, which in turn lead to stabilization of Fe(3d) orbitals and increasing the gap between the ground and excited states.

Figure 3.6 presents the UV-Vis spectra in different pH values. As expected, in alkaline pH when Himpz is neutral the MLCT is at 479 nm (20880 cm^{-1}), whereas in acidic medium it goes to 511 nm (19570 cm^{-1}). This result corroborate our hypothesis above and demonstrate the usefulness of pentacyanidoferrate to probe the electronic structure of the coordinated N-heterocycle.

3.3 Conclusion

The novel complex $\text{Na}_3[\text{Fe}(\text{CN})_5(\text{Himpz})]$ was synthesized in accordance with the synthetic strategy known for pentacyanidoferrate complexed with N-heterocycles.

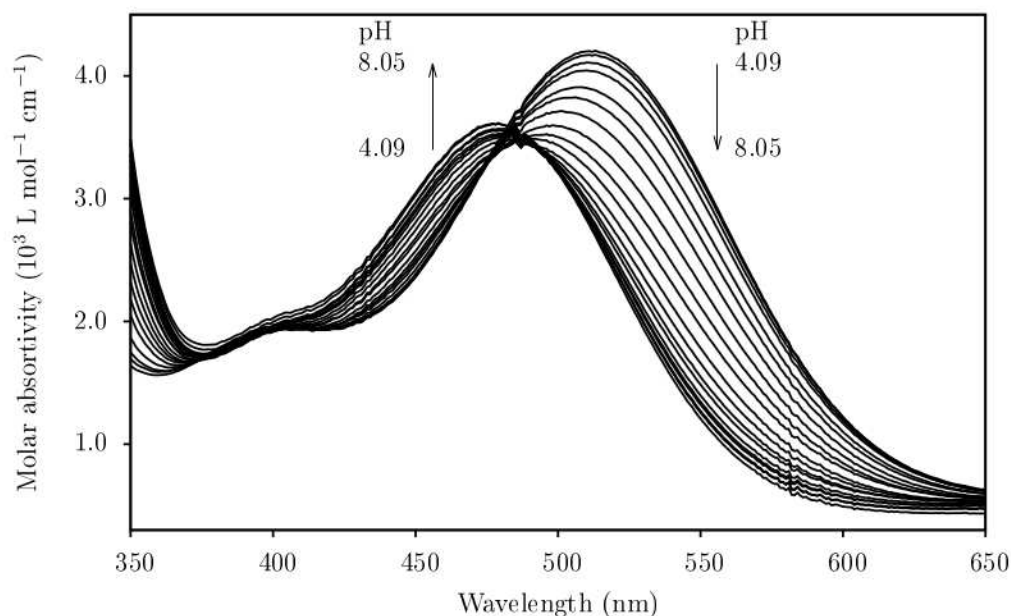


Figure 3.6: Variation of the electronic absorption spectra of $\text{Na}_3[\text{Fe}(\text{CN})_5\text{Himpz}]$ by increasing stepwise the pH by titration with $\text{NaOH } 0.05 \text{ mol L}^{-1}$. The arrows show the evolution of the spectra during the titration and each line represents a pH increase of 0.23 in average.

The characterization by NMR showed that the coordination occurs with the 2-pyrazine moiety via the N4. The cyclic voltammetry results supported the coordination by the pyrazine moiety. Additionally, it showed the redox-active character of the ligand and the pH-dependency of the metal and ligand redox potential. The metal-to-ligand charge transfer band was also found to be pH-dependent in agreement with the electrochemical data, suggesting the stabilization of the π^* LUMO of the Himpz with the protonation of the imidazole moiety leading to a red-shift of the spectrum.

3.4 Experimental

3.4.1 Materials and methods

Materials

2-Pyrazinecarbonitrile (99%), 2,2-diethoxyethylamine (98%), pyrazine ($\geq 99\%$) and ammonium hydroxide (m/v 28%) were purchased from Sigma Aldrich. Sodium nitroprusside dihydrate (99%) was purchased from Acros Organics. Sodium iodide (98%) and ethanol were purchased from Merck. Potassium chloride ($\geq 99\%$) was purchased from Synth. Methanol, acetic acid, hydrochloric acid, diethyl ether (Et_2O), sodium hydroxide and acetonitrile were purchased from Vetec-Sigma (Brazil). Sodium lumps were purchased from Riedel-de Haën. All reagents were used as received from commercial source, with no further purification, except when noted.

The precursor $\text{Na}_3[\text{Fe}(\text{CN})_5(\text{NH}_3)] \cdot 3(\text{H}_2\text{O})$ was synthesized from the sodium nitroprusside dihydrate with ammonium hydroxide, as described in the literature.¹¹³

Physical Measurements

Electronic spectra in the 190-1100 nm range were acquired by using a 1.00 cm quartz cuvette in a diode array HP8453 UV/Visible absorption spectrophotometer equipped with a HP89090A Peltier.

IR spectra were measured using a Bomem MB-Series Model B100 FT-IR spectrophotometer in the $4000 - 400 \text{ cm}^{-1}$ range with resolution of 4 cm^{-1} . Samples were prepared as KBr pellets.

Electrospray ionization mass spectrometry (ESI-MS) measurements were carried out using a Waters Quattro Micro API. Samples were evaluated in the positive mode

in an 1:1 methanol:water solution with addition of 0.10% (v/v) formic acid.

Elemental analysis for carbon, hydrogen and nitrogen were performed using a Perkin Elmer 2400 CHN analyzer.

The values of pH were measured using a Metrohm 827 pH Lab pHmeter.

^1H and ^{13}C NMR spectra were acquired in deuterated dimethylsulfoxide (DMSO) and water (D_2O) solutions and using a Bruker Avance III - 500MHz (11.7T) spectrometer.

Cyclic voltammograms of himpz and the respective pentacyanidoferrate(II) complex were obtained with a Autolab EcoChemie PGSTAT20, using a Britton-Robinson buffer solution¹¹⁴ containing KCl 0.1 mol L^{-1} as supporting electrolyte in all measurements. A glassy carbon electrode was used as working electrode, a Ag/AgCl or saturated calomel electrode as reference electrodes and a platinum electrode as auxiliary electrode. Nitrogen was used before each measurement to avoid the presence of oxygen.

3.4.2 Synthesis of 2-(1H-imidazol-2-yl)pyrazine - Himpz

The ligand was synthesized using the procedure described by Voss *et al.*¹⁷

A 50 mL round-bottom flask was charged with 0.471 mL (5 mmol) of 2-pyrazinecarbonitrile, 5 mL MeOH and 0.47 mL (1 mmol) of a 30% solution of NaOMe in MeOH. The mixture was stirred for 20 minutes at rt.

0.727 mL (5 mmol) of 2,2-diethoxyethanamine followed by 0.6 mL of AcOH were added dropwise to the mixture and the reaction mixture was stirred for 1 hour at 50°C . After the mixture was cooled to rt, 10 mL of MeOH and 2.5 mL of HCl 6 mol L^{-1} were added and the reaction was heated to reflux for 5 hours.

After that, the solution was evaporated to dryness, resolubilised in 15 mL of water and extracted with 3×5 mL of Et_2O , resulting in a deep brown solution. The pH was adjusted to 8-9 with a NaOH 2 mol L^{-1} solution then the volume was reduced to favor the product precipitation. The brown product was filtered and washed with Et_2O . The product was obtained as a brown powder with a 38% yield. Anal. calc. for $(\text{C}_7\text{H}_6\text{N}_4)_3 \cdot (\text{NaCl})$: C 50.76; H 3.65; N 33.83; found: C 51.92; H 3.86 and N 33.95. ESI-MS (MeOH): 146.9 $[\text{H}_2\text{impz}]^+$ and 119.8 $[(\text{H}_2\text{impz})-(\text{CN})]^+$. ^1H NMR (500 MHz, DMSO-d_6) δ (ppm) 13.06 (s, 1H), 9.25 (d, 1H, $J = 1.5$), 8.66 (dd, 1H, $J = 2.5, 1.5$), 8.60 (d, 1H, $J = 2.5$), 7.35 (s, 1H) and 7.17 (s, 1H). ^{13}C NMR (125.7 MHz, DMSO-d_6) δ (ppm) 144.90, 144.24, 143.92, 143.71, 141.80, 130.72 and 120.32.

3.4.3 Synthesis of $\text{Na}_3[\text{Fe}(\text{CN})_5(\text{Himpz})]$

The complex was synthesized using a procedure adapted from the N-heterocycle-pentacyanidoferrate(II) literature, that was extensively studied by Toma *et al.*^{26,92,93}

0.1010 g (0.69 mmol) of Himpz and 10 mL of H_2O were added to a 100 mL beacker and stirred. After partial dissolution, a solution of 0.1754 g (0.55 mmol) of $\text{Na}_3[\text{Fe}(\text{CN})_5(\text{NH}_3)] \cdot 3(\text{H}_2\text{O})$ in 7 mL of water was added dropwise and then stirred for 30 minutes in the dark at 0°C . Posteriorly, a solution of 1.8103 g of NaI in 3 mL of water was added and then absolute ethanol was added in amount enough to precipitate the product. The reddish-orange powder produced was filtered and washed with cold absolute ethanol then dried under reduced pression.

The product was obtained as an reddish-orange powder with a 85% yield. Anal. calc. for $\text{Na}_3[\text{Fe}(\text{CN})_5(\text{C}_7\text{H}_6\text{N}_4)] \cdot 6.5(\text{H}_2\text{O})$: C 27.82; H 3.70; N 24.33; found: C 27.31; H 3.27 and N 24.52. λ_{max} nm ($\text{L mol}^{-1} \text{ cm}^{-1}$) in H_2O : 224 (16932), 270

(8445), 316 (8021) and 481 (3772), FT-IR (KBr) (cm^{-1}): δ_{CN} 2055 and 2095, ^1H NMR (500 MHz, D_2O) δ (ppm) 9.53 (s, 1H), 8.97 (d, 1H, $J = 3.0$), 8.21 (d, 1H, $J = 3.0$) and 6.60 (s, 2H).

3.4.4 Determination of pK_{aH}

The pK_{aH} values of the Himpz and $\text{Na}_3[\text{Fe}(\text{CN})_5(\text{Himpz})]$ were measured spectrophotometrically according to Toma and Malin²⁶ using the expression

$$\text{pH} = \text{pK}_{aH} + \log \frac{[\text{A}]}{[\text{HA}]} \quad (3.1)$$

where $[\text{A}]$ and $[\text{HA}]$ are the molar concentration of base and protonated species respectively calculated using Beer's Law at the wavelengths indicated in Table 3.4. The initial acidic solution was titrated with NaOH 2 or 0.05 mol L^{-1} depending on the proximity of the equivalence point. The pH value was determined using a calibrated pHmeter.

Table 3.4: Experimental conditions for pK_{aH} determination.

A	initial conc. ($\mu\text{mol L}^{-1}$)	initial pH	λ HA (nm)	λ A (nm)
Himpz	58	2.80	292	318
$\text{Na}_3[\text{Fe}(\text{CN})_5(\text{Himpz})]$	127	4.09	300	319

Chapter 4

H₂dimpy as a ligand for Cu(I)-mediated ATRP

4.1 Introduction

Transition metal mediated atom transfer radical polymerization (ATRP) is one of the most versatile and successful that controls living radical polymerization (CRP).¹¹⁵ This method provides a synthetic approach for polymers and copolymers of several architectures with well-defined composition and narrow molecular weight distribution, while maintaining the livingness of the chain.^{116,117}

Cu-mediated ATRP with nitrogen-based ligands has been extensively studied due to their robustness, versatility and low cost.¹¹⁸ Usually, a suitable ligand must be a good electron donor and facilitate a reversible one-electron Cu(I)/Cu(II) redox process.^{119,120} Furthermore, the ligand should also be easily substituted, allowing modification to improve solubility,^{121,122} change in steric topology^{123,124} or immobilization of the catalyst.^{125,126}

Typically bipyridine derivatives or branched N-alkyl polyamines chelators have

utilized. However, other ligands with different denticity, bite angle, basicity and steric topology were also studied in order to provide data of possible rationalization of the synergy between the metal and ligand, showing the crucial role of the ligand in the effectiveness of CRP.^{118, 127, 128}

Imidazol-2-yl ligands play an important role in coordination chemistry due to their higher basicity when compared to pyridines,^{129–132} 1H-deprotonation ability^{28, 133–135} and possible N-derivatization^{136–138} and in this line of reasoning Yamamura and Matyjaszewski¹²⁰ showed that the tripodal ligands bearing 2-pyridyl and 2-imidazolyl moieties were active for Cu-mediated ATRP. Electron donation have been increased with the number of imidazole moieties, leading to complexes with higher formation constants and catalytic activity.

Previous studies revealed that substituted-terpyridines have been successfully used as catalysts in the ATRP,¹²¹ specially for polymerization of vinyl acetate^{139, 140} thus we have decided to explore the 2,6-di(1H-imidazol-2-yl)pyridine (H₂dimp) as a ligand with Cu(I)-mediated for controlled polymerization (ATRP). This ligand combines the denticity of terpyridine, an enhanced electron donor character of the imidazole moieties¹⁴¹ and the possibility of N-derivatization to address solubility demands. In order to prove the structural similarity with terpyridine-Cu(II) complexes,^{142, 143} a thorough characterization of H₂dimp-Cu(II) have been described.

4.2 Results and discussion

4.2.1 Syntheses

The H₂dimpyl ligand was synthesized using the procedure described by Voss and co-workers.¹⁷ The product was characterized using spectroscopic and spectrometric techniques and results were consistent with literature data.^{17,134} The copper(II) complex have been synthesized adapting the method described by Stupka and co-workers¹³⁴ for other transition metal complexes of the H₂dimpyl ligand. The product was obtained as a dark-green powder, that was further dissolved in methanol/H₂O and, after evaporation at rt, yielded single crystals suitable for XRD.

4.2.2 Ligand characterization

The ¹H NMR spectrum in DMSO-d₆ showed two distinct series of peaks in the aromatic region, one that can be assigned to the 2,6-substituted-pyridine moiety in 7.96, 7.90 and 7.88 ppm and two other peaks in 7.47 and 7.14 ppm that can be assigned to the 2-substituted-imidazole moiety. It was also possible to observe the signal of the amine hydrogens in 12.85 ppm. Results show a non-equivalence of the hydrogens in the imidazole moiety that was not described in literature for this molecule.^{17,134} This occurs due to the slow intermolecular proton exchange of dry sample.¹⁴⁴ The ¹³C NMR spectrum of the ligand showed six signals, as expected, in 117.8 118.9, 130.2, 138.2, 146.1 and 148.2 ppm. The ESI-MS spectrum of the ligand showed the mono-protonated molecular ion at m/z 212 and the double protonated molecular ion at m/z 106.5. These results were consistent with literature.¹⁷

4.2.3 Cu(I)-ATRP assays

The synthesis of polystyrene (PS) homopolymers via ATRP is a well-established methodology in literature, hence it was used as a standard reaction to evaluate the performance of H₂dimpy as a ligand for ATRP. Catalysts based on copper have been widely studied and reported in literature.^{121, 145–147} Two independent systems, using the monomer itself (bulk polymerization) or dimethylformamide (solution polymerization) as solvents to prepare Cu(I)/H₂dimpy complexes, were used. Both reactions were carried out at 110 °C during 18 h. The chemical equation is shown in Figure

4.1

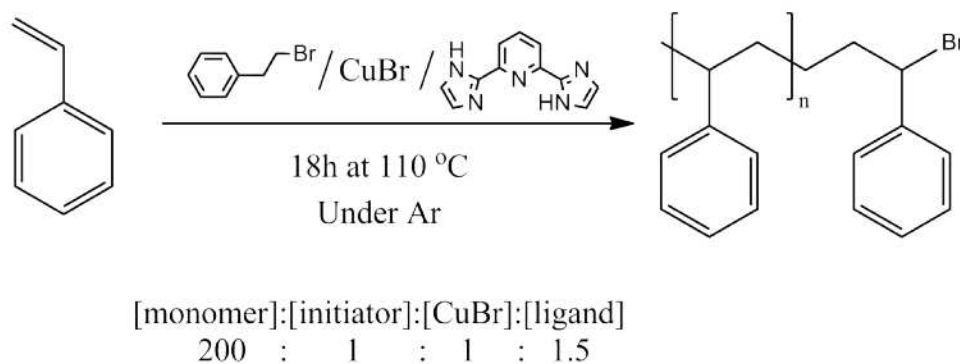


Figure 4.1: Chemical equation of the styrene Cu(I)-ATRP assays.

Gel permeation chromatography (GPC) curves of polystyrene synthesized from bulk (PS-b) or solution (PS-s) polymerization are shown in Figure 4.2. Monomodal and multimodal GPC curves were observed by PS-s and PS-b, respectively. The number average molecular weight (M_n) and polydispersity index ($M_w/M_n = D$) values of PS-b and PS-s are shown in Table 4.1. GPC measurements indicated that PS-b and PS-s presented 1.7 and 1.3 D values, respectively.

One of the literature criteria used to define a controlled polymerization is based on the D values, where $M_w/M_n \leq 1.5$ is considered a narrow molecular weight distri-

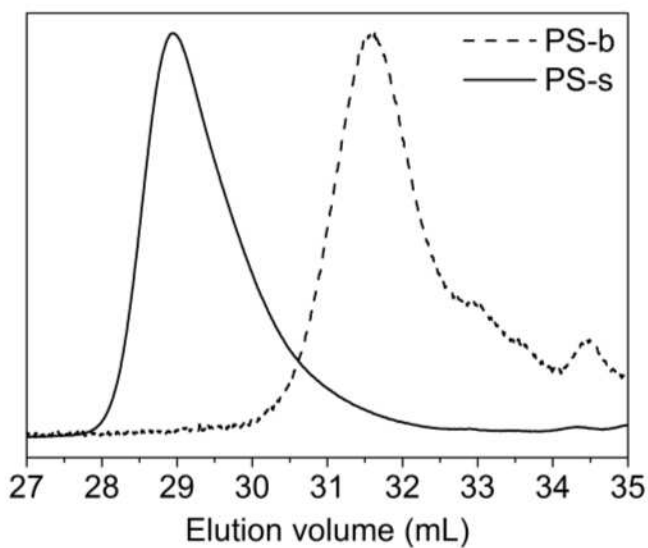


Figure 4.2: GPC curves of PS-s and PS-b homopolymers.

Table 4.1: Molecular parameters obtained for the PS homopolymers.

Polymer	M_n (g mol ⁻¹) ^a	D	M_{RMN} (g mol ⁻¹)	M_n (theo) (g mol ⁻¹)
PS-b	2,100	1.7	6,800	20,800
PS-s	16,300	1.3	20,400	20,800

^a Determined by GPC with THF as the eluent with respect to polystyrene standards.

bution.^{118, 145, 148, 149} Normally, very narrow D values ($M_w/M_n \leq 1.2$) are obtained at low monomer conversion rates and/or by using solvent in the polymerization.^{150–152} Poor controlled reaction was achieved for PS synthesized under bulk condition due to the H₂dimpy hydrophilic character not providing suitable conditions for its solubilization in styrene [1:1.5 molar ratio styrene:H₂dimpy].

Other important observation was the formation of a green suspension in the reaction medium, that is typically assigned to the copper(II) intermediates,^{153–155} suggesting the formation of a resting state that disrupts the polymerization and leads to the product with lower molar mass and high polydispersity. On the other hand, in the PS synthesis in DMF solution the reaction medium was homogeneous and lead to a better controlled polymerization, as determined by GPC, reinforcing the importance of a good solubility of the ligand and the copper(II) intermediate to the controlled catalysis.

According to proton nuclear magnetic resonance (¹H NMR) measurements, the chain end functionality of the PS homopolymers was confirmed. Additionally, these homopolymers were made up of around 91 and 122 styrene monomeric units, per bromide chain end.

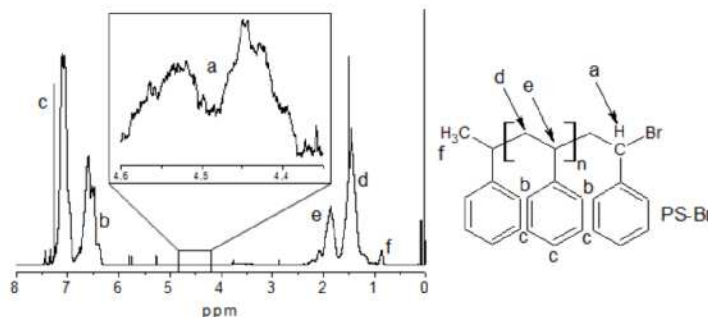


Figure 4.3: ¹H NMR spectrum of the PS-s with inset showing the 4.60–4.35 ppm range magnification obtained in the 500 MHz spectrometer.

Figure 4.3 shows the proton nuclear magnetic resonance (¹H NMR) spectrum of PS-s synthesized via ATRP. The signals at 4.60 - 4.35 ppm were attributed to the hydrogen located in the α position of the bromine chain end (hydrogen “a”), confirming the existence of a bromide end group in the PS homopolymers. The complex asymmetric shape of these signals depends on the differences in the chemical environments of the polymer chain (i.e. polymer tacticity, the restricted motion of the end groups and conformation effects).¹⁵⁶ Based on the signal intensity ratios between the 7.37 - 6.21 ppm range and those in the 4.60 - 4.35 ppm range, the calculated molecular weight by ¹H NMR (M_{RMN}) of PS-s, considering the ratio monomer:chain end, was ca. 20,400 g mol⁻¹.

Comparing this result with the one obtained for the controlled polymerization of styrene using terpyridine and its derivatives,¹²¹ we have also observed that the solubility of the Cu(II) intermediate was a limiting factor for a better controlled reaction with lower polydispersity. Our result, for the polymerization using DMF as solvent, was in agreement with the described for the alkyl-substituted terpyridines with a polydispersity lower than 1.3, suggesting a controlled behaviour and confirming that the solubility of the catalyst and its intermediate is central for Cu(I)-mediated ATRP.

An important feature that H₂dimpyl has is that alkyl-substitution is easier achieved when compared with terpyridines. The reactive amine moiety of the imidazole allows the easy addition of a hydrophobic alkyl group via a simple nucleophilic substitution with the corresponding alkyl halide.^{137, 157–159} While for the terpyridines, a palladium catalyzed coupling is needed for the production of an alkyl-branched derivative. Showing the versatility of the imidazol-2-yl moieties as ligand, allowing the tuning the catalyst for different media, increasing or decreasing the hydrophobic-

ity of the copper complex.

4.2.4 Copper(II) complex

During the polymerization reaction of styrene in the absence of solvent, the formation of a dark-green powder was observed. Attempts to isolate and characterize this residue were unsuccessful and consequently Cu(II) complex was synthesized to provide structural information for possible intermediate. Suitable single crystals were obtained when $\text{CuCl}_2 \cdot (\text{H}_2\text{O})_2$ reacted with H₂dimpY in 1:1 ratio. However even if the halide used in the synthesis is different from the bromide complex possibly produced during the polymerization reaction, these results can give insight into the possible structure of this intermediate. Moreover, analogue copper(II) complexes with the 2,6-di(benzimidazol-2-yl)pyridine and or terpyridine were obtained with chloride.^{121,142,143,160}

Crystal structure

A single crystal suitable for XRD was obtained and refinement revealed a dimeric structure with two chloride bridges with an overall $[\text{Cu}_2(\text{H}_2\text{dimpY})_2(\mu\text{-Cl})_2](\text{PF}_6)_2 \cdot 2\text{H}_2\text{O}$ formula (Table 4.2). The dimeric structure has an inversion center (C_i point group) positioned half-way between the two $\mu\text{-Cl}$ bridges resulting in observation of one unique atom of each type (Figure 4.4). Only one imidazole ring is involved in hydrogen bonding with the unique water molecule in the crystal [$\text{N}(5) \cdots \text{O}(1) = 2.821(3)$ Å, angle $\text{N}(5)\text{-H}(5)\text{-O}(1)$ *ca.* 161.9°]. The presence of the PF_6^- counter-ions confirms that the ligand is not deprotonated in the complex.

Some selected bond distances and angles are shown in Table 4.3. It is possible

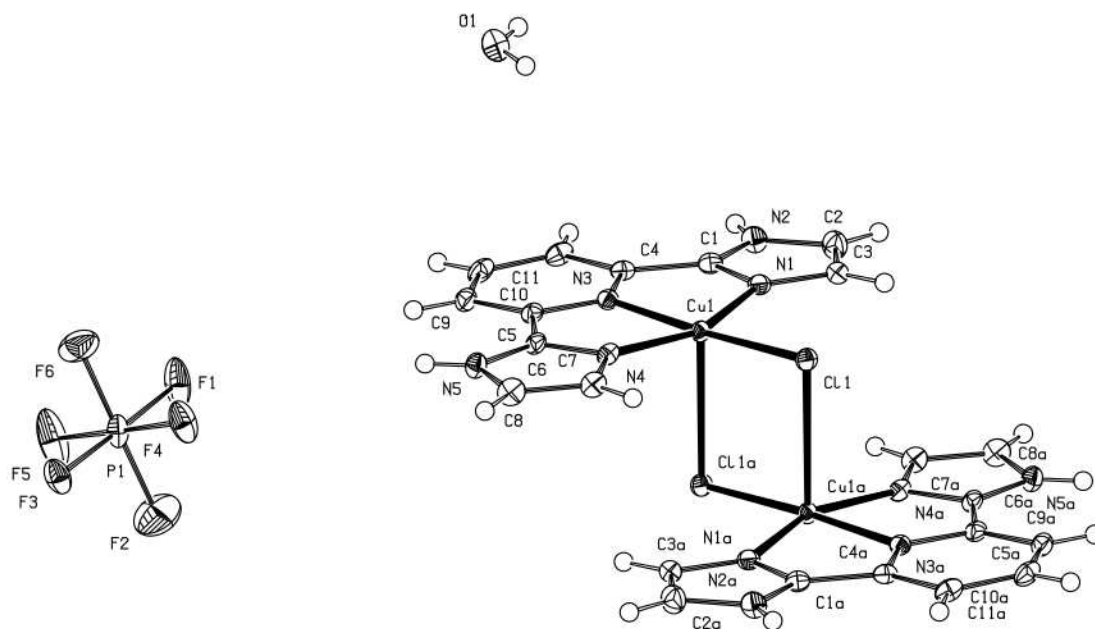


Figure 4.4: ORTEP image of the complex $[\text{Cu}_2(\text{H}_2\text{dimpy})_2(\mu\text{-Cl})_2](\text{PF}_6)_2 \cdot 2 \text{H}_2\text{O}$.

Table 4.2: Data from the single-crystal XRD of the $[\text{Cu}_2(\text{H}_2\text{dimpy})_2(\mu\text{-Cl})_2](\text{PF}_6)_2 \cdot 2 \text{H}_2\text{O}$ complex

Molecular formula	$[\text{Cu}_2(\text{C}_{11}\text{H}_{11}\text{N}_5)_2\text{Cl}_2](\text{PF}_6)_2 \cdot 2 \text{H}_2\text{O}$
Formula weight (<i>Da</i>)	946.44
λ (Mo $\text{K}\alpha$, Å)	0.71073
Space group	$\text{P2}_1/\text{c}$
Crystal System	Monoclinic
<i>a</i> (Å)	12.744(3)
<i>b</i> (Å)	6.873(1)
<i>c</i> (Å)	18.606(4)
β (°)	102.255(4)
<i>V</i> (Å ³)	1592.5(5)
<i>Z</i>	2
<i>T</i> (K)	100
ρ_{calc} (g cm ⁻³)	1.986
<i>F</i> (000)	952
Reflections collected/unique	25865/3653 [$R_{\text{int}} = 0.0528$]
Data/restraints/parameters	3653/0/241
R_1, wR_2 [$I > 2\sigma(I)$]	0.0315, 0.0785
Diff. peak and hole (e/Å ³)	0.55, -0.42
Goodness of fit in F^2	0.902

to conclude that the Cu(μ -Cl)₂Cu core is rhomboid, where the copper is the obtuse vertex (93.61°) and the chloride the acute vertex (86.39°), with the Cu(1)-Cu(1a) distance of 3.4811 Å and the Cl(1)-Cl(1a) of 3.702 Å. Cu(II) is in a distorted square-pyramidal geometry (τ = 0.301, using α = 158.43 and β = 176.48)¹⁶¹ and the Cu(μ -Cl)₂Cu dimer can be classified as parallel showing a 0.562 Å difference between the Cu-Cl_{apical} and the Cu-Cl_{basal} bond distances, which is consistent with literature data for copper(II) complexes with the Cu(μ -Cl)₂Cu core.^{142, 143, 162–164}

The structure is different from one obtained for the analogous complex with 2,6-bis(benzimidazol-2-yl)pyridine¹⁶⁰ that is also neutral but has two chloride ligands per Cu(II) giving the same coordination geometry but without the μ -Cl bridge. This can be related to the presence of PF₆[−] ions in this case but the different Lewis basicity of these ligands cannot be ruled out.

Table 4.3: Selected bond distances and angles from the single-crystal XRD of the complex

Bond distance (Å)		Angle (°)	
Cu(1)-Cl(1)	2.2441(7)	Cu(1)-Cl(1)-Cu(1a)	86.39(2)
Cu(1a)-Cl(1)	2.8063(8)	Cl(1)-Cu(1)-Cl(1a)	93.61(2)
N(3)-Cu(1)	1.978(2)	N(1)-Cu(1)-N(4)	158.43(9)
N(1)-Cu(1)	1.991(2)	N(4)-Cu(1)-Cl(1)	176.48(6)
N(4)-Cu(1)	2.001(2)	N(3)-Cu(1)-Cl(1a)	95.82(6)
Cu(1)-Cu(1a)	3.4811(8)	N(4)-Cu(1)-Cl(2a)	89.81(6)
Cl(1)-Cl(1a)	3.702(1)	N(3)-C(10)-C(5)-N(4)	-1.4(3)
N(3)-Cl(1)	4.220(2)	N(1)-C(1)-C(4)-N(3)	-0.2(3)
O(8)-H(26)	1.992(3)		

The shortest Cu(II)-N distance is for pyridine N(3), 0.023 Å smaller than for imidazole N(4) and 0.013 Å for the other imidazole N(1) which is consistent with the rigidity of the tridentate ligand resulting in a relatively short N(3)-Cu(1)-N(5) angle (158.43°) for the *trans* imidazoles. The three rings in H₂dimpy are almost

coplanar with torsion angles N(3)-C(10)-C(5)-N(4) and N(1)-C(1)-C(4)-N(3) near 0°. Moreover, Cl(1) in the base of the pyramid is *trans* to pyridine with a nearly linear angle (176.48°) which confirms that Cu(II) is sitting in the base of the pyramid.

A powdered sample of the crystals was analysed by FT-IR and compared to the spectrum of the free ligand (Figure 4.5). Two absorption bands at 559 cm⁻¹ and 831 cm⁻¹ present in the spectrum of the complex and absent in the ligand's can be assigned to PF₆⁻ stretching modes.^{165, 166} Bands at 1448 cm⁻¹ and 1467 cm⁻¹ present in the spectrum of the ligand are shifted to 1402 cm⁻¹ and 1431 cm⁻¹ upon coordination and can be assigned to C=N stretching modes suggesting coordination through imine moieties. The N-H stretching bands also corroborates this type of coordination. In the ligand, two bands are observed at 3319 and 3353 cm⁻¹, but in the complex only one broad band is observed at 3371 cm⁻¹, suggesting the gain of symmetry and the strengthening of the bond. This result is in agreement with the structure observed by crystallography.

Magnetic characterization

The magnetic behaviour of the complex was studied in the 2-300 K temperature range and in order to confirm that the crystalline structure did not change with temperature we have determined unit cell parameters at rt and we have observed that the only change was the predicted expansion of the cell (See Support Information) with increasing temperature.

The experimentally determined bulk magnetic properties of the copper complex are shown in Figure 4.6 (Panel A, circles). At 300 K the product $\chi_M T$, where χ_M represents the molar magnetic susceptibility, gives 0.83 K cm³ mol⁻¹, hence value

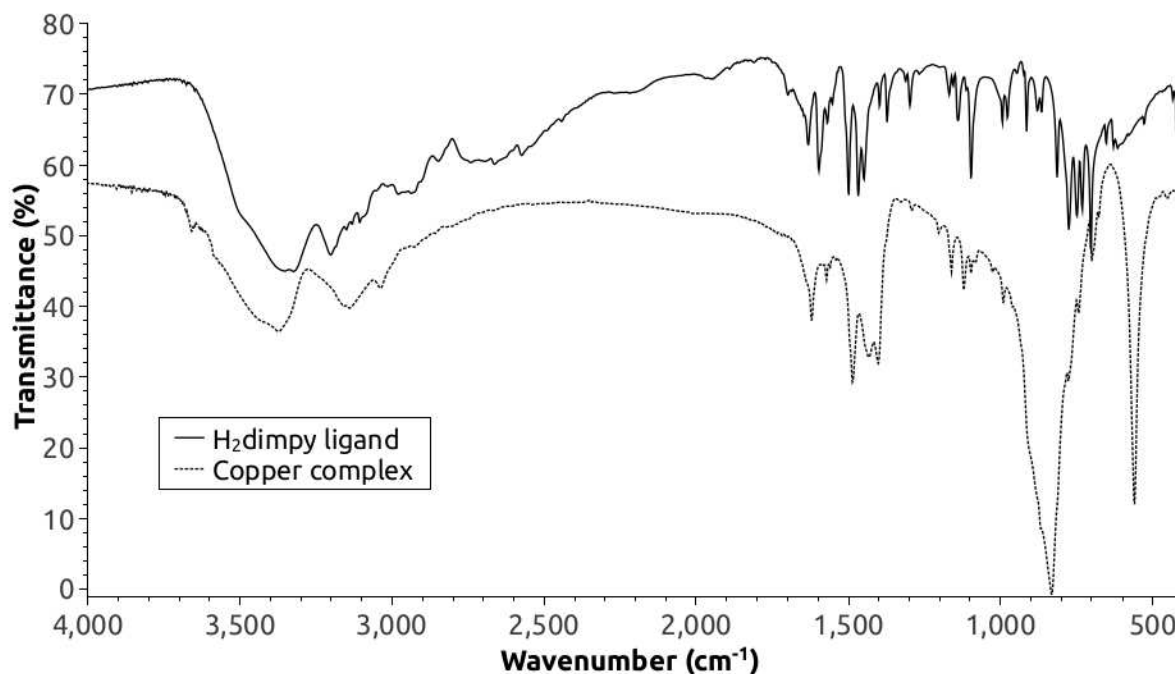


Figure 4.5: FT-IR spectra of the copper(II) complex and the H₂dimpy ligand.

larger than that anticipated for two interacting $S=1/2$ spin-system (where $\chi_M T = 0.75 \text{ K cm}^3 \text{ mol}^{-1}$ with $g_{avg} = 2.00$) being in thermal equilibrium according to the Boltzmann distribution between triplet and singlet states. Upon lowering the temperature, the $\chi_M T$ product increases slowly and then sharply below 25 K, providing a clear indication that the dominating inter and intramolecular interactions in the bulk material are ferromagnetic in nature. However, the observed magnetic trend is very complex.

The crystalline material shows formation of zig-zag chains with short intermolecular contacts among the dimeric units. The system can be best described according to the Heisenberg Hamiltonian ($H = \sum_{i,j} J_{i,j} S_i S_j$) including Zeeman effect in terms of three interacting ($S=1/2$)-spin system ($S_T=3/2$, quartet) according to the model A in the temperature range 5-300 K (Figure 4.6 Panel B) and as fully interacting

dimers (quintet) below 5 K, according to the model B (Figure 4.6 Panel C). The numerical results are given within the panel B and C for simplicity, where positive J indicates antiferromagnetic interactions and negative J the ferromagnetic interactions. Simulations have been carried out by considering an applied field of 0.5 T in line with the experimental conditions employed, an averaged g -value (g_{avg}) of 2.00 and a diamagnetic contribution of $9.2 \times 10^{-4} \text{ cm}^3 \text{ mol}^{-1}$.

In order to investigate in more detail the exchange interaction between the metal centers we performed broken-symmetry U-DFT calculations with the structure obtained by XRD. Calculations considered only the dimeric structure, neglecting water and PF_6^- . Magnetic coupling analysis resulted in data presented in Table 4.5 and use of Equation 4.1^{167, 168} results in $J = 1.1 \text{ cm}^{-1}$. This is indicative of a ferromagnetism in agreement with the experimental results.

$$J = -\frac{E_{HS} - E_{BS}}{(S_{max})^2} \quad (4.1)$$

The spin density (Figure 4.7) reveals a great contribution from Cu(II) $d_{x^2-y^2}$ orbitals and H₂dimp σ orbitals from both centers. This was expected based on the fact that the unpaired electron must be in the more destabilized $3d$ orbital, the one directed to the ligands. It can be seen that spin density is also spread over both chloride bridges, suggesting that the mechanism for exchange interaction may be through them.

Characterization in solution

A solubility assay was made and showed that crystals are very soluble in water, soluble in DMF and methanol and almost insoluble in non-polar solvents, revealing

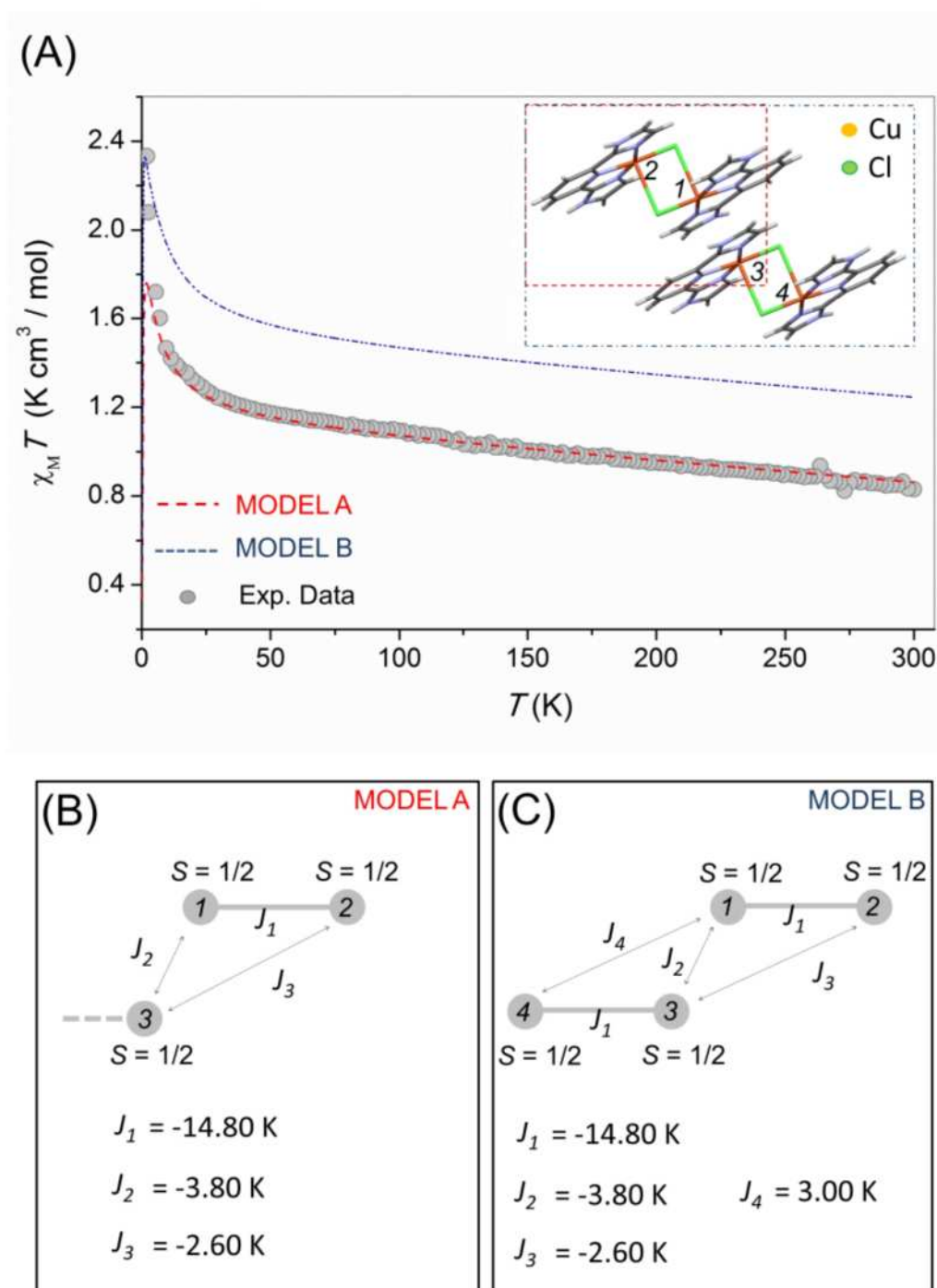


Figure 4.6: A) Experimental magnetic susceptibility in the 2-300 K temperature range and theoretical fittings based on two different models (B and C) for exchange interaction in dimeric $[\text{Cu}_2(\text{H}_2\text{dimpy})_2(\mu\text{-Cl})_2](\text{PF}_6)_2 \cdot 2\text{H}_2\text{O}$.

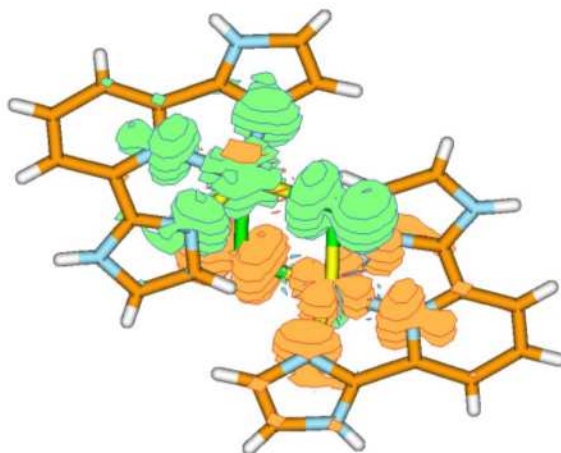


Figure 4.7: Spin density obtained from U-B3LYP/def2-TZVP using the experimental geometry of the dimeric $[\text{Cu}_2(\text{H}_2\text{dimpy})_2(\mu\text{-Cl})_2]^{2+}$ unit in the triplet state ($S = 1$).

the high polarity of the complex.

The ESI-(+)-MS spectrum (See Support Information in the end of the chapter) shows the $[\text{Cu}(\text{H}_2\text{dimpy})\text{Cl}]^+$ molecular ion at m/z 309 and 311 but the most intense peaks were assigned as the $[\text{Cu}(\text{Hdimpy})]^+$ fragment at m/z 273 and 275. Moreover, the fragments $[\text{Cu}(\text{Hdimpy})(\text{MeOH})]^+$ at m/z 305 and 307 and $[\text{Cu}(\text{Hdimpy})(\text{H}_2\text{O})]^+$ at m/z 291 and 293 were observed. All three fragments originated from the loss of HCl from the molecular ion suggesting the lability of the chloride and the protic character of the amine hydrogen in the complex. All peaks have copper isotopic pattern distribution.

The MS/MS analysis of the molecular ion at m/z 309 showed the formation of an intense peak at m/z 273, confirming the assignment of the $[\text{Cu}(\text{Hdimpy})]^+$ fragment as well as the 1:1:1 copper:H₂dimpy:chloride proportion in the first coordination sphere for the compound.

UV-Vis spectra of both H₂dimpy ligand and complex are shown in Figure [4.8](#).

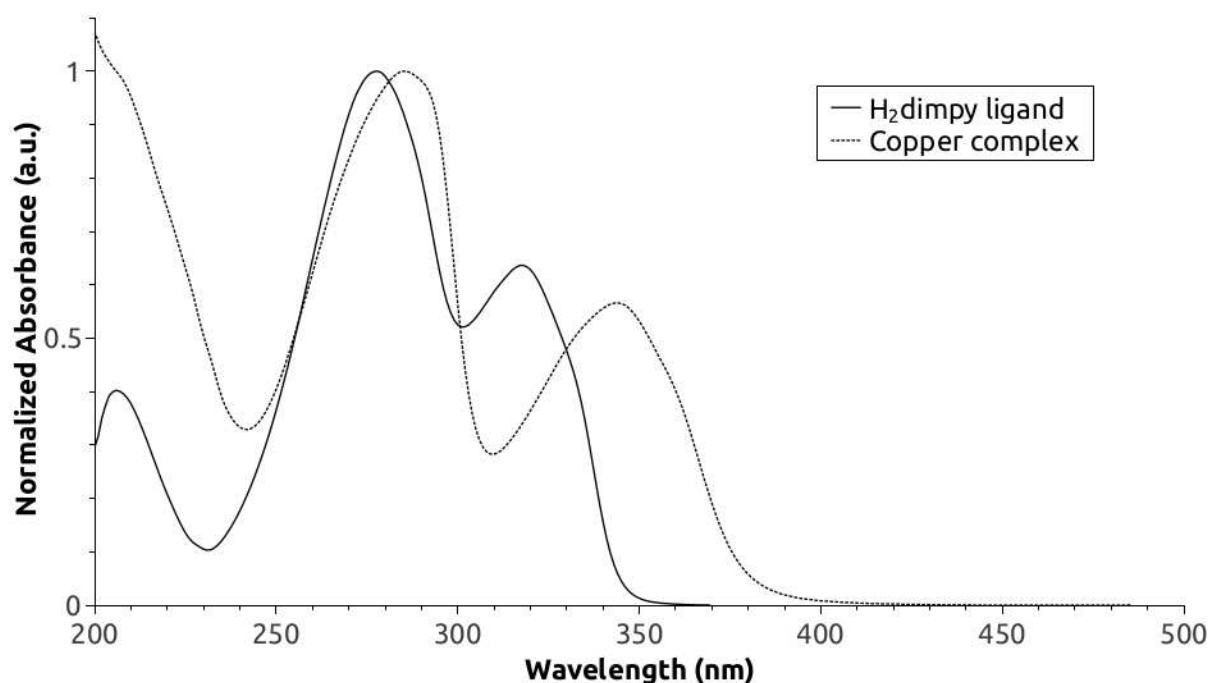


Figure 4.8: UV-Vis spectra of the H₂dimpy in MeOH and the copper(II) complex in H₂O.

The ligand spectrum shows three intense bands at 206, 277, 318 nm that could be assigned to $\pi \rightarrow \pi^*$ bands. It is possible to observe a redshift in all three bands upon coordination with Cu(II). The spectrum of the complex also revealed a very weak and broad band at 680 nm that can be assigned to a $d \rightarrow d$ band. In comparison with the UV-Vis spectrum of copper(II) chloride dissolved in water (814 nm) there is a blueshift, which is consistent with an increase in ligand field after coordination through the imine moiety (See Support Information).

The energy of the $d - d$ band is consistent with pentacoordinated Cu(II) in a square-pyramidal structure,¹⁶⁹ suggesting presence of the solvent molecule as the fifth ligand or maintenance of the dimer observed in the solid state in analogy with other examples with chloride and N-donor ligands.^{142, 143, 162, 164}

Cyclic voltammetry of the complex in acetonitrile solution (Figure 4.9) revealed

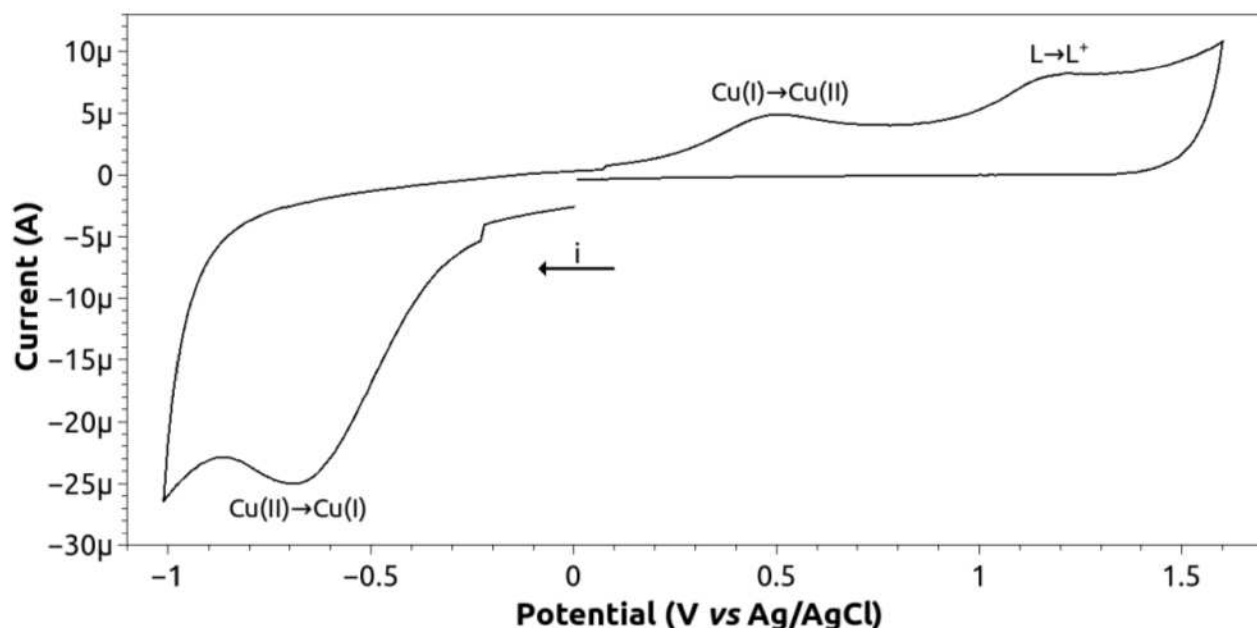


Figure 4.9: Cyclic voltammetry of the complex in acetonitrile at 100 m V s⁻¹.

that Cu(II)/Cu(I) reduction occurs irreversibly at $E_{pc} = -0.69$ V vs Ag/AgCl. There are two irreversible processes at $E_{pa} +0.51$ and $+1.22$ V that can be assigned to oxidation of Cu(I) and the ligand, respectively. This electrochemical behaviour is in agreement with similar complexes, e.g. with modified terpyridines with imidazol in the central pyridine ring in which the Cu(II)/Cu(I) reduction occur around $E_{pc} = -0.2$ vs Ag/AgCl.¹⁷⁰ The lower reduction potential observed in the present case confirms the higher Lewis basicity of H₂dimpy in comparison to the terpy ligand. The irreversibility of the Cu(II)/Cu(I) reduction process can be explained by a high lability of the [Cu^I(H₂dimpy)Cl] formed upon reduction. The high lability can be associated with the efficiency of the Cu(I) assisted polymerization since the catalyst must be regenerated in each step of the catalytic cycle.

4.3 Conclusion

The Cu(I)/H₂dimp complex was successfully applied to obtain polystyrene via ATRP using DMF as a solvent. Furthermore, polystyrene synthesized in these conditions presents controlled molecular weight and a relatively narrow polydispersity, similar to the result obtained with terpyridine derivatives.¹²¹ Without DMF as solvent, a non-controlled polymerization occurs and can be assigned partially to the low solubility of the ligand H₂dimp in styrene and to the formation of a green copper(II) intermediate, highly insoluble, that removes the catalyst from the medium. To investigate this possible catalyst intermediate, a novel copper(II) complex with 2,6-(1H-imidazol-2-yl)pyridine was synthesized and obtained as a green powder that crystallized in water/MeOH to give dark green-bluish crystals. The ESI-(+)-MS showed the 1:1:1 proportion between H₂dimp:Cu(II):chloride and the lability of the chloride in aqueous solution. Spectroscopic analysis confirmed the coordination via the imine moieties and suggested the formation of a pentacoordinated copper(II) complex that was confirmed via single-crystal XRD. The crystal structure showed a dimeric complex with formula [Cu₂(H₂dimp)₂(μ-Cl)₂](PF₆)₂ · 2 H₂O, in which Cu(II) is in a distorted square-pyramidal geometry.

In the ATRP reaction, it is expected a similar "square-like" structure for the copper(II) bromide intermediate, without the halide bridge due the size of bromide, and with a similar hydrophilicity, reinforcing the importance of the solvent for the homogeneity of the catalytic system.

4.4 Experimental

4.4.1 Materials and methods

Materials

Styrene (>99%), copper(I) bromide (98%), (1-bromoethyl)benzene (97%), 2,6-pyridinedicarbonitrile (97%) and 2,2-diethoxyethylamine (98%) were purchased from Sigma-Aldrich. Potassium hydroxide ($\leq 85\%$) was purchased from Fluka Analytical. Methanol, diethyl ether (Et₂O), dimethylformamide (DMF), tetrahydrofuran (THF) and copper(II) chloride dihydrate (>99%) were purchased from Vetec-Sigma (Brazil). Sodium lumps were purchased from Riedel-de Haën. All reagents were used as received from commercial source, with no further purification, except when noted.

Removal of inhibitors present in the monomers

Equal volumes of styrene and aqueous NaOH solution (10% w/v) were vigorously stirred in a 500 mL separation funnel. Then, phase separation was observed and the bottom phase was discarded. The upper phase was washed three times with distilled water, always discarding the bottom phase. After that, the styrene fraction was distilled at 40 ± 2 °C and the pure styrene was collected in a flask immersed in liquid nitrogen.

Physical Measurements

Electronic spectra in the 190-1100 nm range were acquired by using a 1.00 cm quartz cuvette in a diode array HP8453 UV/Visible absorption spectrophotometer

equipped with a HP89090A Peltier.

Electrospray ionization mass spectrometry (ESI-MS) measurements were carried out using a Waters Quattro Micro API. Samples were evaluated in the positive mode in an 1:1 methanol:water solution with addition of 0.10% (v/v) formic acid.

IR spectra were measured using a Bomem MB-Series Model B100 FT-IR spectrophotometer in the 4000 - 400 cm⁻¹ range with resolution of 4 cm⁻¹. Samples were prepared as KBr pellets.

Gel permeation chromatography (GPC) measurements were performed using a Viscotek GPCmax VE 2001, equipped with Viscotek VE 3580 RI Detector and three Shodex KF-8060M columns working at 40 °C. Degassed THF was used as an eluent (1 mL min⁻¹) and as a solvent to prepare 8.0 mg mL⁻¹ sample solutions. The PS molecular weights were determined using polystyrene standards.

¹H NMR spectra of the polymers were obtained in deuterated chloroform solutions (CDCl₃) using a Bruker Avance III - 500MHz (11.7T) spectrometer operating at 499.8731 MHz.

The cyclic voltammetric (CV) measurements were performed using a PGSTAT-30 potentiostat model from AUTOLAB (Eco Chemie, Netherlands) interfaced to a computer controlled by the NOVA (v.1.10) software. A conventional electrochemical cell with three electrodes was used. Ag/AgCl as reference electrode, a coil of platinum wire as auxiliary and glassy carbon electrode (GCE) without modifications as working electrode were used for all the measurements in acetonitrile medium containing lithium perchlorate (0.1 mol L⁻¹). Oxygen was removed by bubbling nitrogen for 10 min through the solution before each electrochemical measurement. GCE surface was previously cleaned mechanically by polishing with 1.0, 0.3, then 0.05 μm

alumina in water slurry on microcloth pads. Adherent particles were removed from the electrode surface by rinsing with double distilled water, followed by sonication in ethanol:water (50:50, v/v) solution and further rinsed with double distilled water before dried at air.

Temperature dependent dc magnetic susceptibility was performed on dried powder sample using Quantum Design MPMS XL Superconducting Quantum Interference Device (SQUID) magnetometer during cooling from 300 K to 5 K under an applied field of 0.5 T.

The crystallographic measurements were obtained with a Bruker Kappa APEX II Duo diffractometer with Mo-K α radiation ($\lambda = 0.71073$ Å). The measurement was made at 100 K using the Oxford Cryostream 700 cryostat. The structure was solved and refined using SHELXL97.¹⁷¹ ORTEP diagrams was generated using PLATON.¹⁷²

4.4.2 Ligand Synthesis

A 100 cm³ flask was filled with 2,6-pyridinedicarbonitrile (10 mmol) and MeOH (10 cm³), and a 30% solution of NaOMe in MeOH (0.4 cm³, 1 mmol) freshly prepared. The reaction mixture was stirred for 2 h at rt. and 2,2-diethoxyethanamine (2 equiv.) was added followed by AcOH (1.2 cm³, 20 mmol). The reaction mixture was heated to 50 °C for 1 h and cooled to rt. MeOH (20 cm³) and 6 mol L⁻¹ HCl in H₂O (5 cm³) were added, and the reaction mixture was kept under reflux for 5 h.

Once the previous step was completed, the solvent was removed on a rotatory evaporator, and the residue was taken up in a 1:1 mixture of H₂O and Et₂O (30 cm³) and two layers separated. The pH of the aqueous layer was adjusted to 8-

9 with 2 mol L⁻¹ aqueous KOH, and aqueous mixture was stirred for 30 min to allow complete precipitation of the product. The solid was collected by filtration and dried under vacuum to provide pure 2,6-di(1H-imidazol-2-yl)pyridine (H₂dimp). The compound was obtained as a white solid with 70% yield. ESI-MS (MeOH): m/z 212 [H₃dimp]⁺ and 106.5 [(H₄dimp)]₂⁺. ¹H NMR (400 MHz, DMSO-d₆) δ 12.85 (s, 1H), 7.96 (s, 1H), 7.90 (s, 1H), 7.88 (s, 1H), 7.47 (s, 1H) and 7.14 (s, 1H). ¹³C NMR (125.7 MHz, DMSO-d₆) δ 148.2, 146.1, 138.2, 130.2, 118.9 and 117.8.

4.4.3 Preparation of polystyrene via ATRP

The [monomer]:[initiator]:[CuBr]:[ligand] ratios used in this section were 200:1:-1:1.5. Styrene (10.0 mL, 87.3 mmol) and (1-bromoethyl)benzene (0.060 mL, 0.436 mmol) were added to a Schlenk flask under continuous argon flux (positive pressure). The mixture was degassed by four freeze-pump-thaw cycles. After each thaw, the Schlenk was opened under argon flux (5 seconds), to remove the released gases from the solution and again closed under argon atmosphere. Then, CuBr (0.062 g, 0.436 mmol) and H₂dimp (0.125 g, 0.654 mmol) were dissolved in DMF (5 mL) and were added dropwise into the frozen mixture under argon flux. The mixture was degassed by further two freeze-pump-thaw cycles. The Schlenk flask was then immersed in a pre-heated oil bath at 110 °C. After 18 h, THF (20.0 mL) was added to solubilize the solid product. The resulting mixture was permeated through a column filled with alumina (0.15 m length), using THF as an eluent in order to remove the metal complex catalyst from the polymeric solution. The polymeric solution was precipitated in methanol followed by drying under vacuum at 40 °C until reaching constant mass, thus obtaining a white solid product.

4.4.4 Complex synthesis

A solution of CuCl₂ · 2 H₂O (34.1 mg, 0,2 mmol) in 3 cm³ of water was added to the solution of 2,6-di(1H-imidazol-2-yl)pyridine (42.1 mg, 0,2 mmol) in 3 cm³ of methanol. After 15 min, a saturated solution of NH₄PF₆ was added to promote the crystallization of the product. The resulting deep green solution was reduced by rotatory evaporation and upon cooling the complex precipitated as a dark green powder which was filtered off and washed with Et₂O and single crystals suitable for XRD were obtained by slow evaporation of a H₂O/MeOH solution. The compound was obtained as a deep green solid with 52% yield. ESI-MS (MeOH): m/z 309 and 311 [Cu(H₂dimp_y)Cl]⁺, 273 and 275 [Cu(Hdimp_y)]⁺. λ_{max} nm (L mol⁻¹ cm⁻¹) in MeOH: 257 (2991), 311 (3244), 376 (1502) and 707 (14).

4.4.5 DFT calculations

Magnetic coupling constants were calculated by the broken-symmetry U-DFT approach, as implemented in Orca version 3.0.0.¹⁷³ The calculations were run on top of the structure determined by X-ray diffraction using B3LYP^{174,175} functional with a triple zeta valence polarized basis set constructed considering relativistic effects (def2-TZVP).¹⁷⁶ The reported *J* values were calculated according to the literature.^{167,168}

Support Information - H₂dimpy as a ligand for Cu(I)-mediated ATRP.

Table 4.4: Data from the single-crystal XRD of the [Cu₂(H₂dimpy)₂(μ-Cl)₂](PF₆)₂ · 2 H₂O complex sample at room temperature.

λ (Mo K α , Å)	0.71073
Space group	P2 ₁ /c
Crystal System	Monoclinic
a (Å)	12.8088(5)
b (Å)	6.9009(3)
c (Å)	18.8547(6)
β (°)	102.050(2)
V (Å ³)	1629.89(11)
T (K)	296(2)

Table 4.5: Magnetic coupling analysis obtained with broken-symmetry U-B3LYP/def2-TZVP. The XRD experimental geometry was used neglecting water and PF₆⁻.

S_{HS}	1.0
S_{HS}^2	2.0054
S_{BS}^2	1.0054
E_{HS}	-5628.915503 hartree
E_{BS}	-5628.915498 hartree

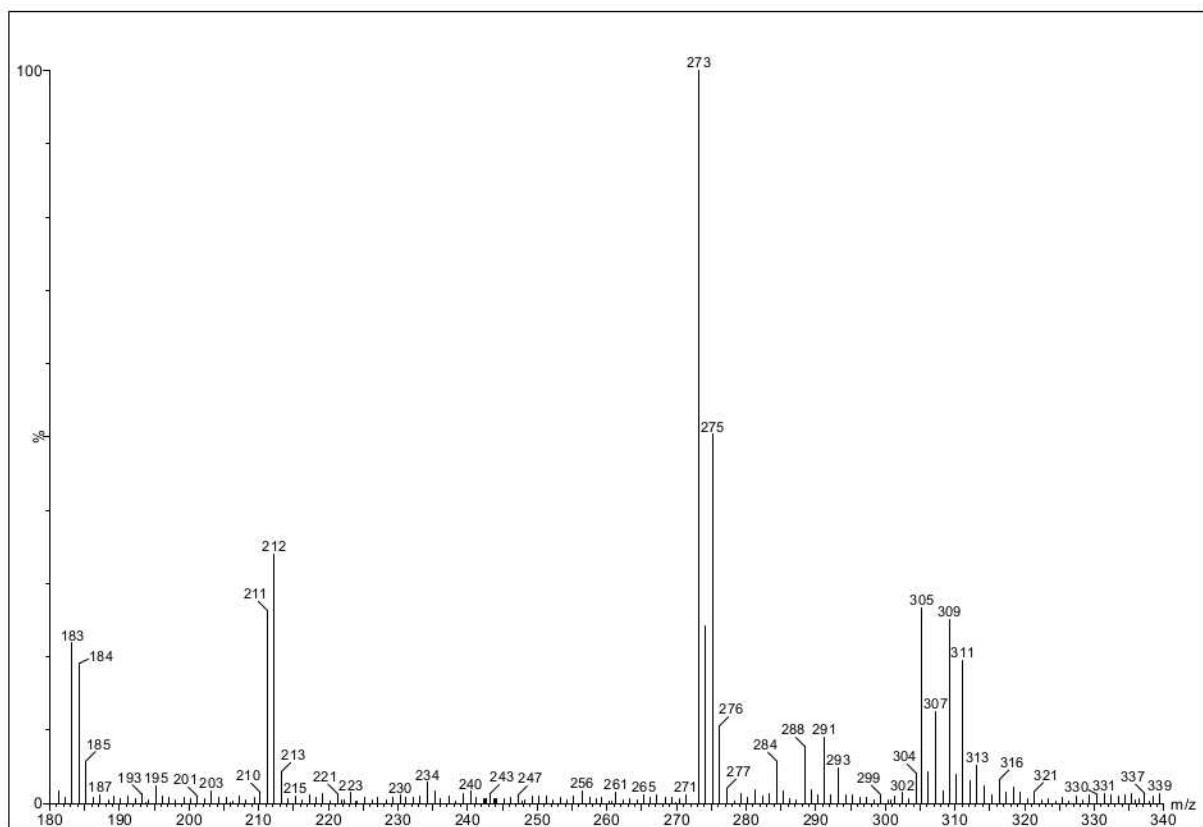


Figure 4.10: ESI-(+)-MS spectrum of the copper complex in MeOH/H₂O.

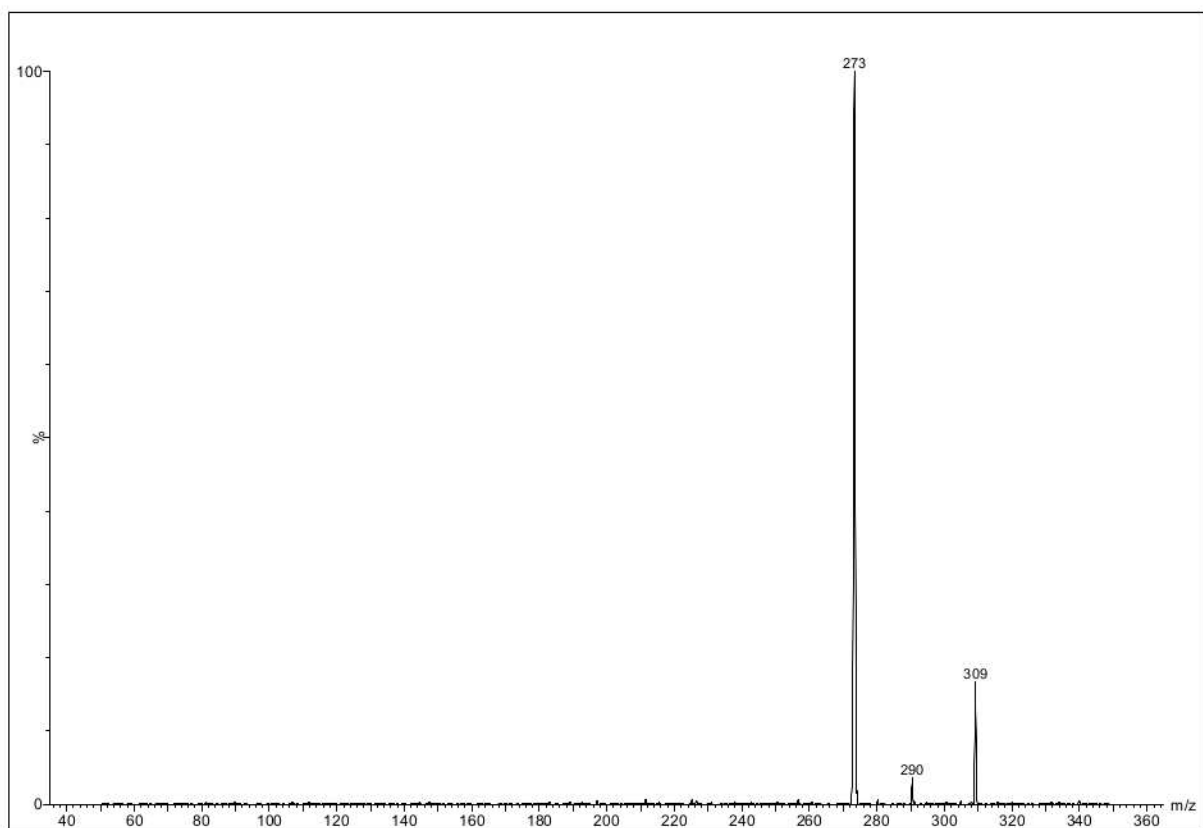


Figure 4.11: ESI-(+)-MS-MS spectrum of the peak at $m/z = 309$ corresponding to the $[\text{Cu}(\text{H}_2\text{dimpy})\text{Cl}]^+$ fragment.

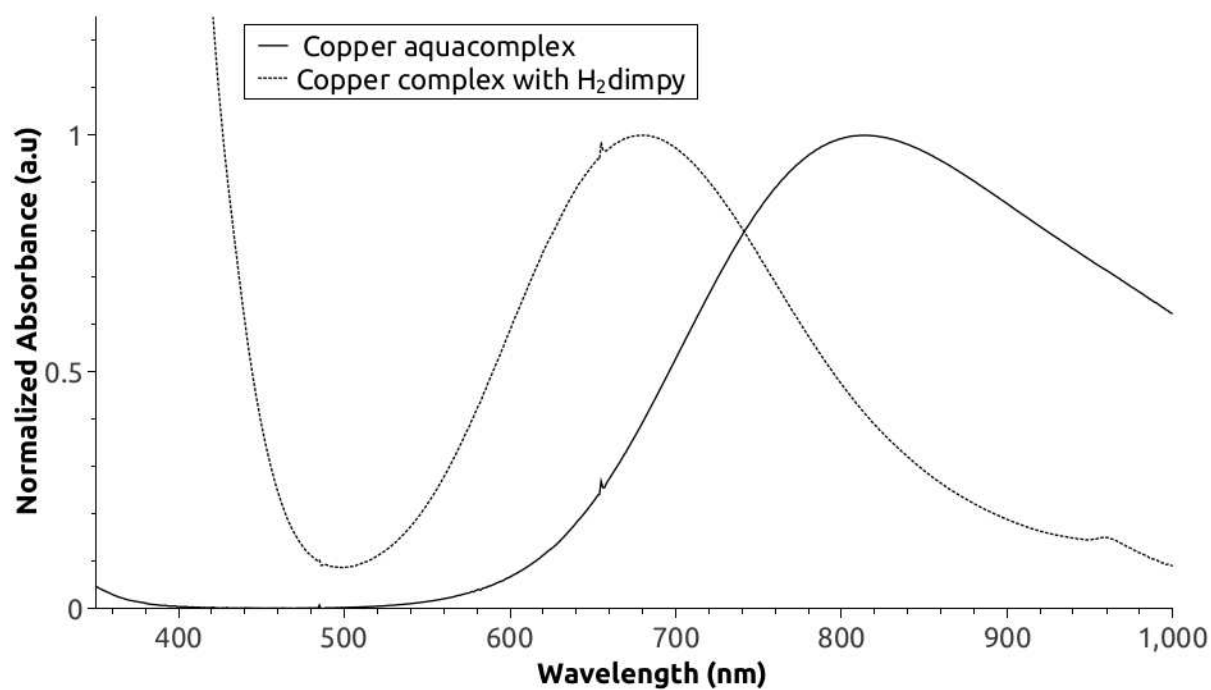


Figure 4.12: UV-Vis spectra of the copper(II) complex and CuCl₂ in H₂O.

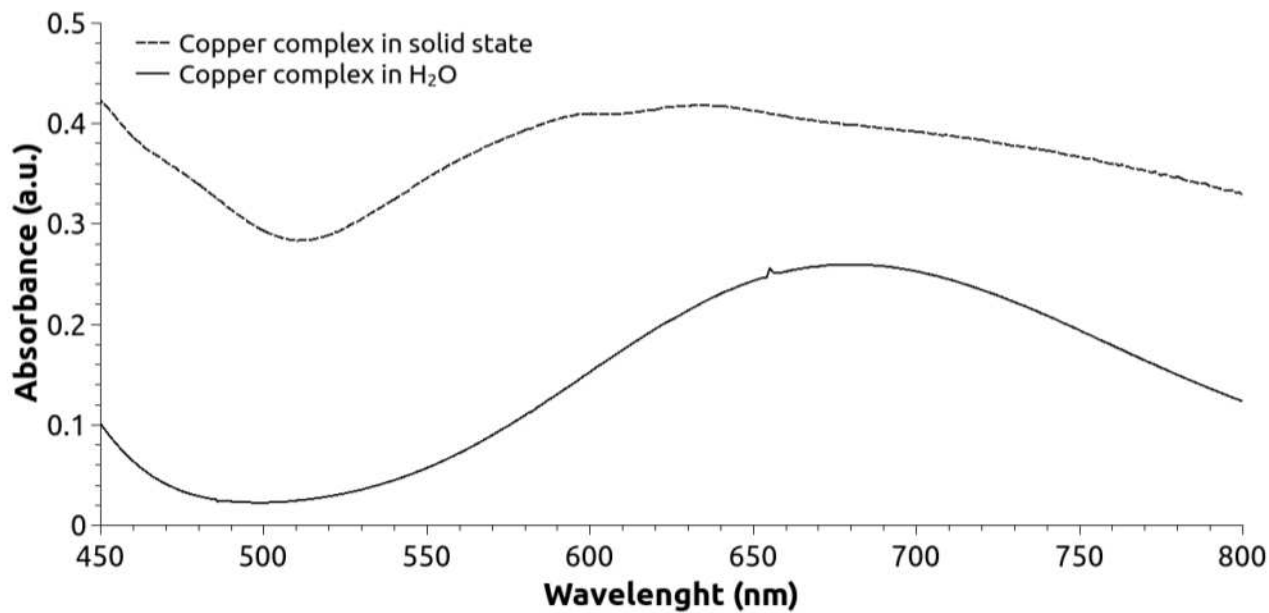


Figure 4.13: UV-Vis spectra of the copper(II) complex in H₂O and in the solid state.

Chapter 5

Conclusion and Perspectives

5.1 Conclusion

A series of 2-(1H-imidazol-2-yl)heteroaryl ligands were synthesized and their properties were investigated extensively. The effect of the number and relative position of nitrogens, in the six-membered N-heterocycles, were evaluated by ^1H and ^{13}C NMR and pK_aH measurements. It showed that increasing the number of nitrogens leads to a strong electron-withdraw effect of the N-heterocycles over the imidazole moiety, but the relative position of the nitrogen can tune the properties and even increase the basicity of the system.

The 2-(1H-imidazol-2-yl)pyridine (Himpy), the simplest ligand of the series, was used to synthesize a Ru(II) complex, previously described in literature,²⁸ in order to evaluate the bidentate binding site of this ligands. Due to the non-symmetric behaviour of the ligand, two possible isomers were expected. However, only the *meridional* isomer was observed. The solvatochromic behaviour of the complex was investigated, but for a accurate description of the MLCT transition a theoretical study is proposed.

In order to evaluate the monodentate binding sites of the pyrazine moiety of the 2-(1H-imidazol-2-yl)pyrazine (Himpz) ligand, a pentacyanidoferrate(II) complex was synthesized. The characterization confirmed the expected coordination and showed interesting electrochemical and spectroscopic properties. The pH-dependent behaviour of the redox potentials and electronic spectra is strongly related with the free imidazole moiety that is uncoordinated and free to be protonated.

Aiming at a synthetic application, the tridentate ligand 2,6-di(1H-imidazol-2-yl)pyridine (H₂dimpy) ligand was used in a Cu(I)-mediated controlled polymerization catalysis. During the catalytic reaction a Cu(II) intermediate was observed and in order to evaluate its properties a new Cu(II) complex was synthesized. The solution characterization of the complex suggested a pentacoordinated complex with 1:1:1 proportion between copper:H₂dimpy:chloride. This was confirmed by the single-crystal XRD structure that showed a dimeric complex with μ -chloride bridges as the fifth ligand. The magnetic measurements showed a ferromagnetic coupling in the solid that was consistent with the theoretical data for the dimeric system. The cyclic voltammetry showed the Cu(I/II) redox potential and the redox active behaviour of the ligand.

5.2 Perspectives

It was proved that the 2-(1H-imidazol-2-yl)heteroaryl compounds are an interesting class of ligand for coordination chemistry. Their versatility arises from the tuning of their properties by changing the number and relative position of nitrogens in the N-heterocycle or the number of 1H-imidazol-2-yl moieties. A diversity of prop-

erties could be observed in their complexes due to the π -acceptor character of the azine/diazine moiety and the protonation versatility of the imidazole. The investigation of the kind of ligands is suggested due to their promising application for it, such as in catalysis, magnetic materials, spin-crossover complexes, supramolecular chemistry and molecular devices.

Bibliography

- [1] D. C. G. A. Pinto, C. M. M. Santos, A. M. S. Silva. *Recent Research Developments in Heterocyclic Chemistry*. Research Signpost (2007).
- [2] Y.-T. Wang, S.-C. Yan, G.-M. Tang, C. Zhao, T.-D. Li, Y.-Z. Cui. *Inorg. Chim. Acta* 376 (2011) 492–499.
- [3] J. J. Perry IV, J. A. Perman, M. J. Zaworotko. *Chem. Soc. Rev.* 38 (2009) 1400–1417.
- [4] M. D. Allendorf, C. A. Bauer, R. K. Bhakta, R. J. T. Houk. *Chem. Soc. Rev.* 38 (2009) 1330–1352.
- [5] O. K. Farha, J. T. Hupp. *Acc. Chem. Res.* 43 (2010) 1166–1175.
- [6] Y.-J. Liu, H. Chao, J.-H. Yao, L.-F. Tan, Y.-X. Yuan, L.-N. Ji. *Inorg. Chim. Acta* 358 (2005) 1904–1910.
- [7] D. Kalyani, K. B. McMurtrey, S. R. Neufeldt, M. S. Sanford. *J. Am. Chem. Soc.* 133 (2011) 18566–18569.
- [8] J. Diez, J. Gimeno, A. Lledos, F. J. Suarez, C. Vicent. *ACS Catal.* 2 (2012) 2087–2099.
- [9] M. Delower Hossain, R. Ueno, M.-a. Haga. *Inorg. Chem. Commun.* 3 (2000) 35–38.
- [10] A. M. Bond, F. Marken, C. T. Williams, D. A. Beattie, T. E. Keyes, R. J. Forster, J. G. Vos. *J. Phys. Chem. B* 104 (2000) 1977–1983.
- [11] L. N. Ashbrook, C. M. Elliott. *J. Phys. Chem. C* 117 (2013) 3853–3864.
- [12] L. Dharmarathne, M. Ashokkumar, F. Grieser. *J. Phys. Chem. C* 116 (2011) 1056–1060.

- [13] R. Ziessel. *J. Am. Chem. Soc.* 115 (1993) 118–127.
- [14] M. R. Norris, J. J. Concepcion, D. P. Harrison, R. A. Binstead, D. L. Ashford, Z. Fang, J. L. Templeton, T. J. Meyer. *J. Am. Chem. Soc.* 135 (2013) 2080–2083.
- [15] C. Stangel, K. Ladomenou, G. Charalambidis, M. K. Panda, T. Lazarides, A. G. Coutsolelos. *Eur. J. Inorg. Chem.* 2013 (2013) 1275–1286.
- [16] D. L. Ashford, D. J. Stewart, C. R. Glasson, R. A. Binstead, D. P. Harrison, M. R. Norris, J. J. Concepcion, Z. Fang, J. L. Templeton, T. J. Meyer. *Inorg. Chem.* 51 (2012) 6428–6430.
- [17] M. E. Voss, C. M. Beer, S. A. Mitchell, P. A. Blomgren, P. E. Zhichkin. *Tetrahedron* 64 (2008) 645–651.
- [18] D. Shugar, A. Psoda. In: W. Saenger (ed.), *Physical Data II. Theoretical Investigations, Landolt-Börnstein - Group VII Biophysics*, volume 1d. Springer Berlin Heidelberg (1990). 315–315.
- [19] R. M. Balabin. *J. Chem. Phys.* 131 (2009) 154307.
- [20] G. S. K. Donald L. Pavia, Gary M. Lampman, J. R. Vyvyan. *Introduction to Spectroscopy*. 4^a ed. Brooks/Cole CENGAGE Learning (2009).
- [21] N. Begum, A. C. Ghosh, S. E. Kabir, M. A. Miah, G. G. Hossain. *Polyhedron* 24 (2005) 3074–3081.
- [22] H.-B. Luo, C. Zheng, Y.-K. Cheng. *J. Chromatogr. B* 853 (2007) 114–122.
- [23] R. Linnell. *J. Org. Chem.* 25 (1960) 290–290.
- [24] T. P. Selvam, C. R. James, P. V. Dniandev, S. K. Valzita. *Research in Pharmacy* 4 (2012) 01–09.
- [25] A. Kozak, M. Czaja, L. Chmurzyński. *J. Chem. Thermodyn.* 38 (2006) 599–605.
- [26] H. E. Toma, J. M. Malin. *Inorg. Chem.* 12 (1973) 1039–1045.
- [27] A. I. Baba, J. R. Shaw, J. A. Simon, R. P. Thummel, R. H. Schmehl. *Coord. Chem. Rev.* 171 (1998) 43–59.

- [28] G. Stupka, L. Gremaud, A. F. Williams. *HCA* 88 (2005) 487–495.
- [29] V. R. Souza, H. R. Rechenberg, J. A. Bonacin, H. E. Toma. *Spectrochim. Acta A* 71 (2008) 1296–1301.
- [30] S. A. V. Jannuzzi, B. Martins, M. I. Felisberti, A. L. B. Formiga. *J. Phys. Chem. B* 116 (2012) 14933–14942.
- [31] W. H. F. Sasse. *Org. Synth.* 46 (1966v) 5. Check by Victor A. Snieckus and V. Boekelheide.
- [32] G. F. Smith, C. A. Getz. *Chem. Rev.* 16 (1935) 113–120.
- [33] B. E. Halcrow, W. O. Kermack. *J. Chem. Soc.* (1946) 155–157.
- [34] G. T. Morgan, F. H. Burstall. *J. Chem. Soc.* (1932) 20–30.
- [35] H. Hofmeier, U. S. Schubert. *Chem. Soc. Rev.* 33 (2004) 373–399.
- [36] L. H. Berka, R. R. Gagne, G. E. Philippon, C. E. Wheeler. *Inorg. Chem.* 9 (1970) 2705–2709.
- [37] M. McDevitt, Y. Ru, A. Addison 18 (1993) 197–204–.
- [38] K. Zeitler. *Angew. Chem. Int. Ed.* 48 (2009) 9785–9789.
- [39] C. Herrero, A. Quaranta, R.-A. Fallahpour, W. Leibl, A. Aukauloo. *J. Phys. Chem. C* 117 (2013) 9605–9612.
- [40] M. Natali, F. Puntoriero, C. Chiorboli, G. La Ganga, A. Sartorel, M. Bonchio, S. Campagna, F. Scandola. *J. Phys. Chem. C* (2015) –.
- [41] A. M. Cargill Thompson. *Coord. Chem. Rev.* 160 (1997) 1–52.
- [42] V. Balzani, G. Bergamini, F. Marchioni, P. Ceroni. *Coord. Chem. Rev.* 250 (2006) 1254–1266.
- [43] H. Takashima, S. Shinkai, I. Hamachi. *Chem. Commun.* (1999) 2345–2346.
- [44] S. Xu, C. Lu, J. Shao, Q. Li, H. Li, W. Li. *J. Electroanal. Chem.* 661 (2011) 287–293.
- [45] H. Song, J. T. Kaiser, J. K. Barton. *Nat Chem* 4 (2012) 615–620.

- [46] X. Sun, Y. Du, L. Zhang, S. Dong, E. Wang. *Anal. Chem.* 79 (2007) 2588–2592.
- [47] M. Jeong, H. Nam, O.-J. Sohn, J. I. Rhee, H. J. Kim, C.-W. Cho, S. Lee. *Inorg. Chem. Commun.* 11 (2008) 97–100.
- [48] A. Heller, B. Feldman. *Chem. Rev.* 108 (2008) 2482–2505.
- [49] K. Kalyanasundaram. *Coord. Chem. Rev.* 46 (1982) 159–244.
- [50] A. Juris, V. Balzani, F. Barigelletti, S. Campagna, P. Belser, A. von Zelewsky. *Coord. Chem. Rev.* 84 (1988) 85–277.
- [51] J. P. Sauvage, J. P. Collin, J. C. Chambron, S. Guillerez, C. Coudret, V. Balzani, F. Barigelletti, L. De Cola, L. Flamigni. *Chem. Rev.* 94 (1994) 993–1019.
- [52] B. P. Sullivan, D. J. Salmon, T. J. Meyer. *Inorg. Chem.* 17 (1978) 3334–3341.
- [53] S. W. Gersten, G. J. Samuels, T. J. Meyer. *J. Am. Chem. Soc.* 104 (1982) 4029–4030.
- [54] J. V. Caspar, T. J. Meyer. *J. Am. Chem. Soc.* 105 (1983) 5583–5590.
- [55] J. J. Concepcion, J. W. Jurss, M. K. Brennaman, P. G. Hoertz, A. O. T. Patrocinio, N. Y. Murakami Iha, J. L. Templeton, T. J. Meyer. *Acc. Chem. Res.* 42 (2009) 1954–1965.
- [56] D. L. Ashford, M. K. Brennaman, R. J. Brown, S. Keinan, J. J. Concepcion, J. M. Papanikolas, J. L. Templeton, T. J. Meyer. *Inorg. Chem.* 54 (2014) 460–469.
- [57] S. Maji, I. López, F. Bozoglian, J. Benet-Buchholz, A. Llobet. *Inorg. Chem.* 52 (2013) 3591–3593.
- [58] L.-N. Ji, X.-H. Zou, J.-G. Liu. *Coord. Chem. Rev.* 216–217 (2001) 513–536.
- [59] G. C. Vougioukalakis, R. H. Grubbs. *Chem. Rev.* 110 (2009) 1746–1787.
- [60] G. A. Filonenko, D. Smykowski, B. M. Szyja, G. Li, J. Szczygieł, E. J. M. Hensen, E. A. Pidko. *ACS Catal.* (2015) 1145–1154.

- [61] S. P. Shan, X. Xiaoke, B. Gnanaprakasam, T. T. Dang, B. Ramalingam, H. V. Huynh, A. M. Seayad. *RSC Adv.* 5 (2015) 4434–4442.
- [62] M.-E. Moret, I. Tavernelli, M. Chergui, U. Rothlisberger. *Chem. Eur. J.* 16 (2010) 5889–5894.
- [63] M. Shen, A. J. Bard. *J. Am. Chem. Soc.* 133 (2011) 15737–15742.
- [64] A. J. Göttle, F. Alary, I. M. Dixon, J.-L. Heully, M. Boggio-Pasqua. *Inorg. Chem.* 53 (2014) 6752–6760.
- [65] D. Wang, L. Guo, R. Huang, B. Qiu, Z. Lin, G. Chen. *Sci. Rep.* 5 (2015) –.
- [66] R. C. Young, T. J. Meyer, D. G. Whitten. *J. Am. Chem. Soc.* 98 (1976) 286–287.
- [67] W. E. Jones, M. A. Fox. *J. Phys. Chem.* 98 (1994) 5095–5099.
- [68] J. Xuan, W.-J. Xiao. *Angew. Chem. Int. Ed.* 51 (2012) 6828–6838.
- [69] D. P. Rillema, G. Allen, T. J. Meyer, D. Conrad. *Inorg. Chem.* 22 (1983) 1617–1622.
- [70] T. P. Yoon, M. A. Ischay, J. Du. *Nat Chem* 2 (2010) 527–532.
- [71] J. W. Tucker, C. R. J. Stephenson. *J. Org. Chem.* 77 (2012) 1617–1622.
- [72] C. K. Prier, D. A. Rankic, D. W. C. MacMillan. *Chem. Rev.* 113 (2013) 5322–5363.
- [73] R. J. Sundberg, R. F. Bryan, I. F. Taylor, H. Taube. *J. Am. Chem. Soc.* 96 (1974) 381–392.
- [74] R. Sahai, W. Murphy Jr., J. Petersen. *Inorg. Chim. Acta* 114 (1986) 137–140.
- [75] G. Orellana, C. Alvarez-Ibarra, M. L. Quiroga. *Bull. Soc. Chim. Belges* 97 (1988) 731–742.
- [76] D. P. Rillema, R. Sahai, P. Matthews, A. K. Edwards, R. J. Shaver, L. Morgan. *Inorg. Chem.* 29 (1990) 167–175.
- [77] S. J. Milder. *Inorg. Chem.* 28 (1989) 868–872.

- [78] U. Mayer, V. Gutmann, W. Gerger 106 (1975) 1235–1257–.
- [79] U. Mayer. *Pure Appl. Chem.* 51 (1979) 1697–1712.
- [80] Y. Marcus. *Chem. Soc. Rev.* 22 (1993) 409–416.
- [81] J. C. Curtis, B. P. Sullivan, T. J. Meyer. *Inorg. Chem.* 22 (1983) 224–236.
- [82] M. K. Nazeeruddin, S. M. Zakeeruddin, R. Humphry-Baker, M. Jirousek, P. Liska, N. Vlachopoulos, V. Shklover, C.-H. Fischer, M. Grätzel. *Inorg. Chem.* 38 (1999) 6298–6305.
- [83] S. Fantacci, F. De Angelis, A. Selloni. *J. Am. Chem. Soc.* 125 (2003) 4381–4387.
- [84] E. M. Kober, B. P. Sullivan, T. J. Meyer. *Inorg. Chem.* 23 (1984) 2098–2104.
- [85] B. J. Holliday, C. A. Mirkin. *Angew. Chem. Int. Ed.* 40 (2001) 2022–2043.
- [86] R. W. Saalfrank, H. Maid, A. Scheurer. *Angew. Chem. Int. Ed.* 47 (2008) 8794–8824.
- [87] M. J. Wiester, P. A. Ulmann, C. A. Mirkin. *Angew. Chem. Int. Ed.* 50 (2011) 114–137.
- [88] P. J. Lusby. *Annu. Rep. Prog. Chem., Sect. A: Inorg. Chem.* 109 (2013) 254–276.
- [89] R. A. Evans. *Aust. J. Chem.* 60 (2007) 384–395.
- [90] C. Spiteri, J. E. Moses. *Angew. Chem. Int. Ed.* 49 (2010) 31–33.
- [91] H. Stockmann, A. A. Neves, S. Stairs, K. M. Brindle, F. J. Leeper. *Org. Biomol. Chem.* 9 (2011) 7303–7305.
- [92] H. E. Toma, J. M. Malin. *Inorg. Chem.* 12 (1973) 2080–2083.
- [93] H. E. Toma, J. M. Malin, E. Giesbrecht. *Inorg. Chem.* 12 (1973) 2084–2089.
- [94] H. E. Toma, J. M. Malin. *Inorg. Chem.* 13 (1974) 1772–1774.
- [95] H. E. Toma, A. B. P. Lever. *Inorg. Chem.* 25 (1986) 176–181.

- [96] H. E. Toma, F. M. Matsumoto, C. Cipriano. *J. Electroanal. Chem.* 346 (1993) 261–270.
- [97] C. Hidalgo-Luangdilok, A. B. Bocarsly. *Inorg. Chem.* 29 (1990) 2894–2900.
- [98] H. Winnischofer, F. M. Engelmann, H. E. Toma, K. Araki, H. R. Rechenberg. *Inorg. Chim. Acta* 338 (2002) 27–35.
- [99] A. L. B. Formiga, S. Vancoillie, K. Pierloot. *Inorg. Chem.* 52 (2013) 10653–10663.
- [100] B. M. Pires, S. A. V. Jannuzzi, A. L. B. Formiga, J. A. Bonacin. *Eur. J. Inorg. Chem.* 2014 (2014) 5794–5794.
- [101] D. H. Macartney. *Rev. Inorg. Chem.* 9 (1988) 101–152.
- [102] C. C. Corrêa, S. A. V. Jannuzzi, M. Santhiago, R. A. Timm, A. L. B. Formiga, L. T. Kubota. *Electrochim. Acta* 113 (2013) 332–339.
- [103] S. Maji, B. Sarkar, S. M. Mobin, J. Fiedler, W. Kaim, G. K. Lahiri. *Dalton Trans.* (2007) 2411–2418.
- [104] H. E. Toma, M. S. Takasugi. *J. Solution Chem.* 12 (1983) 547–561.
- [105] H. E. Toma, M. S. Takasugi. *J. Solution Chem.* 18 (1989) 575–583.
- [106] I. Deligkiozi, E. Voyiatzis, A. Tsolomitis, R. Papadakis. *Dyes Pigm.* 113 (2015) 709–722.
- [107] L. D. Slep, S. Pollak, J. A. Olabe. *Inorg. Chem.* 38 (1999) 4369–4371.
- [108] A. G. Sharpe. *The Chemistry of Cyano Complexes of Transition Metals*. Academic Press: London (1976).
- [109] J. M. Malin, C. F. Schimdt, H. E. Toma. *Inorg. Chem.* 14 (1975) 2924.
- [110] G. Orellana, C. Alvarez Ibarra, J. Santoro. *Inorg. Chem.* 27 (1988) 1025–1030.
- [111] H. E. Toma, C. Creutz. *Inorg. Chem.* 16 (1977) 545–550.
- [112] L. N. Klatt, R. L. Rouseff. *J. Am. Chem. Soc.* 94 (1972) 7295–7304.
- [113] G. Brauer. *Handbook of Preparative Inorganic Chemistry*, volume 1. 2^a ed. Academic Press: New York (1963).

- [114] H. T. S. Britton, R. A. Robinson. *J. Chem. Soc.* (1931) 1456–1462.
- [115] Y. Wang, Y. Kwak, K. Matyjaszewski. *Macromolecules* 45 (2012) 5911–5915.
- [116] K. Matyjaszewski. Elsevier (2003). 3–11.
- [117] N. Ayres. *Polymer Reviews* 51 (2011) 138–162.
- [118] K. Matyjaszewski, J. Xia. *Chem. Rev.* 101 (2001) 2921–2990.
- [119] K. Matyjaszewski. *Chem. Eur. J.* 5 (1999) 3095–3102.
- [120] Y. Yamamura, K. Matyjaszewski. *J. Polym. Sci. A Polym. Chem.* 46 (2008) 2015–2024.
- [121] G. Kickelbick, K. Matyjaszewski. *Macromol. Rapid Commun.* 20 (1999) 341–346.
- [122] M. H. Acar, N. Bicak. *J. Polym. Sci. A Polym. Chem.* 41 (2003) 1677–1680.
- [123] Y. Inoue, K. Matyjaszewski. *Macromolecules* 37 (2004) 4014–4021.
- [124] W. Tang, Y. Kwak, W. Braunecker, N. V. Tsarevsky, M. L. Coote, K. Matyjaszewski. *J. Am. Chem. Soc.* 130 (2008) 10702–10713.
- [125] J. V. Nguyen, C. W. Jones. *Macromolecules* 37 (2004) 1190–1203.
- [126] M. Kamigaito, T. Ando, M. Sawamoto. *Chem. Rev.* 101 (2001) 3689–3746.
- [127] G. Kickelbick, T. Pintauer, K. Matyjaszewski. *New J. Chem.* 26 (2002) 462–468.
- [128] W. A. Braunecker, K. Matyjaszewski. *Prog. Polym. Sci.* 32 (2007) 93–146.
- [129] H. E. Toma, J. A. Vanin, J. M. Malin. *Inorg. Chim. Acta* 33 (1979) L157–L159.
- [130] G. Orellana, M. L. Quiroga, A. M. Braun. *HCA* 70 (1987) 2073–2086.
- [131] M. O. Santiago, C. L. Filho, I. d. S. Moreira, R. M. Carlos, S. L. Queiroz, A. A. Batista. *Polyhedron* 22 (2003) 3205–3211.
- [132] J. Bezençon, M. B. Wittwer, B. Cutting, M. Smieško, B. Wagner, M. Kansy, B. Ernst. *J. Pharm. Biomed. Anal.* 93 (2014) 147–155.

- [133] R. F. Carina, L. Verzeqñassi, A. F. Williams, G. Bernardinelli. *Chem. Commun.* (1998) 2681–2682.
- [134] G. Stupka, L. Gremaud, G. Bernardinelli, A. F. Williams. *Dalton Trans.* 0 (2004) 407–412.
- [135] M. M. Konnick, S. M. Bischof, R. A. Periana, B. G. Hashiguchi. *Adv. Synth. Catal.* 355 (2013) 632–636.
- [136] M.-a. Haga, H.-G. Hong, Y. Shiozawa, Y. Kawata, H. Monjushiro, T. Fukuo, R. Arakawa. *Inorg. Chem.* 39 (2000) 4566–4573.
- [137] M. S. Saraiva, C. D. Nunes, T. G. Nunes, M. J. Calhorda. *J. Mol. Catal. A: Chem.* 321 (2010) 92–100.
- [138] Y. H. Lee, A. Ohta, Y. Yamamoto, Y. Komatsu, K. Kato, T. Shimizu, H. Shinoda, S. Hayami. *Polyhedron* 30 (2011) 3001–3005.
- [139] H. Tang, M. Radosz, Y. Shen. In: *ACS Symposium Series*, volume 1023. American Chemical Society (2009). 139–157–.
- [140] H. Tang, M. Radosz, Y. Shen. *AIChE J.* 55 (2009) 737–746.
- [141] M. L. Rigsby, S. Mandal, W. Nam, L. C. Spencer, A. Llobet, S. S. Stahl. *Chem. Sci.* 3 (2012) 3058–3062.
- [142] T. Rojo, M. I. Arriortua, J. Ruiz, J. Darriet, G. Villeneuve, D. Beltrán-Porter. *J. Chem. Soc., Dalton Trans.* (1987) 285–291.
- [143] T. Rojo, J. Darriet, J. Dance, D. Beltrán-Porter. *Inorg. Chim. Acta* 64 (1982) L105–L107.
- [144] D. L. Pavia, G. M. Lampman, G. S. Kriz. *Introduction to Spectroscopy*. Saunders Golden Sunburst Series, 2^a ed. Saunders College Publishers (1996).
- [145] J.-S. Wang, K. Matyjaszewski. *J. Am. Chem. Soc.* 117 (1995) 5614–5615.
- [146] T. E. Patten, K. Matyjaszewski. *Acc. Chem. Res.* 32 (1999) 895–903.
- [147] U. S. Schubert, G. Hochwimmer, C. E. Spindler, O. Nuyken 43 (1999) 319–326.
- [148] J.-S. Wang, K. Matyjaszewski. *Macromolecules* 28 (1995) 7901–7910.

- [149] S. Perrier, P. Takolpuckdee. *J. Polym. Sci. A Polym. Chem.* 43 (2005) 5347–5393.
- [150] B. Ray, M. Kotani, S. Yamago. *Macromolecules* 39 (2006) 5259–5265.
- [151] M. U. Kahveci, G. Acik, Y. Yagci. *Macromol. Rapid Commun.* 33 (2012) 309–313.
- [152] S. Chavda, S. Yusa, M. Inoue, L. Abezgauz, E. Kesselman, D. Danino, P. Bahadur. *Eur. Polym. J.* 49 (2013) 209–216.
- [153] H. Tang, N. Arulsamy, M. Radosz, Y. Shen, N. V. Tsarevsky, W. A. Braunecker, W. Tang, K. Matyjaszewski. *J. Am. Chem. Soc.* 128 (2006) 16277–16285.
- [154] N. V. Tsarevsky, W. A. Braunecker, W. Tang, S. J. Brooks, K. Matyjaszewski, G. R. Weisman, E. H. Wong. *J. Mol. Catal. A: Chem.* 257 (2006) 132–140.
- [155] R. M. Johnson, C. Ng, C. C. M. Samson, C. L. Fraser. *Macromolecules* 33 (2000) 8618–8628.
- [156] J.-F. Lutz, K. Matyjaszewski. *J. Polym. Sci. A Polym. Chem.* 43 (2005) 897–910.
- [157] A. O. Eseola, W.-H. Sun, W. Li, J. A. Woods. *J. Mol. Struct.* 984 (2010) 117–124.
- [158] F. S. P. Cardoso, K. A. Abboud, A. Aponick. *J. Am. Chem. Soc.* 135 (2013) 14548–14551.
- [159] S. Khabnadideh, Z. Rezaei, A. Khalafi-Nezhad, R. Bahrinajafi, R. Mohamadi, A. Farrokhrooz. *Bioorg. Med. Chem. Lett.* 13 (2003) 2863–2865.
- [160] G. Bernardinelli, G. Hopfgartner, A. F. Williams. *Acta Crystallogr., Sect. C: Cryst. Struct. Commun.* 46 (1990) 1642–1645.
- [161] A. W. Addison, T. N. Rao, J. Reedijk, J. van Rijn, G. C. Verschoor. *J. Chem. Soc., Dalton Trans.* (1984) 1349–1356.
- [162] M. Delower Hossain, R. Ueno, M.-a. Haga. *Inorg. Chem. Commun.* 3 (2000) 35–38.

- [163] P. C. Christidis, C. A. Bolos, G. St. Nikolov. *Inorg. Chim. Acta* 237 (1995) 123–130.
- [164] M. Scarpellini, A. Neves, E. E. Castellano, D. W. Franco. *J. Mol. Struct.* 694 (2004) 193–198.
- [165] A. Heyns, G. van Schalkwyk. *Spectrochim. Acta, Part A* 29 (1973) 1163–1175.
- [166] A. Heyns. *Spectrochim. Acta, Part A* 33 (1977) 315–322.
- [167] A. P. Ginsberg. *J. Am. Chem. Soc.* 102 (1980) 111–117.
- [168] L. Noodleman, E. R. Davidson. *Chem. Phys.* 109 (1986) 131–143.
- [169] A. B. P. Lever. *Inorganic Electronic Spectroscopy, studies in physical and theoretical chemistry*, volume 33. 2^a ed. Elsevier (1986).
- [170] V. M. Manikandamathavan, B. Unni Nair. *Eur. J. Med. Chem.* 68 (2013) 244–252.
- [171] Sheldrick, George. *Acta Crystallogr., Sect. A: Found. Crystallogr.* 64 (2008) 112–122.
- [172] A. L. Spek. *J. Appl. Crystallogr.* 36 (2003) 7–13.
- [173] F. Neese. *Wiley Interdisciplinary Reviews: Computational Molecular Science* 2 (2012) 73–78.
- [174] C. Lee, W. Yang, R. Parr. *Phys. Rev. B* 37 (1988) 785–789.
- [175] A. D. Becke. *J. Chem. Phys.* 98 (1993) 5648–5652.
- [176] D. A. Pantazis, X.-Y. Chen, C. R. Landis, F. Neese. *J. Chem. Theory Comput.* 4 (2008) 908–919.